SIMGRO 5.0 Theory and model implementation

SIMGRO 5.0.1

Theory and model implementation

P.E.V. van Walsum
A.A. Veldhuizen
P.J.T. van Bakel
F.J.E. van der Bolt
P.E. Dik
P. Groenendijk
E.P. Querner
M.F.R. Smit

Alterra-report 913.1

Alterra, Green World Research, Wageningen, 2004

ABSTRACT

P.E.V. van Walsum, A.A. Veldhuizen, P.J.T. van Bakel, F.J.E. van der Bolt, P.E. Dik, P. Groenendijk, E.P. Querner, M.F.R. Smit. 2004. *SIMGRO 5.0.1, Theory and model implementation.* Wageningen, Alterra. Alterra-Report 913.1. 96 pp.; 28 figs.; 2 tables; 50. refs.

For the (efficient) design and evaluation of integrated water management strategies a model is needed that covers the whole (regional) system, including plant-atmosphere interactions, soil water, groundwater and surface water. SIMGRO is a mechanistic distributed model with a (nearly) unified saturated-unsaturated flow description at its core. Innovative use is made of dynamic 'metamodelling' techniques for the soil water and surface water. The implementation relies on 'intelligent' data that are obtained by a series of computational experiments with comprehensive models. In this way an acceptable degree of accuracy is achieved at a relatively low computational cost. For the drainage of groundwater to surface water a new technique is used to combine analytical formulae with a numerical grid.

Keywords: integrated water management, mechanistic, distributed, dynamic, saturated-unsaturated flow, surface water, drainage

ISSN 1566-7197

This report can be ordered by paying € 20,- into bank account number 36 70 54 612 in the name of Alterra, Wageningen, the Netherlands, with reference to report 913.1. This amount is inclusive of VAT and postage.

P.O. Box 47, NL-6700 AA Wageningen (The Netherlands).
Phone: +31 317 474700; fax: +31 317 419000; e-mail: info.alterra@wur.nl

DWK-Programme 417

Contents

Preface

What started with the simple instruction 'write down what you have got' soon transformed into a creative process, involving a large group of hydrologists at Alterra. As we went along new ideas popped up. Sometimes we could not resist the temptation to describe them here, even though – as yet – they have only been tested in a stand-alone fashion. That applies to the concept for flow in the saturated-unsaturated zone and drainage of groundwater to surface water. Work is now underway to include these new ideas in the SIMGRO-code. More than in the past we are trying to make the submodels 'portable', allowing a flexible use of the software. One of the plans for the immediate future is to couple our soil water and surface water concepts to the MODFLOW code. Also the ongoing activity of linking SIMGRO modules to SOBEK-CF will greatly benefit by portable submodels. We expect that in the medium term most of the modules will be available for implementation within modelling frameworks for dynamic simulation models.

In our description we have attempted to make a distinction between 'theory' and 'implementation'. But where to draw the line is of course a subjective matter, depending on the perspective that one has. Nevertheless we hope that it is functional, for the reader who only wants to a get quick idea of the conceptualization, but even more so for the reader who also wants to understand the implementation. Anyone with experience in the field of integrated modelling knows that the efficiency and tractability of the implementation are the critical success factors, and that – in the end – it's the numbers that do the talking.

The production of this report is part of the upkeep and the maintenance activities of 'core' hydrological models which are financed by DWK-DLO research programme 417 "Changing water management for a sustainable rural environment". The SIMGRO model facilitates the description of the interaction between groundwater and surface water systems at sub-regional and regional scale and is therefore an important key to reaching the programme's objectives.

More information about the model can be found on the SIMGRO-webpage http://www.simgro.alterra.nl to obtain a first impression of the capabilities and performance. For questions about the contents of this report concerning the modelling concepts the reader is referred to main authors mr. P.E.V. van Walsum (paul.vanwalsum@wur.nl) and mr. A.A. Veldhuizen (ab.veldhuizen@wur.nl)

Piet Groenendijk, project leader

Summary

Most regional model codes only partly cover the processes *within* a region. The remedy is then sought by introducing internal boundary conditions. But these conditions are more often than not a gross schematization of reality, lacking essential feedback mechanisms. For coming to grips with many issues of integrated water management it is necessary to have a model that covers the whole (regional) system, including plant-atmosphere interactions, soil water, groundwater and surface water. SIMGRO (a dated acronym of SIMulation of GROundwater, Querner and Van Bakel, 1989, Veldhuizen et al., 1998) was developed for that purpose.

SIMGRO is a mechanistic distributed model with a (nearly) unified saturated-unsaturated flow description at its core. For the saturated groundwater flow a finite element scheme is employed. For the soil water and surface water innovative use is made of dynamic 'metamodelling' techniques. The implementation relies on 'intelligent' data that are obtained by a series of computational experiments with comprehensive models. In this way an acceptable degree of accuracy is achieved at a relatively low computational cost. For the drainage of groundwater to surface water a new technique is used to combine analytical formulae with a numerical grid. Although setting up a model can as such be an expedient way of understanding a region's hydrology, the goal is usually to simulate the effects of potential measures (digging ditches, sprinkling, and so on) on the water-dependent functions. Examples of the latter are the production of crops by agriculture and the biodiversity of wet natural grasslands. So in a separate chapter attention is paid to the simulation of water management.

1 Introduction

The hydrologic cycle operates within a set of constraints and physical laws that control the dynamics, storage and disposition of water within it. It is a closed system that satisfies the principle of conservation of mass. Regional hydrologic models suffer the deficiency that only part of the hydrologic cycle is simulated. In the first place this concerns the spatial limitation of a model, which necessitates the making of assumptions with respect to external boundary conditions. Furthermore, most models only partly cover the processes *within* a region. The remedy is then sought by introducing internal boundary conditions. But these conditions are more often than not a gross schematization of reality, lacking essential feedback mechanisms. That even applies to the commonly used assumption that the precipitation and evaporative demand of the atmosphere can be seen as external boundary conditions: the larger the basin, the less this assumption is valid. For coming to grips with many issues of integrated water management it is necessary to have a model that covers the whole (regional) system, including plant-atmosphere interactions, soil water, groundwater and surface water. SIMGRO (a dated acronym of SIMulation of GROundwater, Querner and Van Bakel, 1989, Veldhuizen et al., 1998) was developed for that purpose.

The description of an integrated model inevitably has to cover areas of common knowledge. We consider innovative the dynamic 'metamodelling' of soil water in the shallow subsoil in §3, part of the drainage concepts given in §4, the metamodelling of surface water in §5, and the modelling of urban water management in §6. The term 'metamodelling' is reserved for model descriptions that rely heavily on making computational experiments with a comprehensive model. By feeding the metamodels with 'intelligent' data they achieve an acceptable accuracy at a relatively low computational cost.

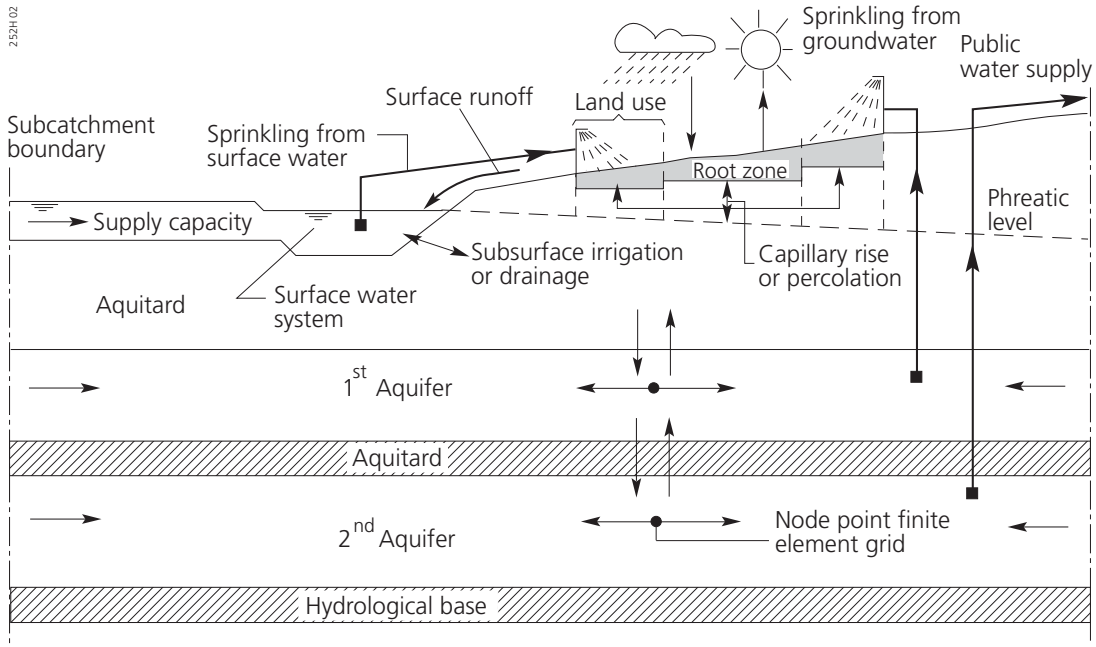

Figure 1 Schematization in SIMGRO of the hydrologic system by integration of saturated zone, unsaturated zone and surface water (Querner and van Bakel, 1989)

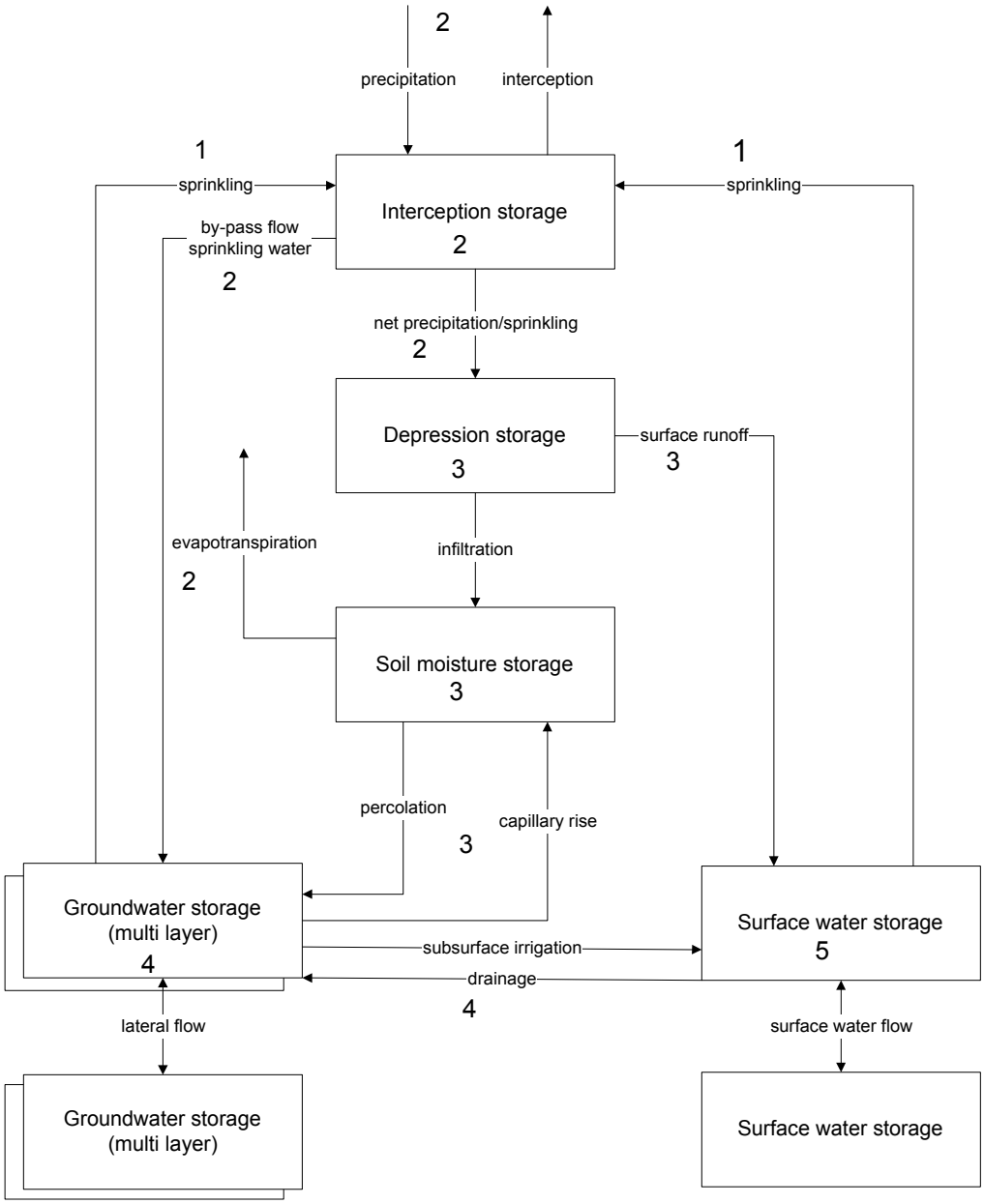

Figure 2 Schematization of water flows in SIMGRO, by means of transmission links and storage elements.

SIMGRO is a mechanistic distributed model. An overview of the modelled processes is given in Figure 1, and the schematization in terms of transmission links and storage elements is given in Figure 2. A finite-element grid is used for the horizontal discretisation of the soil and groundwater modelling, involving nodes and their nodal subdomains. In the vertical direction a schematization is used in terms of aquitards and aquifers, commonly referred to as a 'quasi-threedimensional' approach.

Surface water is modelled as a network of watercourse trajectories. Depending on the way the model has been implemented, this can involve even the smallest of watercourses. But in most applications a certain degree of lumping is done in the headwaters. A detailed area from an example model implementation is given in Figure 3.

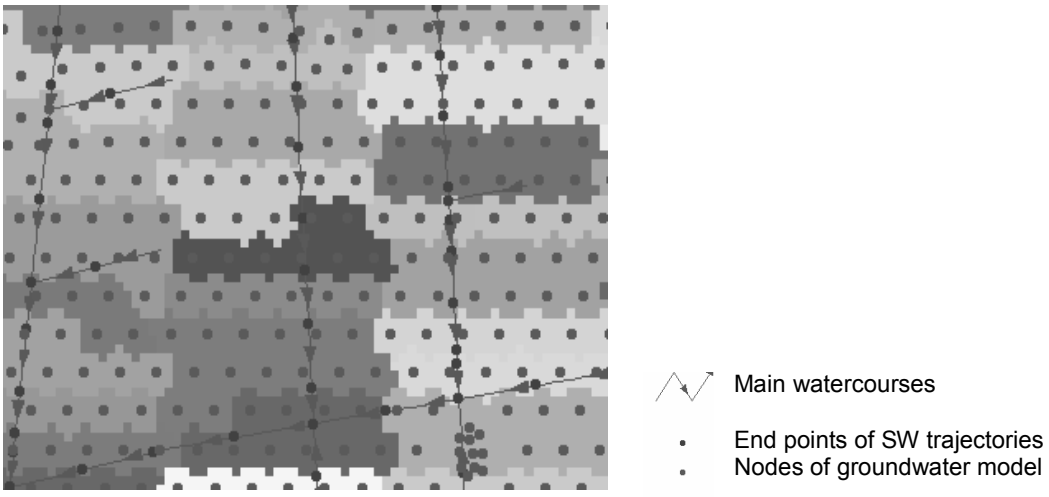

Figure 3 Detail of an example model implementation, showing subcatchments (thematic colouring), main watercourses, end points of watercourse trajectories, and nodes of the groundwater model

The used solutions of fundamental underlying differential equations inevitably involve a certain degree of simplification. Essential for the practical relevance of the model is that it has remained possible to make long simulation runs (30 years) of medium-sized basins (75 000 ha) within acceptable computation times (e.g. one hour per simulation year). During the model development this has been a guiding principle of the utmost consideration.

The model is dynamic, with separate time steps for the surface water system (Δt_s) and the soil water/groundwater system (Δt_g). Typical time steps used in the current modelling practice are Δt_s=0.01 d and Δt_g =0.25 d. These values reflect the large difference between the dynamics of surface water and groundwater. An overview of the modelling cycle is given in Figure 4. Essential for the integrated modelling is that the *feedback* between the compartments takes place at the appropriate time scale. For instance the influence of the surface water level on the drainage fluxes is updated for each time step of the surface water model.

In the following sections a description is given of the used conceptualizations, followed by more detailed descriptions about the way they have been implemented. Heavy rainfall can let a regional hydrologic system undergo a metamorphosis. Such a change of appearance can also be caused by extreme water management measures. The division into 'compartments' of soil water, groundwater and surface water is therefore not a static one. So the arrangement of the material will always have a somewhat arbitrary nature, whichever way it is done. That also applies to the exchanges of water – they have here been described along with the state description of the most naturally associated compartment. Given the obvious limitations of a regional model, the atmosphere is not described as a separate entity. Instead a separate section is devoted to the interactions that it has with the regional system.

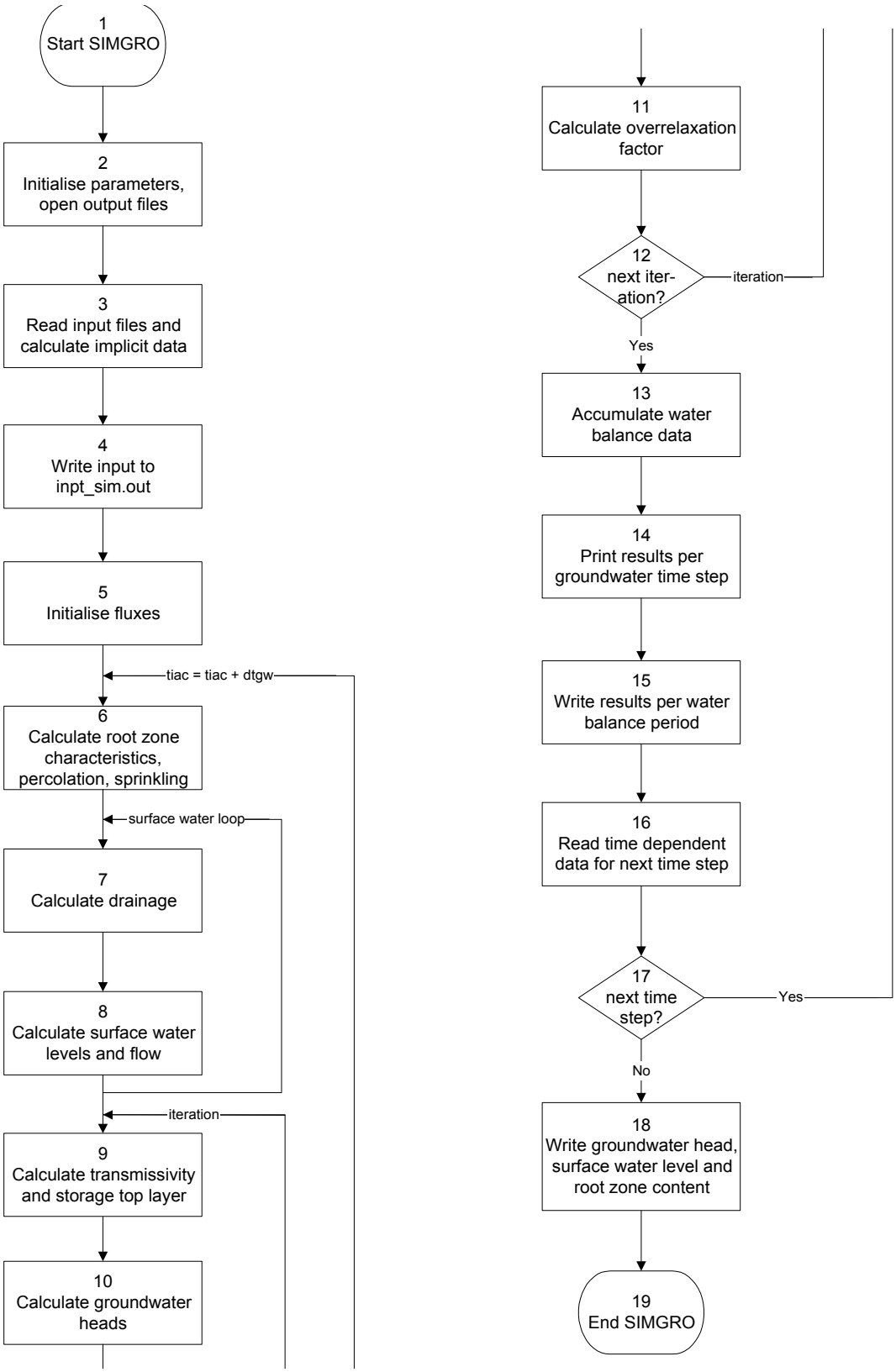

Figure 4 Overview of modelling cycle

The simulation of (possible) changes in water management is the goal of most studies. Given its crucial importance for the practical relevance of the model, the management options are described in a separate section. But of course the distinction between what is considered 'water management' and what 'natural functioning' depends on the perspective that one has. Here any type of land-use involving vegetated soil is considered to be 'natural', even though it is some form of agriculture. In the case of land-use, the term water management is reserved for paved areas, involving some form of interference in the cycle, e.g. urban areas. The layout of man-made ditches is described as if it were part of the natural system, whereas it is of course not. In the case of surface water the term 'management' is reserved for the manipulation of the water flows and levels through the use of structures.

To aid the reader in quickly locating the descriptions, the overview in Figure 2 has been furnished with hyper-links to the subsections.

2 Plant/soil-atmosphere interactions

2.1 Introduction

Interactions with the atmosphere are the drivers of the regional system. The recharge is sensitive to the water balance of precipitation and evapotranspiration: a relative error or change in either of these terms is amplified by a factor 2-3 in the computation of the recharge. In this chapter we therefore describe in some detail the manner in which the interactions between the plant/soil system and the atmosphere are modelled.

2.2 Precipitation

It is well known that the measurement of precipitation usually contains systematic errors due to wind-effects. The size of the error is usually in the order of a few % (<5%), but should be accounted for. The 'natural' precipitation can be augmented by sprinkling. The total (gross) precipitation is then given by:

$$P_{\text{gross}}(t) = P(t) + P_{\text{s,net}}(t) \tag{1}$$

where
$P_{\text{gross}}(t)$ = gross precipitation intensity at time t (m d^{-1})
$P(t)$ = natural precipitation intensity at time t (m d^{-1})
$P_{\text{s,net}}(t)$ = net sprinkling intensity at time t (Eq. 101) (m d^{-1})

2.3 Interception

Incoming precipitation can either fall directly on the ground surface – as free throughfall – or can be intercepted by the vegetation canopy. Subsequently it can either directly evaporate, or else reach the ground surface as stemflow and as drops from the leaves.

The interception reservoir is assumed to have a known maximum capacity S_{ic} for the amount of water that can be stored on a canopy. The capacity is strongly correlated to the leaf area, commonly expressed as the Leaf Area Index (which gives the ratio between the leaf area and the area of the soil surface). The other two important parameters are the 'free throughfall coefficient' p, which is strongly correlated to the soil cover, and the 'stemflow coefficient' p_{sf}. Both these coefficients depend on the type of vegetation and its development stage. This parameterization follows that of Gash (1979). The expression for the intercepted precipitation is given by (for the case that the capacity of the interception reservoir is non-limiting):

$$P_{\text{i}}(t) = [1 - p - p_{\text{sf}}]P_{\text{gross}}(t) \tag{2}$$

where:

$P_{gross}(t)$ = gross precipitation intensity at time t (m d^{-1})
$P_i(t)$ = intercepted precipitation intensity at time t (m d^{-1})
p = free throughfall coefficient (-)
p_{sf} = stemflow coefficient (-)

The potential evaporation from the interception reservoir is given by:

$$E_{i,pot} = C_s E_{wet} \tag{3}$$

where:
$E_{i,pot}$ = potential evaporation from interception reservoir (m d^{-1})
C_s = soil cover (-)
E_{wet} = evaporation of a wet surface (m d^{-1})

An important consideration in the conceptualization for the interception process is the role of time intervals, i.e. the interval with which the data are available. Often the data have the form of a step-function, with 1 day as the integration interval. In that case it is appropriate to use the expression given by Gash (1979) for directly computing the interception evaporation. But if the meteorological data are available at a time scale of 1 hour or less – as they ideally should be – the measurement data can be used in a continuous water balance of the interception reservoir for the time interval of the *surface water* model in the following manner:

$$S_i(t_s) = S_i(t_s - \Delta t_s) + \int_{t_s-\Delta t_s}^{t_s} [P_i(t) - E_i(t)]\,dt \tag{4}$$

where:
t_s = time at end of current surface water time step (d)
$P_i(t)$ = intercepted precipitation intensity at time t (m d^{-1})
$S_i(t_s)$ = water stored in interception reservoir at time t_s (m)
$E_i(t)$ = (actual) evaporation from the interception reservoir (m d^{-1})
Δt_s = time interval of surface water model (d)

In the implementation of the calculation method provisions are made for ensuring that the amount of water in storage does not exceed the maximum capacity S_{ic}. In the final step, the net precipitation is computed with:

$$P_{net}(t_s) = \frac{1}{\Delta t_s} \int_{t_s-\Delta t_s}^{t_s} P_{gross}(t)\,dt - E_i(t_s) - [S_i(t_s) - S_i(t_s - \Delta t_s)]/\Delta t_s \tag{5}$$

2.4 Evapotranspiration

The evapotranspiration is computed using a reference crop evapotranspiration in combination with a 'crop' factor. This method was originally conceived for modelling the evapotranspiration of agricultural crops. But in the course of time it has also been used for natural vegetations. For instance Schouwenaars (1990) calibrated the crop factor for reed vegetation in Dutch bog relicts. For this reason it will not be referred to as the 'crop factor' method, as is commonly done, but simply as the 'vegetation factor' method.

Typically for agricultural crops, the factors are only available for the growing season. When the factors are used in the model, the assumption is made that the factors have been calibrated on the basis of field experiments, involving the *total* evapotranspiration, including that of bare soil. So for the vegetated part of the year no separate calculation of the bare soil evaporation is made. Outside the growing season a special method is used for calculating the evaporation of a bare soil. That does not apply to natural vegetation of course. For these (and for agricultural grassland) it is assumed that a vegetation factor is available all the year round.

The calibration of the vegetation factors (usually) included the interception evaporation. The reason for nevertheless including a separate computation of the interception evaporation in the model is that it can have a significant impact on the actual evapotranspiration that is simulated: the interception evaporation is not subject to the limitations stemming from the soil water pressure head. That limitation was *not* active during the *field* experiments for determining the vegetation factors, because it can be assumed that the conditions were made optimal for growth. But that of course does mean that the *routing* of the precipitation water (directly to the soil, or first through the interception reservoir) should not be taken into account in a *model* that makes use of the vegetation factors. It is important to subtract the interception evaporation from the potential evapotranspiration. Otherwise the model can simulate higher values for the total evapotranspiration than were measured at the experimental sites under optimal conditions.

The followed method makes a clear distinction between the evapotranspiration of the crop and evaporation of the intercepted water. This makes the computed evapotranspiration a better indicator for the growth of crops. But it should be realised that it still contains a substantial term for the bare soil evaporation, which during the growing season is implicitly included in the reference crop evapotranspiration.

2.4.1 Bare soil

The bare soil evaporation is only computed as a separate entity outside the growing season. It is a process involving the very thin upper soil crust layer. When the layer dries out, a self-mulching effect occurs, limiting further loss of moisture. Modelling of the soil water transport at such a detailed scale is beyond the scope of the regional model SIMGRO. Instead, we use the method of Boesten and Stroosnijder (1986).

In the calculation method the sum of the potential evaporation, ΣE_p (m) is used as a time variable:

$$\begin{aligned} \sum E_a &= \sum E_p \qquad \text{for} \qquad \sum E_p \le \beta_2^2 \\ \sum E_a &= \beta_2 \left(\sum E_p \right)^{1/2} \qquad \text{for} \qquad \sum E_p > \beta_2^2 \end{aligned} \tag{6}$$

where β_2 is a soil parameter ($m^{1/2}$), which should be determined experimentally. The default value of $\beta_2 = 0.054$ $m^{1/2}$ and $P_{min} = 0.005$ m d^{-1}. The parameter β_2 determines the length of the potential evaporation period, as well as the slope of the ΣE_a versus $(\Sigma E_p)^{1/2}$ relationship in the soil limiting stage.

The (default) parameters have been derived for application of the method to the daily totals of the meteorological data. So the method is here also applied on a daily basis. The implementation involves several steps. For days with $P_{net} < P_{min}$, the following procedure is used for the updates of ΣE_p. On days of no excess in rainfall ($P_{net} < E_p$), ΣE_p follows from Eq. 6, that is:

$$\left(\sum E_p \right)^j = \left(\sum E_p \right)^{j-1} + \left(E_p - P_{net} \right)^j \tag{7}$$

in which superscript *j* is the day number. $(\Sigma E_a)^j$ is calculated from $(\Sigma E_p)^j$ with Eq. 6 and E_a is calculated with

$$E_a^j = P_{net}^j + \left(\sum E_a \right)^j - \left(\sum E_a \right)^{j-1} \tag{8}$$

On days of excess in rainfall ($P_{net} > E_p$)

$$E_a^j = E_p^j \tag{9}$$

and the excess rainfall is subtracted from ΣE_a

$$\left(\sum E_a \right)^j = \left(\sum E_a \right)^{j-1} - \left(P_{net} - E_p \right)^j \tag{10}$$

The next $(\Sigma E_p)^j$ is calculated from $(\Sigma E_a)^j$ with Eq. 6. If the daily rainfall excess is larger than $(\Sigma E_p)^{j-1}$, then both $(\Sigma E_a)^j$ and $(\Sigma E_p)^j$ are set at zero. That is also done when $P_{net} \ge P_{min}$.

2.4.2 Vegetated soil

The evapotranspiration of a vegetated soil is computed in three steps by:
- computing the reference crop evapotranspiration;
- applying a vegetation factor to obtain the potential evapotranspiration;
- reducing the potential evapotranspiration to the actual evapotranspiration based on the soil moisture content.

For the reference crop evapotranspiration use can be made of the well-known Penman-equation for open water or, as is customary in the Netherlands, the reference crop evapotranspiration according to Makkink. The latter is computed with (e.g. De Bruin, 1987):

$$ET_r = 0.65 \frac{s}{s+\gamma} \frac{K\downarrow}{\lambda} C \tag{11}$$

where:
ET_r = reference crop evapotranspiration according to Makkink (m d^{-1})
λ = latent heat of vaporization of water (J kg^{-1})
C = factor for converting units (m d^{-1}/kg $m^{-2}s^{-1}$)
s = slope of the saturated vapour pressure curve at air temperature (mbar K^{-1})
γ = psychrometer constant (0.66 mbar K^{-1} at MSL)
$K\downarrow$ = global radiation (W m^{-2})

This equation has been calibrated by means of regression analysis. It should be realized that only the summer values were used for this. If the winter values had been included, an intercept term of the regression function would have been required (De Bruin, 1987). So it should be expected that for the winter period the expression has a large relative error. But since the winter evapotranspiration itself is relatively small, the absolute error made by using the Makkink-equation also for the winter period is not very substantial.

At moments that there is evaporation from the interception reservoir, the transpiration can be assumed halted. This fraction of time can be approximated by $E_i/E_{i,pot}$. To account for this the following expression is used for the potential evapotranspiration:

$$ET_{pot} = f\, ET_r \left(1 - \frac{E_i}{E_{i,pot}}\right) \tag{12}$$

where:
ET_r = reference crop evapotranspiration (m d^{-1})
f = vegetation factor (-)
ET_{pot} = potential evapotranspiration (m d^{-1})
E_i = (actual) interception evaporation (m d^{-1})
$E_{i,pot}$ = potential interception evaporation (m d^{-1})

In the above equation the correction for the interception evaporation is *time*-based (using $E_i/E_{i,pot}$) instead of energy-based as in Penman-Monteith (see Rijtema (1965) and Kroes and Van Dam (2003)). We use a time-based correction factor because the Makkink-method is essentially a regression method and not an energy-balance method. The result given in Eq. 12 is not equivalent to the transpiration, because (implicitly) soil evaporation is included in the vegetation factors themselves.

For taking into account the effect of limiting soil moisture conditions on the evapotranspiration the function defined by Feddes et al. (1978) is used (Figure 5):

$$ET_{act} = \alpha_E \, ET_{pot} \tag{13}$$

where:
ET_{act} = actual evapotranspiration (m d^{-1})
ET_{pot} = potential evapotranspiration (m d^{-1})
α_E = soil moisture reduction factor (-)

Water uptake by roots is zero when the soil water pressure head p is below p_4 (Figure 5), which is assumed to be the wilting point. Soil water pressure head p_3 is called the reduction point. In between the wilting point and the reduction point the evapotranspiration rate is linearly reduced. The reduction point depends on the potential evapotranspiration (see E_{low} and E_{high}). Between pressure heads p_2 and p_3 the evapotranspiration is at its maximum ('potential'). As a result of oxygen deficiency in the root zone, water uptake is hampered for some crops between p_2 and p_1.

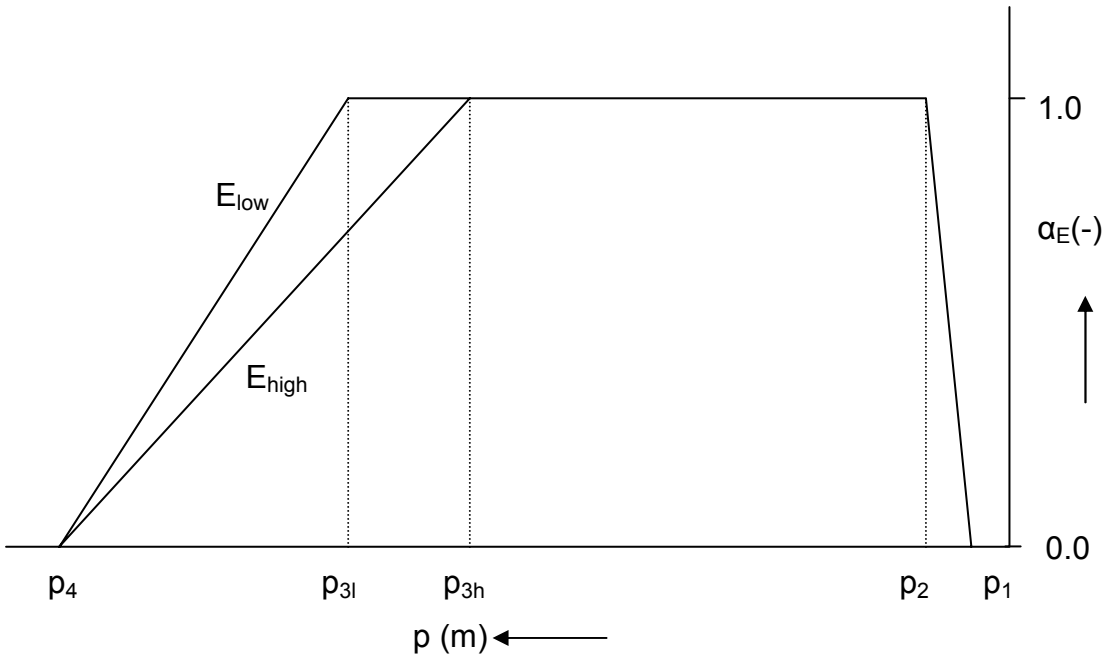

Figure 5 Reduction coefficient for root water uptake, α_E, as a function of soil water pressure head p and potential transpiration rate E_{pot} (see E_{high} and E_{low}) (after Feddes et al., 1978)

2.4.3 Inundated area and surface water

For the inundated area the actual evaporation is computed from the reference crop evapotranspiration multiplied by a factor that not necessarily is equal to the factor commonly used for open water (which is 1.0 for Penman). If the inundation occurs when the surface is vegetated, it is more likely that due to the wind-shade effect the evaporation is not higher than that of grass.

2.4.4 Urban area

Urban areas are considered to be partly vegetated and partly paved. The paved parts of urban areas are considered to have a zero evapotranspiration. The water management of urban area is described in §6.2.1.

2.4.5 Total evapotranspiration

The total evapotranspiration is computed by multiplying the fractional areas by the respective evapotranspiration rates and totalizing:

$$ET_{act,tot} = (1 - a_{in})[C_s ET_{act,veg} + (1 - C_s) E_{bs}] + a_{in} f_{in} ET_r \quad (14)$$

where:
$ET_{act,tot}$ = actual evapotranspiration (m d^{-1})
a_{in} = fraction of area that has become inundated (-)
C_s = soil cover by vegetation (-)
$ET_{act,veg}$ = actual evapotranspiration of vegetation (m d^{-1})
E_{bs} = evaporation of a bare soil (m d^{-1})
f_{in} = 'vegetation factor' of inundation water /surface water (m d^{-1})

This computation does *not* include the interception evaporation, because in the rest of the model we use the *net* precipitation instead of the gross precipitation.

Since the factor method assumes that the bare soil evapotranspiration has been calibrated as part of the total crop evapotranspiration, the value of the soil cover in Eq. 14 is taken to be 1.0 in the part of the year for which a vegetation factor is available, and 0.0 for the remaining part.

2.5 Data summary

For the simulation period, the time series information of the meteorological conditions should be available in the form of a step-function (usually per day, but also shorter intervals can be handled) of:
- precipitation;
- reference crop evapotranspiration.

These data can be supplied for one than one gauging station in the region. In that case the relevant station should be specified for each of the nodal subdomains of the soil water /groundwater model.

A number of land-use types and their fractional areas can be specified per nodal subdomain. But in the current practice usual only one type is given, in view of the relatively small nodal areas. For the calculation of plant-atmosphere relations, four main categories of land use have been defined:
- agricultural areas and natural grasslands;
- forests;
- urban areas;
- surface waters (lakes, ponds);

Within these main categories any number of specific land-use types can be defined. The differentiation should take into account the differences in evapotranspiration, rooting depths and irrigation demands of agriculture for sprinkling.

Two categories of urban areas are distinguished: impermeable surfaces (e.g. homes, streets) and permeable surfaces (gardens, playgrounds, parks etc., §6.2.2).

It is crucial that the vegetation factors supplied in a file are consistent with the chosen method for computing the reference crop evapotranspiration. For agricultural crops in combination with the Makkink reference evapotranspiration use can be made of the factors supplied by Feddes (1987).

The function defined by Feddes et al. (1978) for the effect of limiting soil moisture conditions has to be available for the different crops/ vegetations.

The parameters of the interception reservoir should be given, for each type of vegetated land use.

3 Soil water

3.1 Introduction

Soil water is here defined to include small pools that have come into existence by the limiting capacity of infiltration into the soil. But when the soil column becomes fully saturated, we prefer to consider water on the soil surface as 'visible' groundwater, and treat it accordingly. The soil water dynamics are described using a series of three control boxes: for the root zone, the shallow subsoil and the deep subsoil (Figure 6). The root zone is handled with a separate box because the presence of plant roots is a very dominating influence, leading to moisture patterns that strongly deviate from that of the subsoil. Shallow water tables strongly influence the soil water. That does not only concern the moisture content itself, but also the process of capillary rise reaching the bottom of the root zone. The moisture supply of plants through capillary rise can make

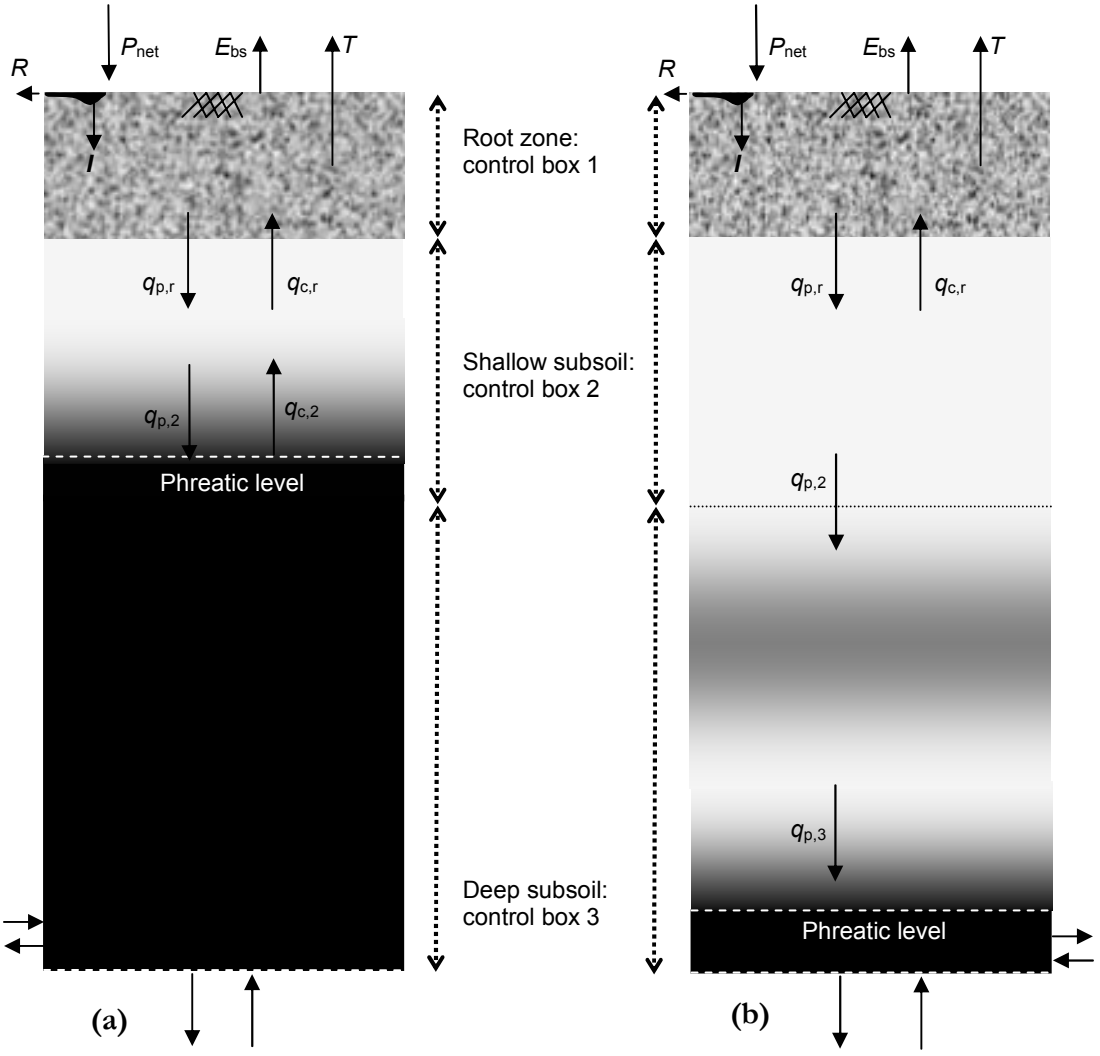

Figure 6 Conceptualization of the soil water system: a) showing a situation with the water table in the shallow subsoil b) showing a situation with the water table in the deep subsoil. Explanation of symbols: P_{net} – net precipitation; I – infiltration; R - surface runoff; E_{bs} – evaporation of bare soil; T – transpiration; q_p – percolation; q_c – capillary rise.

all the difference for surviving a dry period. These influences of the shallow groundwater justify a separate control box in the modelling. The box reaches down to the lowest level from where capillary rise can reach the root zone; so its extent depends on the type of crop (depth of root zone) and type of soil. Very deep water tables are a different matter altogether, justifying a third control box.

In the soil water submodel the flow is assumed in the vertical direction only. As can be seen the boxes extend *into* the groundwater. This reflects the dual identity of the water just below the unsaturated zone. In fact, the distinction between soil water and groundwater is not sharply defined: correct handling of the dual identity thus requires a unified approach for the modelling.

3.2 Theory

3.2.1 Surface runoff

Surface runoff occurs when for some reason the precipitation can not infiltrate quickly enough into the soil, or even can not infiltrate at all. The latter is the case in paved urban areas, but also in situations with a fully saturated soil profile. In these extreme cases all of the rainfall remains on the soil surface, where it gathers in pools that can start to overflow if the rain persists for a long enough period of time. But only when it finds its way to the surface water system does it actually become runoff. Intermediate situations with a semi-permeable ground surface can involve runoff from one spot to another, where it can after all infiltrate from a shallow pool. If the rain continues for long enough, the infiltration capacity can become limiting due to a decreasing vertical gradient of the soil water potential, thus generating runoff after all. Surface runoff is a very complex process that depends on:

- intensity and duration of the rainfall;
- vegetation cover;
- soil physical properties;
- meso- and micro-scale ground surface variations;
- density, geometry and hierarchical structure of the surface water system;
- soil water conditions and groundwater level.

In the conceptualization of the runoff process a distinction is made between:

- runoff that is generated due to a limiting infiltration capacity of the soil surface itself (i.e. the soil physical properties and conditions);
- runoff that is generated due to the full saturation of the soil column.

In the latter case there is a 'fusion' of water in the depression storage and the 'visible' groundwater in the low-lying parts. This fusion of water storages is important for making accurate simulations of shallow groundwater processes.

Since the modelling approach is very much based on the use of empirical functions we describe it in §3.3.1

3.2.2 Unsaturated flow

A unified three-dimensional modelling of saturated-unsaturated flow in the subsoil is of course the ideal. But for application at catchment-scale that is not practical. The first simplification is by assuming vertical flow, leading to the Richards' equation (Richards, 1931):

$$\frac{\partial \theta}{\partial t} = C(p)\frac{\partial p}{\partial t} = \frac{\partial}{\partial z}\left[K(p)\left(\frac{\partial p}{\partial z} + 1\right)\right] - S_a(p) \qquad (15)$$

where:
θ = soil water content (-)
p = pressure head (m)
$K(p)$ = unsaturated conductivity (m d^{-1})
$C(p)$ = differential water capacity ($\partial\theta/\partial p$) ($m^{-1}$)
$S_a(p)$ = sink term (d^{-1})

Even this one-dimensional equation is computationally demanding due to the very non-linear soil hydraulic functions. Its use leads to a model that can only be applied on a relatively small scale or for a subregion of special interest.

Here we follow a simplified 'metamodelling' approach that uses three storage elements, defined by the three 'control boxes' given in Figure 6:
- control box 1 for simulating the water balance of the root zone;
- control box 2 for simulating the soil water dynamics in the shallow subsoil;
- control box 3 for simulating the soil water dynamics in the deep subsoil.

The first two control boxes are tightly coupled in the model; thus for shallow water tables a (semi-)unified approach is followed. The coupling between the shallow and deep subsoil is less tight: capillary rise is assumed non-existent in the deepest compartment. The current concept does not include bypass flow and hysteresis. The non-steady dynamics of a wetting front can lead to a retardation of the infiltration compared to the steady-state profiles. These aspects will be added in the near future.

Since the dynamics in the root zone and the shallow subsoil are closely interlinked, we describe them together in the subsequent section. Then follows the modelling for the deep subsoil.

3.2.2.1 Root zone and shallow subsoil

The dynamics of the soil water are treated as a stream of transitions between steady-state situations, called the 'quasi' or 'pseudo' steady-state approach. For describing the flow the non-steady term in Eq. 15 is set to zero:

$$\frac{\partial \theta}{\partial t} = 0 = \frac{\partial}{\partial z}\left[K(p)\left(\frac{\partial p}{\partial z} + 1 \right) \right] - S_a(p) \tag{16}$$

In control box 2 the sink term is not present. The (constant) moisture flux q_m (sign convention 'upward positive') is then given by the Darcy equation:

$$q_m = -K(p)\left(\frac{\partial p}{\partial z} + 1 \right) \tag{17}$$

Solutions to Eq. 17 can be found by numerical integration. More practical is the use of a transient model like SWAP (Kroes and Van Dam (eds.), 2003) and letting the steady state be reached for a given top-boundary condition in the form of evapotranspiration or precipitation, and a bottom boundary condition in the form of a fixed groundwater level. A sequence of model runs yields a family of curves that is specific for a certain soil type and root zone depth. A few examples for a root zone thickness of 0.5 m are given in Figure 7.

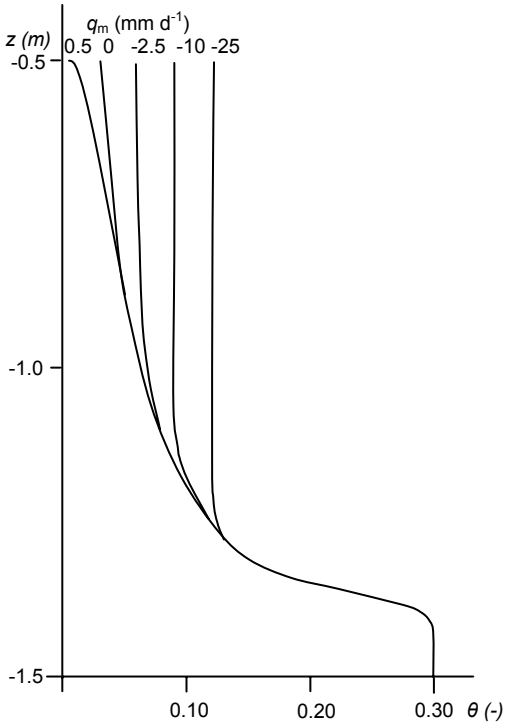

Figure 7 Examples of soil water profiles for steady state percolation/capillary rise (Van der Molen, 1972), generated for a root zone depth of 0.5 m; the moisture flux is taken as positive for upward flow

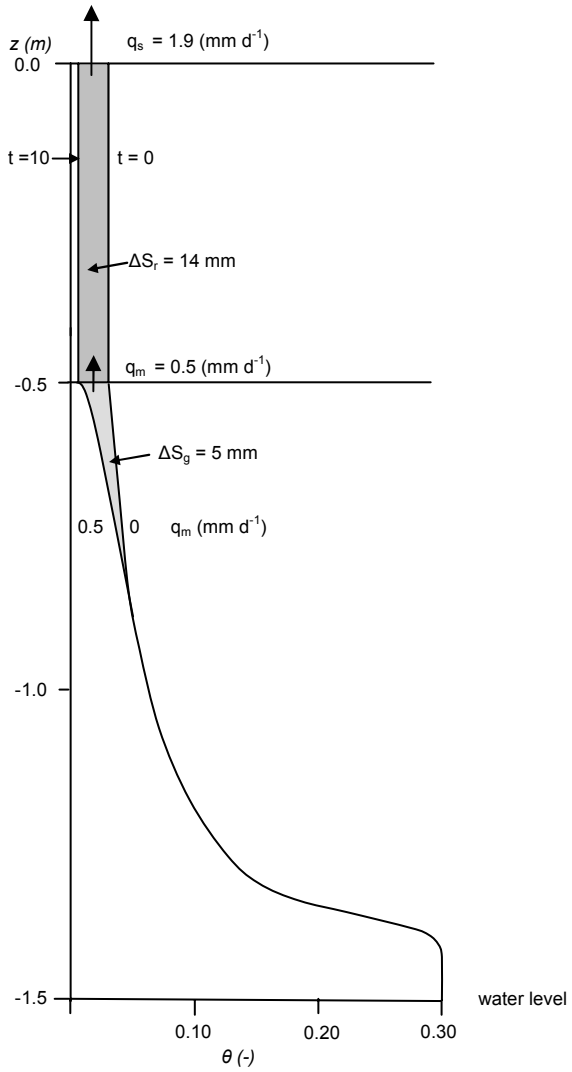

*Figure 8 Illustration of the method of Rijtema (1971) / De Laat (1980): starting from the equilibrium soil moisture profile at t=0 the soil dries out in such a manner that the total moisture extraction during a 10-day period (10*1.9=19 mm) equals the release of water from storage in the root zone (14 mm) and the capillary rise (10*0.5 = 5 mm) from the subsoil*

In the past there has been a development in the use of steady-state profiles for dynamic soil moisture modelling, see Wesseling (1957), Feitsma (1969), Rijtema (1971) and De Laat (1980). A simplified example of the Rijtema method is shown in Figure 8. Starting from the equilibrium profile at t=0 a capillary rise of 0.5 mm d^{-1} is assumed available as long as the soil water pressure head has not dropped below the value obtained from solving Eq. 17. As can easily be verified the final state at the end of the 10-day time step has been computed in such a manner that the total extraction of 19 mm at the top boundary can be made available by the release of water extraction in the root zone (14 mm) and the capillary rise from the subsoil (0.5 mm d^{-1} * 10 d = 5 mm; for the purpose of giving a simplified example we for the moment leave the flux density from the water table out of consideration, though the mentioned references of course do also take this flux into account).

De Laat (1980) computerized the Rijtema method and extended it for handling the transitions from capillary rise profiles to percolation profiles. But for achieving the latter,

various amendments had to be made, making the method relatively complex. This complexity stems from the chosen starting point in the conceptualization, i.e. that the soil moisture pressure head at the *bottom of the root zone compartment* should at all times remain equal to the head at the *top of the subsoil*. As such that seems to be an obvious choice, because it simply follows from 'sound physics'. So it does not appear to be a choice at all. However, it is inevitable that the quasi steady-state method at some point makes concessions with respect to the reality of non-steady flow. Due to the complexity of the procedure given by De Laat (1980), these concessions become less obvious, but they are there all the same. Not that it disqualifies the method: the *results* are what count, and the method has been shown to have a wide range of applicability. Nevertheless we prefer an alternative method. The main justification is the relative simplicity that we have achieved in the coupling to the saturated flow module. The coupling method of De Laat requires an iterative procedure involving an implicit non-linear expression, whereas the current approach is much more straightforward, without loss of accuracy.

In the model formulation given here we use the following state variables:
- the mean pressure head and water content in the root zone (control box 1), p_r and θ_r;
- the pressure head and water content at the top of the subsoil (box 2), p_2 and θ_2;
- the groundwater level h.

In contrast to the approach of De Laat (1980) and others, we do *not* under all conditions force the equality between the pressure head at the bottom of the root zone and the pressure head at the top of the subsoil. Especially in situations following heavy precipitation we accept that there (temporarily) can be a large discontinuity in the pressure head profile at the interface between the root zone and the subsoil. An example of such a situation is given in Figure 9, where precipitation has caused a sudden increase of the root zone water content. In a schematized way, this kind of profile bears a resemblance to the non-steady-state profiles found in the field after rainfall on a dry soil.

Like is done by De Laat we assume that the infiltrated rainfall is instantaneously spread throughout the root zone. Especially with thick root zones that is of course a very schematic assumption. For situations with the soil drying out the assumption is better justified. It is then based on the notion that the plant roots develop a certain (negative) pressure head, depending on the needs of the situation. All water having a higher pressure head is then removed, assuming that the roots are omnipresent in the root zone. Also the redistribution of moisture due to the local soil water gradients plays a role in creating a near-uniform moisture distribution.

The discontinuity of the pressure head at the boundary between root zone and subsoil raises the question of how to compute the percolation/capillary rise flux. We assume that (Figure 9):
- the moisture flux density at the boundary between the root zone ($q_{m,r}$) and subsoil is totally determined by the mean pressure head in the root zone (p_r) and the groundwater level (h);
- the moisture flux to the water table ($q_{m,2}$) is determined by the pressure head at the top of the subsoil (p_2) and the water level (h).

So the pressure head at the top of the subsoil is *not* used here for computing the interaction with the root zone. That avoids the 'locking up' of the model, especially in transition situations with high precipitation on a dried out subsoil. The main further justification for this *heuristic* computational rule is that the *convergence* is correct. In the given example (of Figure 9, assuming a fixed groundwater level) the converged profile is given

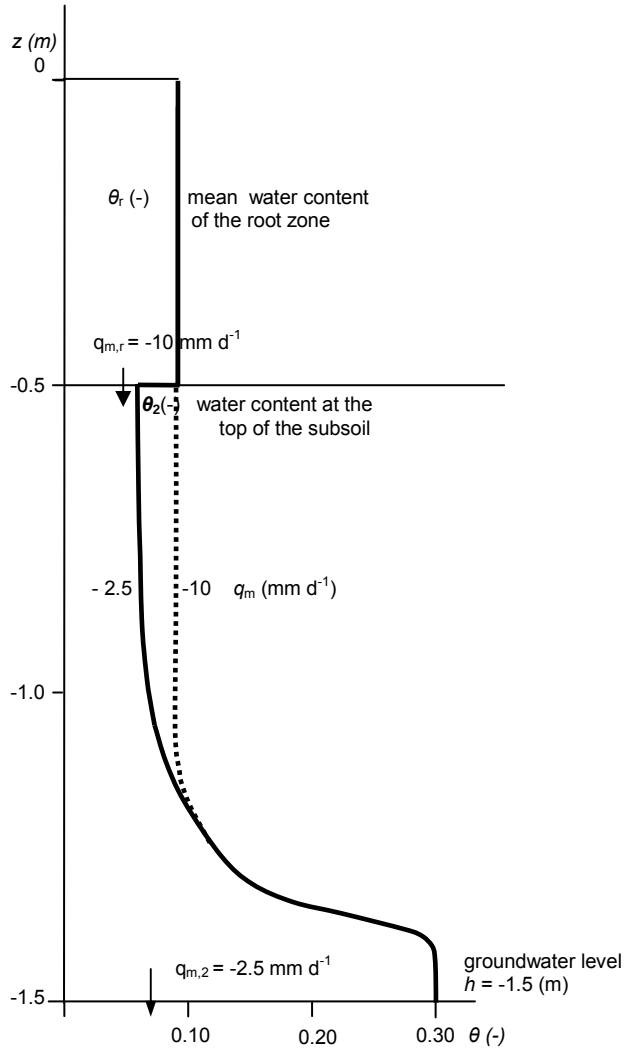

Figure 9 Schematizations of the soil water metamodel. The moisture flux $q_{m,r}$ at the boundary between the root zone and the subsoil is determined by the mean root zone water content θ_r (or pressure head p_r) and the groundwater level h. The moisture flux $q_{m,2}$ to the water table is determined by the moisture content θ_2 (or pressure head p_2) at the top of the subsoil and the groundwater level h

by the dotted line, which is reached when the moisture flux to the water table ($q_{m,2}$) has become equal to the inflow rate from the root zone($q_{m,r}$). The above consideration only applies in situations with percolation. In situations with the soil slowly drying out we revert to the Rijtema-method, which assumes a sequence of steady-state profiles with no discontinuity of the pressure head at the bottom of the root zone.

As stated above, the main advantage of the current approach is the simplicity of the coupling to the saturated flow module. This coupling consists of two elements:

- the 'stress' at the top of the system, in the form a net inflow (+/-) to the root zone;
- a piece-wise linear storage function of the groundwater level; the coefficients of the function itself are updated at each time step, according to the prevailing conditions in the unsaturated zone.

No iteration is needed between the unsaturated flow module and the saturated module (cf. the Newton iterative procedure in the scheme of De Laat (1980, p. 76)). Details are given in §3.3.2, including a verification of the results with SWAP.

3.2.2.2 Deep subsoil

The above given approach is only justifiable for situations with shallow water tables to about 3 m below soil surface. For deeper water tables the dynamics become more complex, involving 'waves' of percolation water. In literature (e.g. Childs, 1936) many examples are known of describing such waves with a diffusion-type equation; in its most simplified form the equation is taken as linear, as is done here. But given the very nonlinear nature of flow in the unsaturated we refrain from giving a derivation from the Richards' equation as a starting point. Instead we 'borrow' a diffusion-type equation for describing the response to a unit step-input starting at t=0, for the percolation from control box 2 to box 3 (Figure 6). The input is given by:

$$q_{p,2}(0,0) = 0; \quad q_{p,2}(0,t) = 1 \tag{18}$$

and we assume that the response at the bottom of control box 3 can be described by:

$$q_{p,3}(z_*,t) = 1 \cdot \tfrac{1}{2}\,\mathrm{erfc}\left(\frac{z_* - At}{2\sqrt{Dt}}\right) = 1 \cdot \mathrm{S}(z_*,t) \tag{19}$$

where

$q_{p,3}(z_*,t)$ = percolation that arrives at the deep water table in control box 3 (m d^{-1});
z_* = depth to the water table measured from the bottom of control box 2 (m);
A = 'wave celerity' (m d^{-1});
D = diffusivity (m^2 d^{-1});
'1' = unit step input (m d^{-1});
$\mathrm{S}(z_*,t)$ = dimensionless function known as the S-curve (-) .

We assume that the response given by Eq. 19 does not differ in time; thus it represents a 'linear time invariant system'. Solutions can then be combined by means of simple superimposition techniques. A highly efficient way of doing that is by employing the unit hydrograph method, as for instance described by Dooge (1959). We now define a unit block input of duration T and intensity $1/T$ by:

$$q_{p,2}(0,0) = 0; \quad q_{p,2}(0,t) = 1/T, \text{ for } 0 < t \le T; \quad q_{p,2}(0,t) = 0, \text{ for } t > T \tag{20}$$

Because Eq. 19 describes a linear time invariant system, the response to the unit block input can be obtained by superimposition. That is done by subtracting two S-curves multiplied by the input intensity (1/T), the one starting at t=0, and the other at $t = T$:

$$u(z_*,T,t) = \frac{1}{T}[\mathrm{S}(z_*,t) - \mathrm{S}(z_*,t-T)], \quad \text{for } t \ge T \tag{21}$$

where $u(z_*,T,t)$ is the so-called T-day unit hydrograph (d^{-1}), also called the pulse response. For $t<T$ the term with $(t-T)$ is omitted.

Eq. 19 is of course a gross simplification of reality. Parameters A and D can only be determined by some form of calibration, yielding 'effective' values. Two examples of the pulse responses are given in Figure 10. It should be kept in mind that accuracy in predicting the dynamics of deep water tables is usually not critical for the performance of the model as a whole. That is because the deep water tables do not make contact with the

local drainage system, and neither is there any ecological function directly dependent on them. The influence on the rest of the region takes place through feeding the regional groundwater flow, which has a long characteristic time. Thus errors in the exact timing of the recharge to the groundwater can be relatively large before there are serious consequences for the performance of the model as a whole.

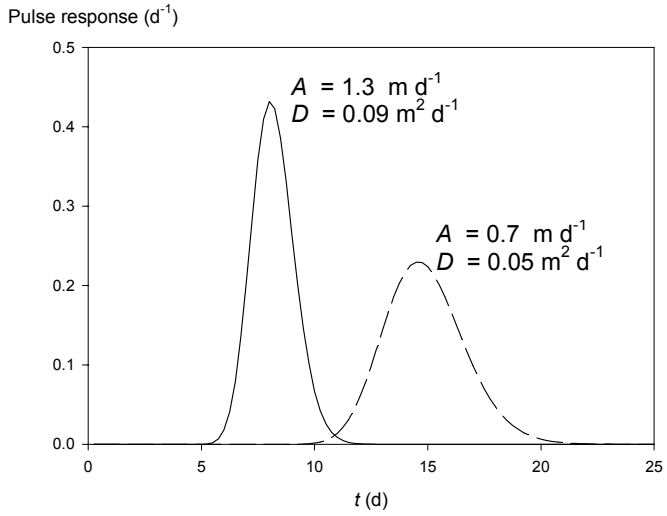

Figure 10 Examples of a unit pulse responses to a unit block input lasting 1 day, for a water-table depth of 10 m below the bottom of control box 2 (cf. Figure 6)

3.3 Model implementation

3.3.1 Surface runoff

Surface runoff is calculated at nodal subdomain level. That implies a certain degree of 'lumping'. A continuing water balance is made of water held in the depression storage (Figure 6). The time step of the *surface water* model is used because surface runoff is a 'fast' process:

$$S_s(t) = S_s(t - \Delta t_s) + [P_{net}(t) - I(t) - R(t)]\,\Delta t_s \qquad (22)$$

where:
$S_s(t)$ = amount of water stored in depression storage reservoir (m)
$P_{net}(t)$ = net precipitation (m d^{-1})
$I(t)$ = infiltration rate from depression reservoir (m d^{-1})
$R(t)$ = runoff rate from depression reservoir (m d^{-1})
Δt_s = time interval of surface water submodel (d)

Infiltration can of course only occur if there is water available in the form of net precipitation and/or water stored from the preceding period. The maximum infiltration rate $I_{max,i}$ is a function of the soil properties. But infiltration can be blocked due to a bottleneck further down in the system, i.e. the amount of storage capacity still available in the root zone and the percolation rate from the root zone to the groundwater.

Water held in the depression reservoir in excess of the 'dead' storage capacity can become runoff. The flow rate is assumed to linearly depend on the amount of water stored above the reservoir threshold:

$$R(t) = [S_s(t) - S_{sd}]/\gamma_s, \quad \text{for } S_s(t) \geq S_{sd} \qquad (23)$$

where:
S_{sd} = 'dead' part (maximum) of depression storage reservoir (m)
γ_s = flow resistance of surface runoff (d)

Surface runoff can be become (partly) obstructed by the surface water level in the ditches In that case the amount of 'dead' storage increases.

The infiltration rate of a non-paved soil is computed at the time step of the soil water model. But the runoff itself is computed at the time step of the surface water system, because it is a fast process. In order to make the most of the available information, the chosen time step of the surface water system should not be larger than that of the meteorological data. By using the surface water time step the numerical integration of Eq. 23 can be done using an explicit evaluation of the runoff $R(t)$, without much loss of accuracy.

Implementation of Eqs. 22 and 23 is done in a number of steps. First a check is made to see if there is a bottleneck in the soil-groundwater system for actually absorbing the water during the time interval of the soil water model. The maximum rate that can be absorbed is given by:

$$I_{\max,s} = [S_{rs} - S_r(t_g - \Delta t_g)] / \Delta t_g + q_{p,r}(t_g) \quad (24)$$

where:
$I_{max,s}$ = maximum infiltration rate that the soil can absorb (m d^{-1})
S_{rs} = saturated water content of root zone (m)
$S_r(t_g)$ = water content of root zone (m)
Δt_g = time step of soil water/ groundwater submodels (d)
$q_{p,r}(t_g)$ = percolation rate from the root zone to the groundwater (m d^{-1})

The maximum infiltration rate is computed as:

$$I_{\max} = \min(I_{\max,i}; I_{\max,s}) \quad (25)$$

This value remains the same for the surface water time steps within the groundwater time step. For each time step of the surface water model the following procedure is followed:
- evaluation of $R(t)$ using Eq. 23;
- evaluation of the new storage $S_s(t)$ using Eq. 22;
- if $S_s(t)$ is found to be <0, then
  - first see if the balance can be made square at zero by reducing the runoff;
  - if that (partly) fails, then reduce the infiltration rate so that the new $S_s(t)$ becomes zero after all.
- adding of $R(t)\Delta t_s$ to the integrated runoff flux $R(t_g)$.

So in the case of the depression storage falling dry, the infiltration has priority over the runoff. Since this procedure is applied at the small time step of the surface water system, the error made by this (arbitrary) prioritization is negligible.

In the case that the soil becomes fully saturated, the amount of water in the depression storage reservoir is added to the groundwater, and the runoff is routed though the groundwater module as 'gulley' drainage. But that can only be done for the *new* time step of the soil water/groundwater model. So the above algorithm is still used after conditions become fully saturated at some point in time during the surface water time steps within the current groundwater time step. The gulley drainage-resistance for full inundation conditions is equal to the resistance for surface runoff; thus no discontinuities occur in the runoff computation due to the rerouting of the water in the depression reservoir. The depression storage reservoir is activated again as soon as the soil water content falls below the saturated value. Then a starting value of zero is given to this storage, even though the groundwater model signals that part of the area of a nodal subdomain is inundated in its relatively low-lying parts.

3.3.2 Unsaturated flow

3.3.2.1 Schematization

The unsaturated zone is modelled at the nodal subdomain level, with per soil column the three control boxes given in Figure 6. For each nodal subdomain the dominant soil physical unit should be determined: the model assumes that the soil physical properties are uniform in the horizontal sense (but can of course be heterogeneous within a vertical column). Root zone depths are assumed to not vary in time. The depth can be specified per nodal subdomain for each combination of land use and soil physical unit. Various types of land use and root zone depths may exist within a single subdomain. Their exact locations are not included in the input files: only the relative surface areas that they occupy are known. However, in the current modelling practice the nodal subdomains are at field scale, so usually only one type of land use is specified. The used time step is the same as that of the groundwater model, Δt_g.

As stated in the introduction (§3.1) we model water on the soil surface as 'visible' groundwater. This requires taking an extra storage term into account.

3.3.2.2 Soil physical metafunctions

The soil physical parameters are not used in a direct way. In the pre-processing stage they are converted to metafunctions for the capillary rise /percolation flux density and the storage in the shallow subsoil. These functions are derived by making a series of simulations with a transient model like SWAP (Kroes and Van Dam (eds.), 2003). The runs must be long enough for the steady state to be reached. The use of a steady-state model is an alternative, but experience has shown that to be less practical. By using the same (transient) model for deriving the metafunctions and for verifying the metamodel simulations, consistency in the handling of the nonlinear soil-hydraulic functions is ensured.

For each soil physical schematization a series of calculations are done in which the following conditions are varied:

- the root zone depth d_r for 0.10 m, 0.20 m, and so on, for all of the root-zone depths in the land-use schematization;
- the phreatic level h in steps of 0.10 m, down to the bottom of control box 2;
- the flux density at the top of the soil column in steps of 0.5 mm d^{-1} for the precipitation and 0.05 mm d^{-1} for the potential evapotranspiration.

The latter requires some explanation. The goal of the computational experiments is to derive functions that cover the full range of (steady-state) conditions that can occur in a soil column, including the root zone. That makes it logical to vary the boundary condition at the *soil surface*, and not at the bottom of the root zone. The maximum precipitation should be high enough to generate surface runoff, thus ensuring that the situation with maximum percolation is covered. The highest evapotranspiration rate should equal the highest possible value of the potential evapotranspiration (of forest). The root water uptake reduction function given by Figure 5 then plays a role in the determining the steady state that is reached.

From the series of computational experiments the following tabular functions are derived for each soil physical schematization:

- $s_{r,u}(d_r,p_r,h)$ = total storage of water in the root zone (control box 1), as a function of the root zone thickness d_r , the mean root zone pressure head p_r and the groundwater level h (storage in $m^3\ m^{-2} = m$);
- $s_2(d_r,p_2,h)$ = total storage of water in the shallow subsoil (control box 2) as a function of the pressure head at the top of the subsoil p_2 and the groundwater level h (m)
- $q_{m,r}(d_r,p_r,h)$ = moisture flux density from the root zone to the shallow subsoil (m d^{-1})
- $q_{m,2}(d_r,p_2,h)$ = moisture flux density from the shallow subsoil to the water table(m d^{-1})

The moisture flux functions of course pertain to the same flux, because the model is built on the use of steady-state profiles. So in fact there is only *one* function in the computer code. But for the sake of convenience we use separate notations, involving different independent variables. For the root zone we use the mean pressure head because we can then directly apply the root water uptake function given in Figure 5. In most notations we leave out the d_r-variable, for the purpose of being concise. Likewise we leave out the dependency on the soil physical unit.

An example of a root zone storage function for a loamy soil is given in Figure 11. As can be expected, the storage is nearly completely determined by the mean pressure head in

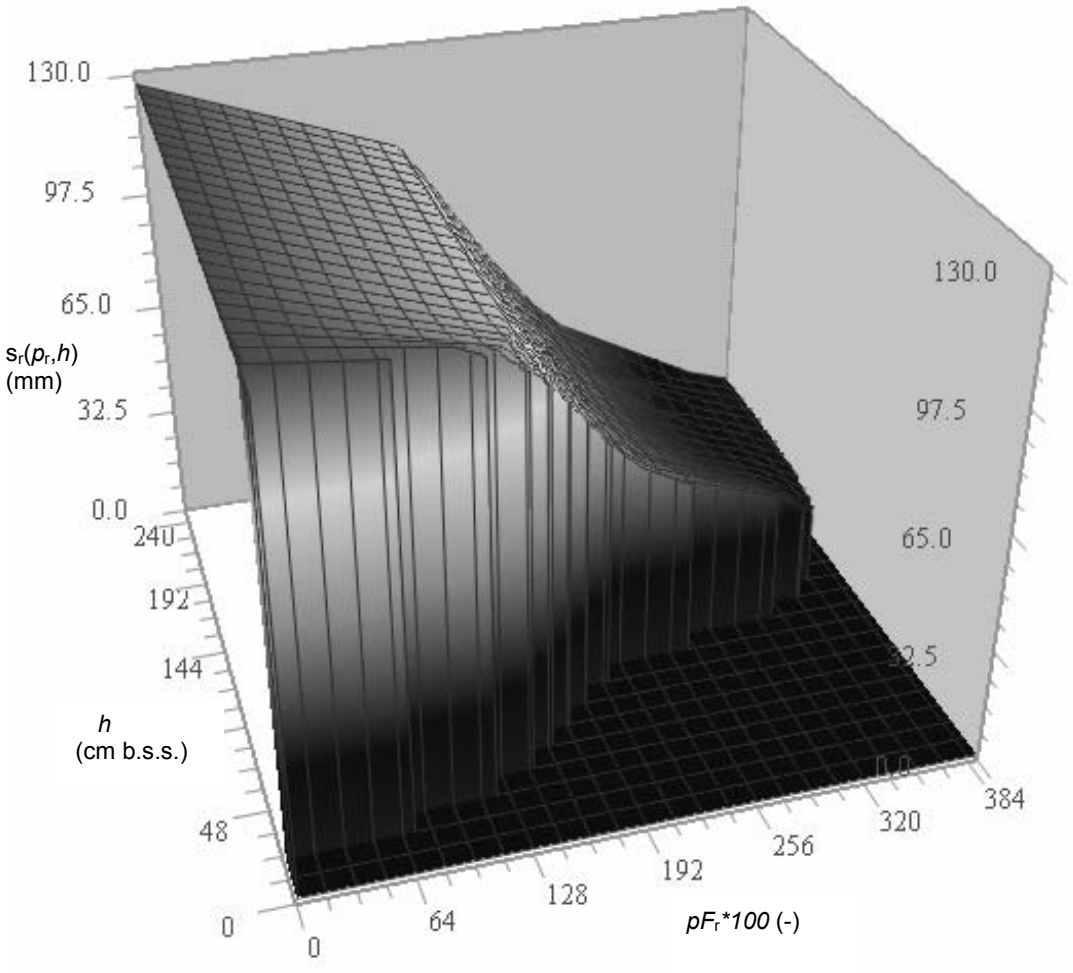

Figure 11 Example of a root zone storage function $s_r(p_r,h)$ for a loamy soil and a root zone depth of 0.30 m. Explanation of symbols – pFr = pF of root zone; h = groundwater level (cm b.s.s.)

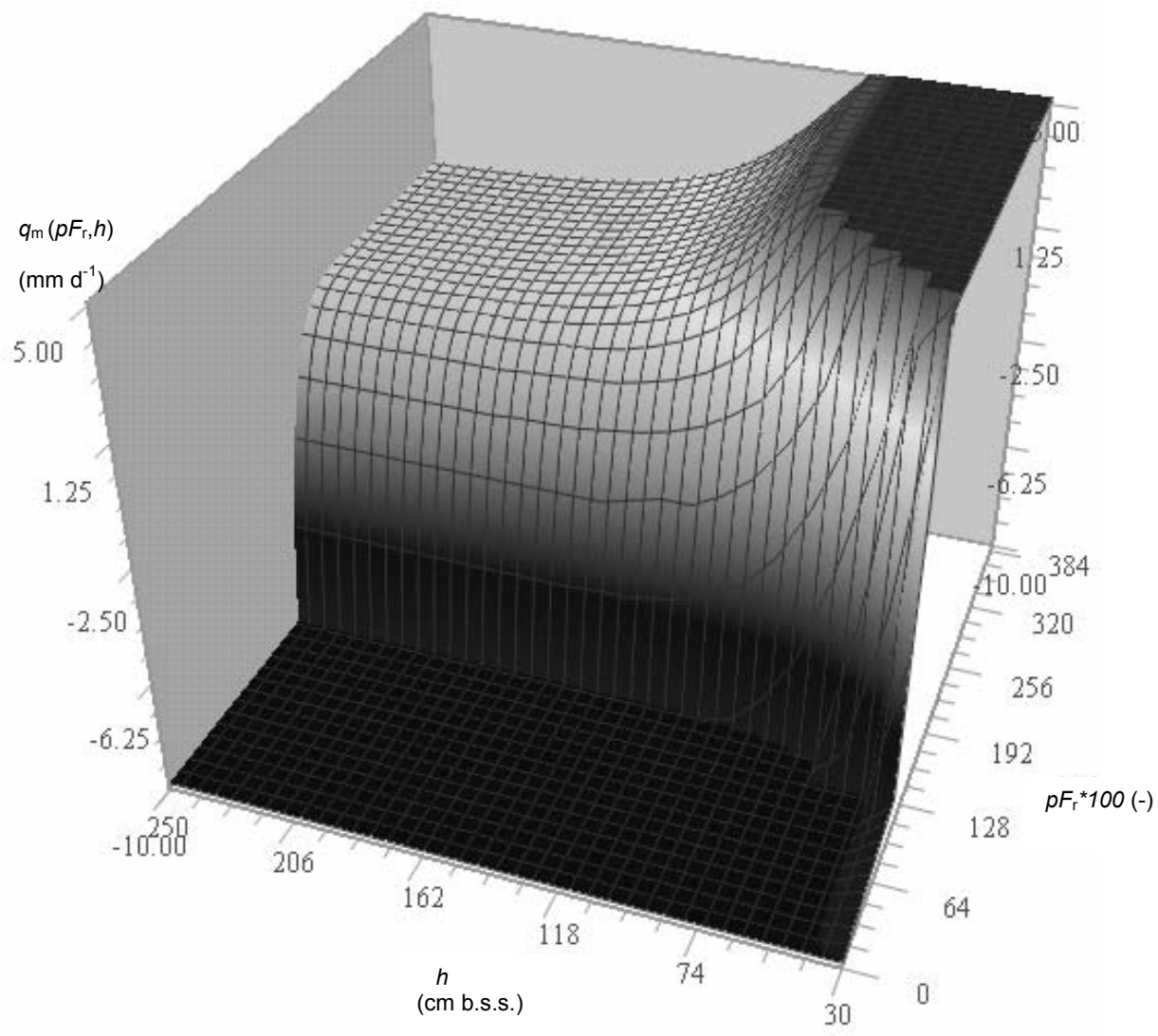

Figure 12 Example of a moisture flux function obtained from computational experiments with SWAP for a loamy soil. Explanation of symbols – pFr = pF of root zone; h = groundwater level (cm b.s.s.)

the root zone; the influence of the groundwater is only felt at extremely high levels. An example of a moisture flux function is given in Figure 12. In the example the flux densities range from +5 mm d^{-1} (capillary rise) to -10 mm d^{-1} (percolation).

When the groundwater level starts to approach the mean soil surface elevation, the nodal subdomain will start to become inundated: first the lower parts become submerged, then the higher ones. In the model this water is treated as 'visible' groundwater. It is essential that the inundation water in this way makes contact with the groundwater; otherwise the interaction between the head of the inundation water and that of the groundwater can not be modelled. The further assumption is made that – when the inundation starts to take place – the water level does not have a horizontal gradient within a nodal sub-domain. Then it is possible to derive the storage function of the inundated water through the cumulative frequency distribution of the soil surface. That distribution is determined for each nodal subdomain. The storage function of the inundated areas is then given by:

$$s_{DTM}(h) = \int_{-\infty}^{h} F_i(y)dy \qquad (26)$$

where:
$s_{DTM}(h)$ = function for the amount of water stored on the soil surface (m)
$F_i(h)$ = fraction of area that is inundated at a certain mean groundwater level h (-)

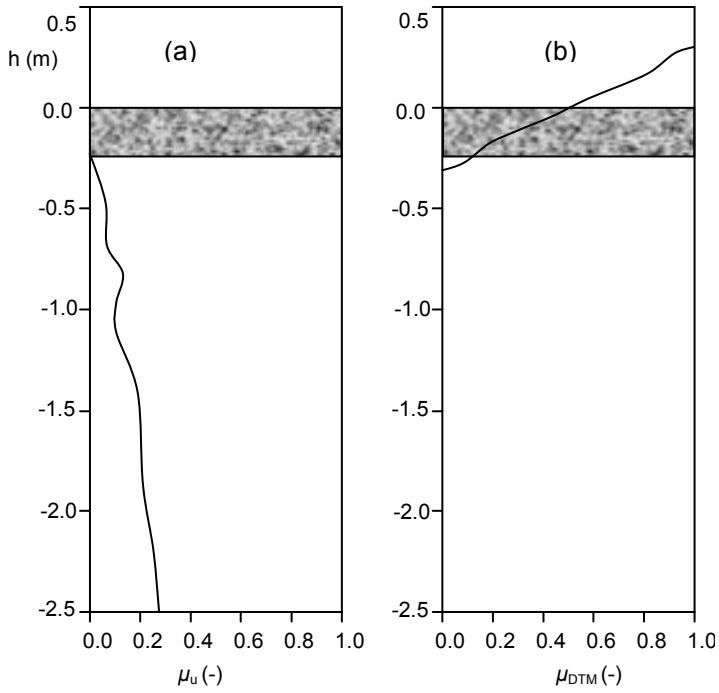

Figure 13 Storage coefficient of shallow groundwater (control box 2) for a certain pressure head in the root zone (a); storage coefficient of water stored on the soil surface (b), for a situation with a varying level of the soil surface within a nodal subdomain

This function is then added to the root zone storage function derived from the SWAP-experiments, to yield the aggregated storage function for the root zone in control box 1:

$$s_r(p_r, h) = s_{r,u}(p_r, h) + s_{DTM}(h) \qquad (27)$$

The storage function of shallow subsoil can be converted to a function for the storage *coefficient* by differentiating with respect to the groundwater level:

$$\mu = \frac{\partial}{\partial h} s_2(p_2, h) \qquad (28)$$

This conversion is useful in the solution scheme for the groundwater model. An example is given Figure 13.

For control box 3 the storage function $s_3(h)$ is derived from equilibrium soil water profiles.

3.3.2.3 Root zone and shallow subsoil

Overview of solution scheme

The update of soil water in the shallow subsoil involves three state variables:

- the mean pressure head and water content in the root zone (control box 1), p_r and θ_r;
- the pressure head and water content at the top of the subsoil (box 2), p_2 and θ_2;
- the groundwater level h.

The groundwater level is of course only involved in this part of the solution scheme if it starts within control box 2. (The scheme for when it starts in box 3 is given in §3.3.2.4.). The interdependency of the state variables is governed by the storage and flux functions given in the preceding section and in §3.2.2.1). To get an as accurate possible solution for a new time step would require an iterative procedure that also involves the groundwater submodel. But this would lead to a long algorithm. Therefore we have designed a step-by-step procedure. The price paid is a slight loss of accuracy, and the requirement that the time step should be ≤1 d. But such a short time step is anyhow needed for simulating the dynamics of drainage to surface water. And the resulting algorithm is extremely efficient.

The solution procedure consists of three steps, in which the state variables are updated in the above given order, one at a time:

1. the mean pressure head p_r of the root zone is updated, using the groundwater level $h(t_g\text{-}\Delta t_g)$ of the preceding time step as a boundary condition;
2. the pressure head p_2 at the top of the subsoil is updated, making use of the latest information about the situation in the root zone, and the groundwater level of the preceding time step;
3. the groundwater level is updated to obtain $h(t_g)$, in conjunction with the groundwater submodel.

In the case of a slowly drying out soil, the steps 1 and 2 are combined into a single step, in which we assume that the soil water profile exactly resembles one of the profiles derived in the computational experiments with SWAP (or an interpolation between two of them). As will subsequently be seen, the first two steps yield updated storage functions which specify the way in which the storage in the shallow subsoil depends on the groundwater level, for the prevailing pressure heads in the root zone and at the top of the subsoil. So the information supplied by the soil water model to the groundwater model consists of an aggregated storage function that is updated at each time step. The groundwater model then supplies the new groundwater level, which is then used for finalizing the amount of water $S_r(t_g)$ stored in control box 1, and the amount $S_2(t_g)$ stored in control box 2.

Update of mean root zone pressure head

The update of the mean root zone pressure head (and water content) is done in step 1 of the solution scheme. It is based on the water balance given as:

$$S_r'(t_g) = S_r(t_g - \Delta t_g) + [P_{net}(t_g) - R(t_g) - ET_{act,tot}(t_g) + q_{m,r}(p_r(t_g), h(t_g - \Delta t_g))]\Delta t_g \qquad (29)$$

where:

$S_r(t_g\text{-}\Delta t_g)$ = amount of water stored in the root zone at beginning of time step (m)
$S_r'(t_g)$ = first estimate of water stored in the root zone at end of time step (m)
$p_r(t_g)$ = mean pressure head in the root zone (m)
$h(t_g\text{-}\Delta t_g)$ = groundwater level at the beginning of the time step (m)

P_{net} (t_g) = net precipitation rate during time step (m d^{-1})
$R(t_g)$ = mean runoff rate during time step (m d^{-1})
$ET_{act,tot}(t_g)$ = actual evapotranspiration rate (m d^{-1})
$q_{m,r}(p_r,h)$ = moisture flux density function (m d^{-1})

The moisture flux density $q_{m,r}$ at the boundary between box 1 and 2 is computed as a function of the pressure head in the root zone and the groundwater level, for reasons explained in §3.2.2.1. As can be seen from the above equation, we use the water level at the *beginning* of the time step (explicit method) and the mean pressure head at the *end* of the time step (implicit method). This leads to the first estimate of the new storage, indicated by $S_r'(t_g)$. The final update of $S_r(t_g)$ is done in step 3 of the solution scheme, in conjunction with the groundwater submodel. To solve for the new pressure head we first rewrite the balance as:

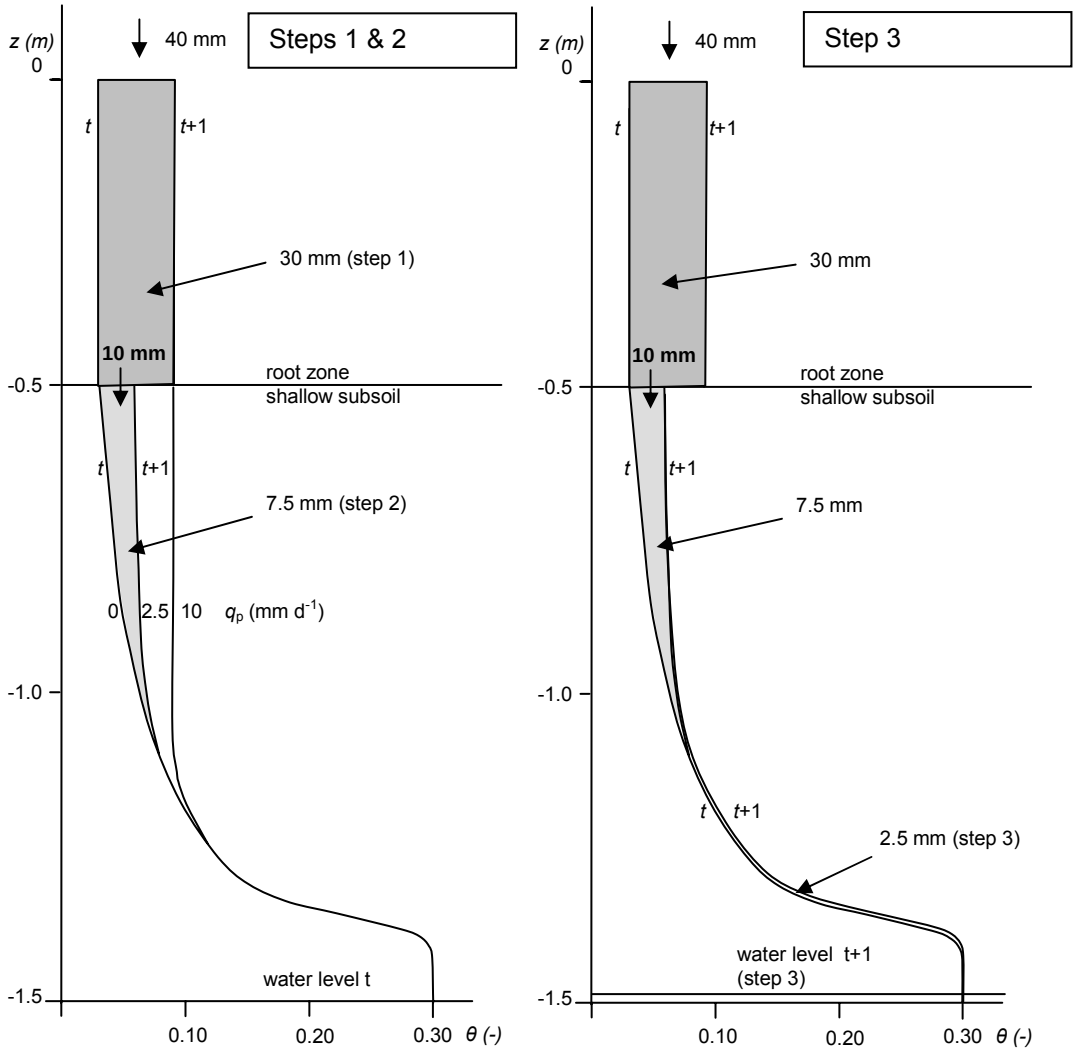

*Figure 14 Transition from one steady-state situation to the next, as a consequence of increased percolation from the root zone to the shallow subsoil. In the example there is 40 mm of rainfall in the time interval of 1 day. Of that 40 mm, an amount of 30 mm (root zone thickness of 500 mm * change of water content by 0.06) is used for increasing the storage in the root zone, and 10 mm flows to the shallow subsoil (step 1): the root zone water content makes the connection with the soil water distribution that has a steady-state percolation flux density of 10 mm d^{-1}. Of that 10 mm, 7.5 mm is used (in step 2) for adjusting the water content at the top of the subsoil to the profile that has a steady-state percolation flux of 2.5 mm d^{-1}. That 2.5 mm is then used (in step 3) for raising the groundwater level (right-hand figure).*

$$S_r'(t_g) - q_{m,r}(p_r(t_g), h(t_g - \Delta t_g))\Delta t_g = S_r(t_g - \Delta t_g) + [P_{net}(t_g) - R(t_g) - ET_{act,tot}(t_g)]\Delta t_g \quad (30)$$

All the terms on the right-hand side are known when the update is done. That makes it possible to solve for the unknown $S_r'(t_g)$ and $p_r(t_g)$ in the following manner. A function is prepared at programme initialization in the form of:

$$\sigma_r(p_r, h) = s_r(p_r, h) - q_{m,r}(p_r, h)\Delta t_g \quad (31)$$

For a given water level h and a given right-hand side value of Eq. 30, the unknown $p_r(t_g)$ can directly be found from an inverse table interpolation of $\sigma_r(p_r,h)$. The solution also yields the new storage $S_r'(t_g)$ and the moisture flux density $q_{m,r}$. The latter is registered as $q_{p,r}(t_g)$ in the case of percolation or as $q_{c,r}(t_g)$ in the case of capillary rise. This solution procedure is analogous to the one used in the surface water model, which is graphically explained in §5.3. A simple example for the root zone update is given below.

Simple numerical example of the root zone update

Let us assume that the initial situation involves the equilibrium profile ($q_{m,r}$=0) of Figure 7. The total amount of water stored in the root zone is 0.03 (water content)*500 mm (thickness root zone) = 15 mm. Then during one day there is 40 mm of rainfall. Our knowledge about the soil hydraulics is contained in the percolation profiles of Figure 7. We start by trying out each of the profiles, to see what would happen if the water content in the root zone changes from the equilibrium value to the value belonging to one of the percolation profiles. The moisture content (of the root zone) for the percolation profile of 2.5 mm d^{-1} is 0.06, and the storage thus 30 mm. That means a storage change of 15 mm. We assume that the percolation during the whole day is equal to the value belonging to the soil water content that is reached at the end of the day, the implicit method. In this case it means that the increase of the water content also causes a percolation of 1 d* 2.5 mm d^{-1} = 2.5 mm. So if we assume that the water content becomes 0.06 at the end of the day, then the total amount of water that can be absorbed by the soil is 15 mm (storage change) plus 2.5 mm (percolation) = 17.5 mm. Given the rainfall of 40 mm during the day, the 0.06 is clearly not the correct solution for the root zone update. We therefore also try out the other percolation profiles of Figure 7, and collect the results as in Table 1. It then becomes clear that the amount water absorbed by the profile matches the rainfall for a new water content of 0.09 (normally this would have to be found by interpolation, of course). The mass balance is further illustrated by step 1 in Figure 14.

Table 1 Simple example of a combined storage-flux function used for the root zone update for a time step of 1 day and a precipitation of 40 mm. The root zone thickness is 0.5 m. The initial condition is an equilibrium profile, with a water content of 0.03(Figure 7), so the initial amount of water stored in the root zone is 0.03 500 mm = 15 mm. The amount of water absorbed by the soil is found by adding the percolation during 1 day to the storage change.*

Percolation profile (mm d^{-1})	Water content of root zone (-)	Storage in root zone (mm)	Storage change, from initial state (mm)	Total amount of water absorbed by the soil (mm)
0.0	0.03	15	-	-
2.5	0.06	30	15	17.5
10	0.09	45	30	40
25	0.12	60	45	70

Update of pressure head at top of subsoil
Similar to the root zone, the update of the pressure head at the top of the subsoil is done using the groundwater level at the beginning of the time step. The method takes into account that part of the percolation from the root zone is needed for making the transition to a new steady-state water profile. The remainder is available for percolation to the water table. For the update of the pressure head at the top of the subsoil we make a water balance in the form of

$$S_2'(t_g) = S_2(t_g - \Delta t_g) + [q_p(t_g) - q_c(t_g) + q_{m,2}(p_2(t_g), h(t_g - \Delta t_g))]\Delta t_g \quad (32)$$

where
$S_2(t_g - \Delta t_g)$ = amount of water stored in shallow subsoil at beginning of time step (m)
$S_2'(t_g)$ = first estimate of water stored in the shallow subsoil at end of time step (m)
$p_2(t_g)$ = pressure head at top of subsoil (m)
$h(t_g - \Delta t_g)$ = groundwater level at the beginning of the time step (m)
$q_p(t_g)$ = percolation from the root zone during time step (m d^{-1})
$q_c(t_g)$ = capillary rise to the root zone during time step (m d^{-1})
$q_{m,2}(p_2,h)$ = moisture flux density function for the flow to the water table (m d^{-1})

To solve for the pressure head $p_2(t_g)$ at the top of the subsoil we rearrange Eq. 32 in the following manner:

$$S_2'(t_g) - q_{m,2}(p_2(t_g), h(t_g - \Delta t_g))\Delta t_g = S_2(t_g - \Delta t_g) + [q_p(t_g) - q_c(t_g)]\Delta t_g \quad (33)$$

This equation can then be efficiently solved for $p_2(t_g)$ by preparing the following function for the shallow subsoil, analogous to the root zone algorithm:

$$\sigma_2(p_2,h) = s_2(p_2,h) - q_{m,2}(p_2,h)\Delta t_g \quad (34)$$

We then follow the same solution technique as used for the root zone pressure head: first the right-hand side of Eq. 33 is evaluated; then an inverse table interpolation is done of $\sigma_2(p_2,h)$. Apart from yielding an updated p_2, that gives values for the storage $S_2'(t_g)$ and the moisture flux density $q_{m,2}(p_2,h)$.

A numerical example is given in Figure 14, for a time step of 1 day: the percolation of 10 mm d^{-1} from the root zone is used for the transition of the soil water storage ($S_2'(t_g) - S_2(t_g - \Delta t_g)$ = 7.5 mm) and for the percolation flux to the water table (2.5 mm d^{-1}). So in this substep we handle the influence of the unknown $p_2(t_g)$ in a fully *implicit* manner (based on the value at t_g) and the influence of the water table depth in a fully *explicit* manner (based on the value at $t_g - \Delta t_g$).

Once the net moisture flux has been found, it can be registered as either $q_{p,2}$ in the case of percolation or $q_{c,2}$ in the case of capillary rise. If the groundwater level is in control box 3, then the calculation method given below for the new groundwater level is skipped. Instead the calculated $q_{p,2}$ is used as input to the unit hydrograph method given in §3.3.2.4.

Solution scheme for the shallow groundwater level

In the third step of the solution scheme the update of the groundwater level is done in conjunction with the groundwater submodel. That requires arranging the information about the soil water system in an appropriate manner. To that end we make a water balance for the whole of the shallow subsoil, comprising boxes 1 and 2:

$$S_{\mathrm{r}}(t_{\mathrm{g}}) + S_2(t_{\mathrm{g}}) = S_{\mathrm{r}}(t_{\mathrm{g}} - \Delta t_{\mathrm{g}}) + S_2(t_{\mathrm{g}} - \Delta t_{\mathrm{g}}) + [P_{\mathrm{net}}(t_{\mathrm{g}}) - R(t_{\mathrm{g}}) - ET_{\mathrm{act,\,tot}}(t_{\mathrm{g}})]\Delta t_{\mathrm{g}} + \int_{t-\Delta t_g}^{t} \Sigma q_{\mathrm{sat}}\, dt \qquad (35)$$

where q_{sat} is the saturated flow towards the control boxes 1 and 2. We now rewrite Eq. 35 in a form that makes it possible to solve for the unknown $h(t_{\mathrm{g}})$. To this end we replace the unknown $S_{\mathrm{r}}(t_{\mathrm{g}})$ and $S_2(t_{\mathrm{g}})$ by the storage functions, with $h(t_{\mathrm{g}})$ as one of the arguments. Then after rearranging to a form that is convenient for the coupling of submodels we have

$$\mathrm{s}_{\mathrm{r}}(p_{\mathrm{r}}(t_{\mathrm{g}}), h(t_{\mathrm{g}})) + \mathrm{s}_2(p_2(t_{\mathrm{g}}), h(t_{\mathrm{g}})) - S_{\mathrm{r}}(t_{\mathrm{g}} - \Delta t_{\mathrm{g}}) - S_2(t_{\mathrm{g}} - \Delta t_{\mathrm{g}}) - \ldots$$
$$[P_{\mathrm{net}}(t_{\mathrm{g}}) - R(t_{\mathrm{g}}) - ET_{\mathrm{act,\,tot}}(t_{\mathrm{g}})]\Delta t_{\mathrm{g}} = \int_{t-\Delta t_g}^{t} \Sigma q_{\mathrm{sat}}(h(t_{\mathrm{g}}))\, dt \qquad (36)$$

which can be solved for the groundwater level $h(t_{\mathrm{g}})$, in conjunction with the system of equations of the groundwater model, as explained further in §4.3.1. Here we suffice by stating that at the end of each update of the unsaturated zone the result is available in the form of a (piece-wise linear) function of h as given in the left-hand side of Eq. 36. This function of h is updated for each time step, to take into account the changing conditions in the unsaturated zone. Once the new groundwater level is known, the storage in the root zone and subsoil can be finalized by evaluating the storage functions for the new h. In the case that the new groundwater level is within the root zone, equilibrium conditions are assumed in the part that remains unsaturated. The mean pressure head is recomputed accordingly; likewise is done for the pressure head at the top of the subsoil. In the computer code this situation is anticipated upon in the construction of the storage functions. If the groundwater level starts in the root zone (or even above soil surface) and the saturated flow module dictates that it should drop to a level below the *bottom* of the rootzone, then the assumption is made that the pressure head at the top of the subsoil is equal to the equilibrium value in the first time step.

In Figure 14 the simplified example is continued for when the saturated flows are zero. Then all of the 2.5 mm that flows to the water table is used for the update of the soil water distribution at the bottom of the compartment in the form of a slight upward shift.

Verification with SWAP

In Figure 15 an example is given using the soil hydraulic metafunctions of Figure 11 and Figure 12 (expanded to percolation rates of up to 100 mm d^{-1}), for a root zone depth of 0.3 m, and a drainage system at 2 m b.s.s. with a resistance of 200 d. A time step of 1 d was used. In order to test the response to extreme situations a fictitious year was constructed. This year was followed by the years 1975 and 1976; these are less extreme, but both are still very dry. The SWAP-model simulates a more dried out root zone in the initial phase of drying out, which is due to non-steady conditions in the profile.

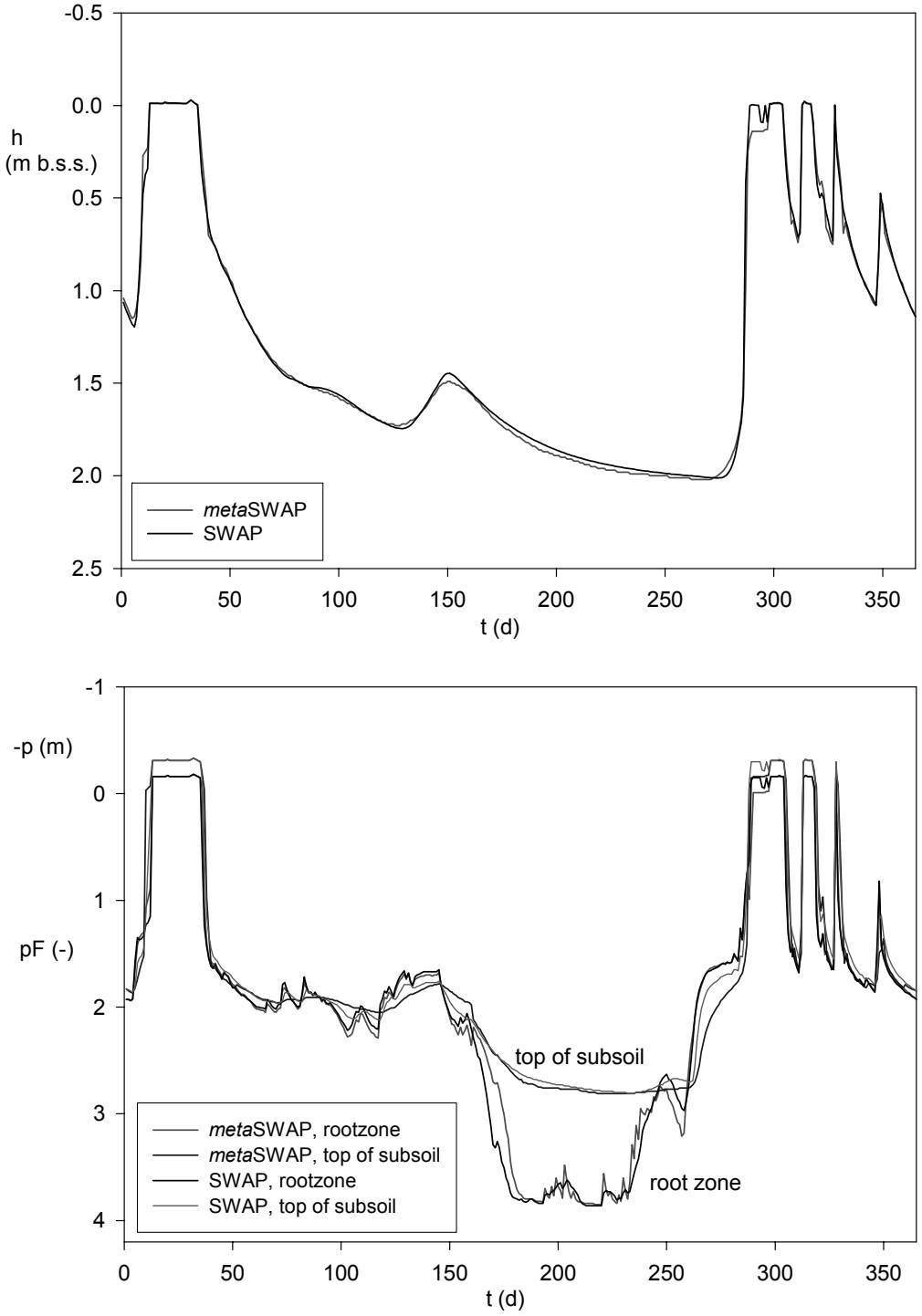

Figure 15 Verification of the metaSWAP-model with SWAP. The soil profile has a root zone depth of 0.3 m, and a drainage system at 2 m b.s.s. with a drainage resistance of 200 d

Especially during this period the SWAP model has a higher reduction of the evapotranspiration due to relatively more moisture stress. The example demonstrates that the rigid coupling of the rootzone to the subsoil (as also employed in the Rijtema/De Laat method) has the drawback of leading to an optimistic calculation of the actual evapotranspiration. As can be seen from the water balance terms in Table 2, the *meta*SWAP model overestimates the actual evapotranspiration by 4-5%. That explains why the groundwater level takes a few days longer to reach the soil surface after the prolonged dry period. But in modelling practice the soil physical properties are not known exactly anyhow. Then some form of calibration will be necessary. This calibration can easily compensate for the type of 'modelling error' shown in the example.

Table 2 Comparison between metaSWAP and SWAP for three simulation years

	Year			
Description	19xx	1975	1976	Total
P (mm)	1806.6	635.0	536.3	*2977.9*
ET_{ref} (mm)	693.0	577.7	614.8	*1885.5*
ET_{act}, SWAP (mm)	495.1	464.2	394.7	*1354.0*
ET_{act}, *meta*SWAP (mm)	515.0	480.6	413.0	*1408.6*
Q_{sat}, SWAP (mm)	1330.3	324.4	131.0	*1785.7*
Q_{sat}, *meta*SWAP (mm)	1314.0	312.7	118.6	*1745.3*
ΔS, SWAP (mm)	-18.9	-153.7	10.6	*-162.0*
ΔS, *meta*SWAP (mm)	-22.4	-158.3	4.6	*-176.1*
h final, SWAP (m b.s.s.)	1.16	1.94	1.97	*1.69*
h *final*, metaSWAP *(m b.s.s.)*	*1.16*	*1.98*	*2.03*	*1.72*

The run time for a single year is about 0.009 s on a 2.4GHz Pentium computer. That is roughly 200 times less than the time neeed by SWAP for the verification (with the IO-time discounted).

3.3.2.4 Deep subsoil

The pulse response function given in Eq. 21 is used in combination with discrete time intervals. So it is used in its integrated form, which is known as the 'distribution graph':

$$U(z_*, T, j) = \int_{(j-1)T}^{jT} u(z_*, T, t)dt \tag{37}$$

where $U(z_*,T,j)$ gives the fraction of the percolation pulse that passes z_* during the time interval $[(j-1)T; jT]$ (-). The response to a series of percolation pulses from control box 2 to box 3 can be calculated with the convolution integral (Dooge, 1959). Here it is given in its discrete form applied to the distribution graph, with the length of the block input T taken as the time step Δt_g of the groundwater model:

$$q_{p,3}(z_{*d}, t_g) = \sum_{j=1}^{N_j} q_{p,2}(t_g - (j-1)\Delta t_g) \cdot U(z_{*d}, \Delta t_g, j) \tag{38}$$

where

$q_{p,3}(t_g)$ = percolation to the deep water table during time interval $[t_g-\Delta t_g ; t_g]$ (m d^{-1})
$q_{p,2}(t_g)$ = percolation pulse from box 2 to box 3 during time interval $[t_g-\Delta t_g ; t_g]$ (m d^{-1})
z_{*d} = depth of the water table with respect to the top of control box 3 (m)
N_j = number of time steps that have passed since the start of the simulation

The water balance for the deep groundwater is given by:

$$S_3(t_g) = S_3(t_g - \Delta t_g) + q_{p,3}(z_{*d}, t_g)\,\Delta t_g + \int_{t-\Delta t_g}^{t} \Sigma q_{sat}(h)dt \tag{39}$$

The interpretation of this water balance is somewhat involved, because the description of the percolation wave is superimposed on the equilibrium soil water profile of the deep subsoil. The given balance is in fact for the latter, because the dynamic storage involved in the percolation wave is contained in the 'blocks' of the unit hydrograph model that have not yet arrived at the water table. Thus for water tables in control box 3, the storage function is not bivariate like for control box 2 (the function $s_2(p_2,h)$ given in §3.2.2.1) but a *uni*variate function given by $s_3(h)$, based on equilibrium profiles For the used U-function we need to make an assumption with respect to the average depth to the water table, here indicated by z_{*d}. The actual update of a deep groundwater level is based on combining the storage function $s_3(h)$ with Eq. 39, and solving for $h(t_g)$, as further explained in §4.3.1:

$$s_3(h(t_g)) = S_3(t_g - \Delta t_g) + q_{p,3}(z_{*d}, t_g)\,\Delta t_g + \int_{t-\Delta t_g}^{t} \Sigma q_{sat}(h(t_g))dt \tag{40}$$

or, more conveniently for the coupling with the groundwater model submodel:

$$s_3(h(t_g)) - S_3(t_g - \Delta t_g) - q_{p,3}(z_{*d}, t_g)\,\Delta t_g = \int_{t-\Delta t_g}^{t} \Sigma q_{sat}(h(t_g))dt \tag{41}$$

3.4 Data summary

For describing the surface runoff, parameters are needed for
- maximum infiltration rate;
- the 'dead' storage, S_{sd};
- the flow resistance of surface runoff, $\gamma_{s.}$

For the unsaturated flow the soil physical metafunctions should be supplied for:
- the percolation/capillary rise;
- the storage in the shallow subsoil (box 2);
- the storage in the deep subsoil (box 3)

These functions should be given in tabular form, for discrete steps of:
- the root zone depth;
- the soil water content;
- the phreatic level.

The given function values are then used as vertices of piece-wise linear functions.

For constructing the contribution of inundated fractions to the storage coefficient, the cumulative frequency distribution of the soil surface elevation should be given per nodal subdomain.

For simulating the dynamics of the soil water in control box 3 we needed values of the diffusivity D and the wave celerity A, and the average depth to the water table z_* (measured or estimated).

4 Groundwater

4.1 Introduction

For shallow water tables a unified approach is followed in the modelling of the soil/groundwater in a vertical column, as explained in the introduction of §3. So if the groundwater level is in 'control box 2' (Figure 6), the water in that box is seen as belonging to both the soil water *and* the groundwater. If the water level drops below the bottom of control box 2, the groundwater simulation uses the simple concept of the unit hydrograph for transmitting the outflow from box 2 down to the water table.

At the other extreme, the soil column can become fully saturated. In that case the groundwater 'overrules' the soil water, and the water on the soil surface is treated as 'visible' groundwater. This overruling can occur on an ephemeral basis or it can be permanent, as in the case of a lake. We assume that in a lake the hydraulic head is everywhere the same. A lake is of course connected to the surface water system with some sort of a link, as described in §5.

4.2 Theory

Darcy's Law for the flow of a homogeneous incompressible fluid through a porous medium can be generalized to the three-dimensional form given by (e.g. Bear 1979):

$$\mathbf{q} = \mathbf{K} \cdot \mathbf{J} = -\mathbf{K} \cdot \text{grad}\,\varphi \qquad (42)$$

where
$\mathbf{q}$ = the specific discharge vector (m d^{-1})
$\mathbf{K}$ = the so-called conductivity tensor (m d^{-1})
φ = hydraulic head (m)
$\mathbf{J}$ = $-$ grad φ, the hydraulic gradient with components $J_x = -\partial\varphi/\partial x$, $J_y = -\partial\varphi/\partial y$, and $J_z = -\partial\varphi/\partial z$ (-)

The conductivity tensor $\mathbf{K}$ is symmetric (see e.g. Bear , 1979). And in the case that x, y, and z-axes are (through a transformation) made to correspond with the principal directions of the anisotropic medium, only the elements on the diagonal are non-zero, i.e. K_{xx}, K_{yy}, K_{zz}. In the following these symbols will be abbreviated to K_x, K_y, K_z.

The experimentally derived Darcy's Law for groundwater motion has its limitations with respect to applicability. But this does not apply to the unconsolidated sediments that the SIMGRO-model is intended for.

The equation of motion given by Eq. 42 just describes the flow in a point. (Strictly speaking that is not true, of course, due to the irregularities of the soil matrix. But use of the 'representative elementary volume'-concept, allows us to describe the flow in terms of continuum mechanics). For making it operational at a finite scale it has to be combined with the mass conservation equation. It then becomes possible to scale up the flow description to a domain of finite dimensions that is embedded in the surrounding environment by means of boundary conditions. The SIMGRO-model is intended for

describing the flow at the scale of a drainage basin. That also requires describing the local flows to watercourses and wells. But the embedding of detailed descriptions of the local flows in the regional model would not be practical. In order to arrive at a manageable formulation we decompose the flow into:

- regional flow components that are described explicitly;
- local flow components that are described using metafunctions.

We derive the local-flow metafunctions by solving subproblems for the local flows. These subproblems are stated in such a manner that they take place within local subdomains, involving zero-flux boundaries in the horizontal direction. It is then possible to superimpose the local flow formulations on the regional flow, by simply adding the metafunctions as extra leakage terms to the regional flow equation.

In the following, the formulation for the regional flow is given first, followed by those for the local flows.

4.2.1 Regional flow

In the flow formulation we assume that the regional groundwater system can be schematised to alternating layers of:

- aquifers, with essentially horizontal flow;
- aquitards, with essentially vertical flow.

In this schematization the top layer can either be an aquitard or an aquifer. The bottom layer of the (modelled) system is always an aquifer.

For essentially horizontal flow in an aquifer, the equation of motion can be integrated in the vertical direction, and then be written as (Bear, 1979; for x and y in principal directions of conductivity):

$$\mathbf{q}^{\mathrm{a}} = \mathbf{T} \cdot \mathbf{J}^{\mathrm{a}} \; ; \quad q_{\mathrm{x}}^{\mathrm{a}} = T_{\mathrm{x}} J_{\mathrm{x}}^{\mathrm{a}} = -T_{\mathrm{x}} \frac{\partial \varphi}{\partial x}; \quad q_{\mathrm{y}}^{\mathrm{a}} = T_{\mathrm{y}} J_{\mathrm{y}}^{\mathrm{a}} = -T_{\mathrm{y}} \frac{\partial \varphi}{\partial y} \tag{43}$$

where

$\mathbf{q}^{\mathrm{a}}(x,y,l)$ = the integrated discharge vector for flow through the layer l ($m^2\ d^{-1}$)
$q_{\mathrm{x}}^{\mathrm{a}}(x,y,l)$ = x-component of $\mathbf{q}^{\mathrm{a}}(x,y,l)$ ($m^2\ d^{-1}$)
$q_{\mathrm{y}}^{\mathrm{a}}(x,y,l)$ = y-component of $\mathbf{q}^{\mathrm{a}}(x,y,l)$ ($m^2\ d^{-1}$)
$\mathbf{T}(x,y,l)$ = transmissivity tensor, with non-zero components T_{x} and T_{y} ($m^2\ d^{-1}$)
$\mathbf{J}^{\mathrm{a}}(x,y,l)$ = gradient of the mean hydraulic head in the vertical section (-)

The validity of this equation hinges on the assumption that "the gradient of the mean head in the vertical section" is the same as "the mean gradient of the head in the vertical section" (Bear, 1979). If – within an aquifer – the conductivity does not vary for the z-coordinate, then the components of the transmissivity tensor can simply be obtained by

$$T_{\mathrm{x}} = K_{\mathrm{x}} D \; ; \; T_{\mathrm{y}} = K_{\mathrm{y}} D \tag{44}$$

where $D(x,y,l)$ is the thickness of the layer l in m.

The flow to and from the aquitards that are above and/or below an aquifer is commonly referred to as the 'leakage' term. Given the fact that we assume 'essentially vertical flow' in the aquitards, this flow can described by applying Eq. 42 only in the z-direction. The leakage to the aquifer l is then given by the sum of the vertical flow from the layer above and from the layer below it, respectively from (l -1) and from (l +1). The used sign convention is that flows to the layer l are taken as positive. So we have:

$$q_z(x,y,l) = -K_z(x,y,l-1)\frac{\partial \varphi}{\partial z}(x,y,l-1) + K_z(x,y,l+1)\frac{\partial \varphi}{\partial z}(x,y,l+1) \qquad (45)$$

where
$q_z(x,y,l)$ = leakage to layer l (m d^{-1})
$\varphi(x,y,l-1)$ = hydraulic head in the middle of layer $l-1$ (m)
$\varphi(x,y,l-1)$ = hydraulic head in the middle of layer $l+1$ (m)
$K_z(x,y,l-1)$ = vertical conductivity of layer $l-1$ (m d^{-1})
$K_z(x,y,l+1)$ = vertical conductivity of layer $l+1$ (m d^{-1})

Storage effects in groundwater can be due to elasticity of the soil matrix and of the water itself, and due to the desorption/resorption of the soil matrix. The storage effect is parameterized in the form of an aggregated storage coefficient given by:

$$\mu = D S_{0p} + S_y \qquad (46)$$

where
μ = storage coefficient (-)
S_{0p} = specific storativity (m^{-1})
D = layer thickness (m)
S_y = specific yield of desorption/resorption (-)

The specific yield is not a constant; it depends on the conditions in the unsaturated zone. In its integrated form it is implicitly contained in the storage function given §3.3.2.2. In that form it is also used in the model. For the top layer the storage coefficient also includes the water that is stored on the soil surface.

In the regional flow equation, all flux terms involving leakage and local flow are treated as diffuse vertical flux densities. That is because such vertical flux densities satisfy the requirement of being 'local', i.e. not directly involving lateral flows at the boundaries of local subdomains that are used in the model implementation (§4.3.1). That may seem trivial, but in fact it is not: it is an essential requirement for performing the decomposition that was put forward in §4.2. These flux densities form the link between the regional model and the 'local' models for flow to watercourses. By combining the equation of motion with mass conservation, the flow description can now be stated with:

$$-\text{div}\ \mathbf{q}^a = \frac{\partial}{\partial x}\left(T_x \frac{\partial \varphi}{\partial x}\right) + \frac{\partial}{\partial y}\left(T_y \frac{\partial \varphi}{\partial y}\right) = \mu \frac{\partial \varphi}{\partial t} - \sum q_{unsat} - q_z + q_d + q_s + q_e - q_b \qquad (47)$$

where
$\mathbf{q}^a(x,y,l)$ = the integrated specific discharge vector for flow through the layer l (m^2 d^{-1})
$q_z(x,y,l)$ = leakage (taken positive for flow towards the domain) (m d^{-1})
$q_d(x,y,l)$ = drainage to surface water (*negative* for flow towards groundwater)(m d^{-1})
$q_s(x,y,l)$ = extraction for sprinkling (m d^{-1})

$q_e(x,y,l)$ = extraction for public water supply (m d^{-1})
$q_b(x,y,l)$ = boundary flux (taken positive for flows to the domain)(m d^{-1})
$\sum q_{unsat}(x,y,l)$ = total unsaturated flow to the groundwater (only for l=1) (m d^{-1})

The unsaturated flow term only applies to the phreatic layer. In the case that the phreatic level is in control box 2 (for its definition see Figure 6), it corresponds to the terms for the unsaturated flow in the left-hand side of Eq. 36. In the case that the phreatic level is in control box 3, the unsaturated flow terms is the percolation given in Eq. 41. More is said about the coupling between the soil water and groundwater submodels in §4.3.1.

4.2.2 Drainage

Drainage to a watercourse is a gravity flow involving relatively small differences in the hydraulic head. The head differences depend very much on the preceding history of events, involving the precipitation, and so on. So the involved fluxes must be simulated through time.

In the sense that was expounded in §4.2 the flows to watercourses can be seen as 'local' if there is a surface water system involving parallel watercourses at equal spacing, in the presence of a uniformly distributed recharge from the unsaturated zone to the groundwater: in that case the drainage can be seen as a diffuse process that is 'spread over' the local-flow subdomain, with no boundary effects to the regional system. But the conceptualization of the regional model should of course be capable of dealing with situations that differ from the mentioned one. Before going into that, the schematized situation will be discussed first.

In order to arrive at a manageable numerical implementation for the computation of drainage fluxes a number of simplifying assumptions are made. The first is that the local flow can be adequately described as a stream of steady-state situations, like is done for the soil water modelling. This assumption neglects the fast-flow terms that are present if the shallow groundwater receives a heavy percolation pulse. The fast flow terms are due to the locally steep hydraulic gradient in the direct vicinity of the watercourse, involving a more 'square' shape of the water table than under steady-state conditions. These terms were given by for instance Dumm (1954), and Kraijenhoff van de Leur (1958).

The second main assumption is that the local flow can be decomposed, using the method given by Ernst (1962), as adapted by Van der Molen (1972). The decomposition involves the following components, which are illustrated in Figure 16 (adapted from Jousma & Massop, 1996):
- vertical flow from where the percolation water enters the groundwater body, to the 'main stream' of the aquifer;
- essentially horizontal flow in the aquifer towards the watercourse;
- radial flow in the vicinity of the watercourse;
- entrance flow to the watercourse itself (Van der Molen, 1972).

The assumption is that the total hydraulic head difference between the local groundwater culmination point and the water level in the watercourse can be written as the sum of the head differences for the separate flow components:

$$\Delta h = \Delta h_v + \Delta h_h + \Delta h_r + \Delta h_e \qquad (48)$$

where
Δh = total head difference between groundwater culmination point and surface water level (m)
Δh_v = head difference for vertical flow to the 'main stream' of the aquifer (m)
Δh_h = head difference for horizontal flow to watercourse (m)
Δh_r = head difference for radial flow to watercourse (m)
Δh_e = head difference for entrance flow to watercourse (m)

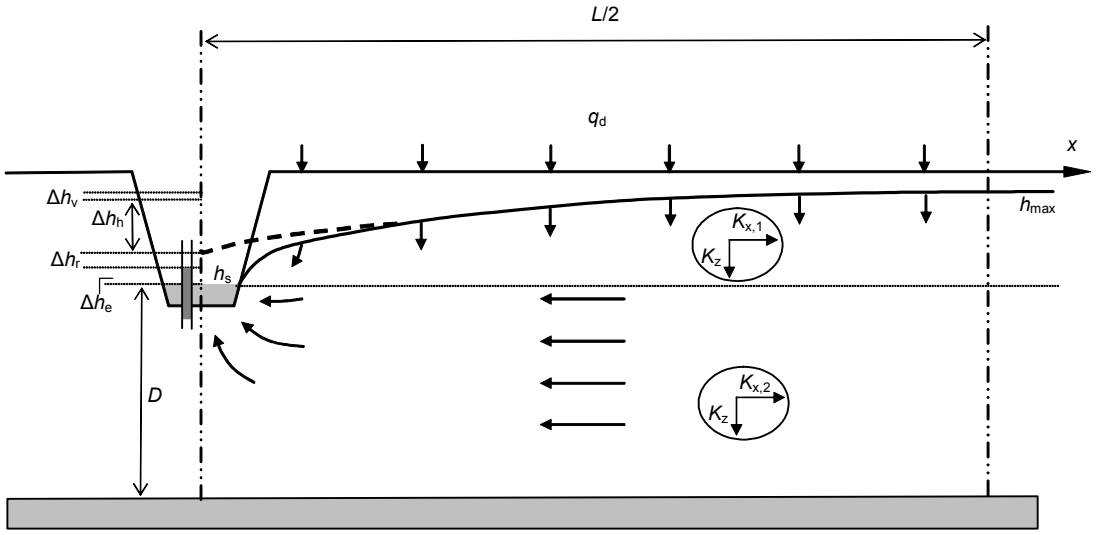

Figure 16 Decomposition of the head loss in the flow towards a watercourse, according to Ernst (1962) and Van der Molen (1972); figure adapted from Jousma & Massop (1996).

The conceptualization thus involves four flow resistances that are connected 'in series'. That is of course an approximation. There is for instance an overlap between the horizontal flow and the radial flow, involving the same part of the flow domain. Here we give the flow formulation for parallel watercourses. The geometry of the flow situation is governed by the following parameters:
- L = distance between the parallel watercourses (m)
- D = thickness of the aquifer below the drainage base (m)
- P = wetted perimeter of a watercourse (m)

For the horizontal conductivity a distinction is made between the subdomain above the drainage base ($K_{x,1}$) and the subdomain below it ($K_{x,2}$).

In order to 'feed' the lateral flow in the aquifer, the vertical flow must on average travel a distance of $D/2$ (disregarding the flow above the drainage base). Using the one-dimensional form of Eq. 42, and integrating over the interval $[0;D/2]$, the head difference for the vertical flow can then simply be computed with:

$$\Delta h_v = \frac{q_d D/2}{K_z} = q_d L \omega_v; \quad \omega_v = \frac{D/2}{L K_z} \tag{49}$$

where:
q_d = drainage flux (sign positive for flow towards the watercourse) (m d^{-1})
K_z = vertical conductivity (m d^{-1})
ω_v = vertical drainage resistance (d m^{-1})

In situations where the drainage flux stems from upward seepage through the semi-pervious layer that in Figure 16 forms the lower 'boundary' of the flow domain, the vertical flow resistance is already taken into account in the regional flow equation. In such a situation the head loss given by Eq. 49 should be left out, to avoid double counting of this flow resistance.

For the horizontal flow between parallel watercourses, the flow equation reduces to a one-dimensional form of Eq. 47, with only the steady-state drainage term. This equation is also known as the Dupuit discharge formula (e.g. Bear, 1979). Here it is written as:

$$-\text{div}\ \mathbf{q}^{\mathbf{a}} = \frac{d}{dx}\left([h(x)-D]\,K_{x,1}\frac{dh}{dx} + D\,K_{x,2}\frac{dh}{dx}\right) = q_d \tag{50}$$

where $h(x)$ is the hydraulic head with reference to the bottom of the aquifer (m), at distance x from the watercourse. The sign of the drainage term q_d is positive for flow to surface water. If the breadth of the watercourse itself is neglected, integration between x=0 and x=L/2, and insertion of the boundary condition $h(0)=h_s$, then yields

$$h(x) = h_s + \sqrt{D^2\frac{K_{x,2}^2}{K_{x,1}^2} + \frac{q_d}{K_{x,1}}(xL - x^2)} - D\frac{K_{x,2}}{K_{x,1}} \tag{51}$$

Inserting x=L/2 yields the head elevation at the culmination point (h_{max}), and thus the head difference for the horizontal flow:

$$\Delta h_h = h_{max} - h_s = h(L/2) - h_s = \sqrt{D^2\frac{K_{x,2}^2}{K_{x,1}^2} + \frac{q_d L^2}{4K_{x,1}}} - D\frac{K_{x,2}}{K_{x,1}} \tag{52}$$

with the horizontal drainage resistance ω_h (d m^{-1}) given by:

$$\omega_h = \frac{\Delta h_h}{q_d L} = \frac{1}{q_d L}\left(\sqrt{D^2\frac{K_{x,2}^2}{K_{x,1}^2} + \frac{q_d L^2}{4K_{x,1}}} - D\frac{K_{x,2}}{K_{x,1}}\right) \tag{53}$$

The expression for the drainage flux as a function of the head difference can be made explicit by rearranging Eq. 52:

$$q_d = \frac{8K_{x,2}D}{L^2}\Delta h_h + \frac{4K_{x,1}}{L^2}\Delta h_h{}^2 \tag{54}$$

For implementation in the model the mean head-elevation is also needed; it is given by:

$$\bar{h} - h_s = \frac{\sqrt{\frac{K_{x,1}}{q_d}\frac{K_{x,2}^2}{K_{x,1}^2}D^2 + \sqrt{\frac{q_d}{K_{x,1}}\frac{L^2}{4}}}}{L}\arctan\left(\sqrt{\frac{q_d}{K_{x,1}}}\frac{K_{x,1}L}{2K_{x,2}D}\right) - \frac{K_{x,2}D}{2\,K_{x,1}} \tag{55}$$

The ratio between the mean head difference and Δh_h is commonly referred to as the *form factor* (Ernst, 1983*)*:

$$\zeta_h = \frac{h - h_s}{h_{max} - h_s} \tag{56}$$

which in the simplified case of only flow below the drainage base (i.e. neglecting the quadratic term in Eq. 54) is equal to 2/3. For situations where also the radial and entrance flow resistance play a role, the form factor assumes higher values. In the extreme case of no vertical or horizontal resistance ($\Delta h_v = \Delta h_h = 0$) the form factor approaches unity.

For the radial flow to a watercourse Ernst (1962) gives:

$$\Delta h_r = \frac{q_d L}{\pi K_e}\ln\left(\frac{\alpha D_e}{P_e}\right) = q_d L \omega_r; \quad \omega_r = \frac{1}{\pi K_e}\ln\left(\frac{\alpha D_e}{P_e}\right) \tag{57}$$

where ω_r is called the radial drainage resistance (d m^{-1}), and α is a geometry factor that depends on the specific configuration of the aquifer in relation to the watercourse. In the presence of anisotropy, the value of the conductivity in the equivalent isotropic domain is taken as $\sqrt{(K_x K_z)}$. The D-value has then to be transformed with: $D_e = D\sqrt{(K_x/K_z)}$; assuming that de wetted perimeter is mostly in the x-direction, the P-value has to be transformed with $P_e = P\sqrt{(K_z/K_x)}$. The relevant expressions for field drains are e.g. given by Van der Molen (1972).

For the entrance flow Van der Molen (1972) gives:

$$\Delta h_e = q_d\left(\frac{c_b L}{P}\right) = q_d L \omega_e; \quad \omega_e = \frac{c_b}{P} \tag{58}$$

where c_b is the local entrance resistance (d), and ω_e the entrance resistance (d m^{-1}). This description of radial and entrance resistance neglects the presence of a seepage face in the watercourse, just above the surface water level.

Summarizing, the total head difference for the mean head between the watercourses can be written as:

$$\bar{h} - h_s = q_d L\,(\omega_v + \zeta_h \omega_h + \omega_r + \omega_e) \tag{59}$$

and for the culmination point between the watercourses the head difference can be written as:

$$h_{\max} - h_s = q_d L\,(\omega_v + \omega_h + \omega_r + \omega_e) \tag{60}$$

For deep watercourses, it is assumed that the above given drainage theory can also be applied to the deeper layers of the geohydrologic schematization that are cut into by the watercourses. This should not be considered equivalent to applying a multi-layer drainage formula, like given in Appendix 1. For situations with relatively small vertical resistances to the subsoil, it is relevant to use a multi-layer drainage formula for the *local* flow: the drainage water seeks a route with the lowest flow resistance, which can mean 'taking a detour over the highway' in the deeper subsoil. Since this flow takes place *within* the local subdomain, it is not a flow that is modelled by the regional flow equation: the local flow is superimposed upon the regional one. In comparison to a single layer formula, that can lead to a substantial decrease of the computed drainage resistance.

The above given derivations are for a uniformly distributed recharge situation, which also applies to situations with seepage from a leaky layer. In a regional model all kinds of different situations can occur, of course. The question is whether the above given approach can then still be used. Consider for instance the situation with zero recharge and regional flow that is locally drained. Depending on the strength of the regional flux, the horizontal drainage resistance of the local flow can vary. It thus should be realized that the used approach is an approximate one.

When the groundwater level starts to approach the mean soil surface, the lowest-lying places start to act as a drainage medium. With increasing level, more parts become inundated, thus leading to a sharp reduction of the horizontal flow resistance. Also the radial resistance and entrance resistance show a sharp decrease, due to the increase of the wetted perimeter involved in the inundation.

4.3 Model implementation

4.3.1 Regional flow

The implementation of the regional flow equation for the phreatic layer requires rearranging Eq. 47 and integrating over the time step of the groundwater model, Δt_g. A number of q-terms are assumed to remain constant during a time interval, so the expression simplifies to:

$$\int_{t-\Delta t_g}^{t} \left(\mu \frac{\partial \varphi}{\partial t} - \sum q_{\text{unsat}} \right) dt = \int_{t-\Delta t_g}^{t} (-\text{div } \mathbf{q}^{\mathbf{a}} + q_z - q_d)\, dt + (q_b - q_s - q_e)\Delta t_g \tag{61}$$

Replacing the left-hand side by the left-hand side of Eq. 36 gives:

$$\begin{aligned} &s_r(p_r(t_g), h(t_g)) + s_2(p_2(t_g), h(t_g)) - S_r(t_g - \Delta t_g) - S_2(t_g - \Delta t_g) - \\ &[P_{\text{net}}(t_g) - R(t_g) - ET_{\text{act, tot}}(t_g)]\Delta t_g = \int_{t-\Delta t_g}^{t} (-\text{div } \mathbf{q}^{\mathbf{a}} + q_z - q_d)\, dt + (q_b - q_s - q_e)\Delta t_g \end{aligned} \tag{62}$$

where in the left-hand side the values of p_r and p_2 for t_g are already known, but the value of h still has to be found together with the terms in the right-hand side. The storage functions $s_r(p_2,h)$ and $s_2(p_2,h)$ are given in the form of piece-wise linear table functions. This equation applies to situations with the groundwater level above the bottom of 'control box 2' of the shallow subsoil (Figure 6). If the water level is in the 'control box 3' for the deep subsoil, then the left-hand side is replaced by the left-hand side of Eq. 41:

$$\begin{aligned} &s_3(h(t_g)) - S_3(t_g - \Delta t_g) - q_{p,3}(z_{*d}, t_g)\Delta t_g = ... \\ &.. = \int_{t-\Delta t_g}^{t} (-\text{div } \mathbf{q}^{\mathbf{a}} + q_z - q_d)\, dt + (q_b - q_s - q_e)\Delta t_g \end{aligned} \tag{63}$$

If the water level starts in box 2, then the algorithm takes the possibility into account that the water level drops to a position in box 3. If the water level starts in box 3, a rise to box 2 is a possibility. For handling the smooth transition of the water level from one box to the other the storage functions s_2 and s_3 are extended into the domain of the other box. In its original form the storage function s_2 remains constant for water levels below the bottom of box 2. The extension is done by assuming that below the bottom of box 2 the storage *change* is the same as that of the s_3-function for that trajectory. The extension of the s_3-function into box 2 is done in a similar fashion.

In the case that the phreatic layer is an aquitard, the div $\mathbf{q}^{\mathbf{a}}$ term in Eq. 61 is not present. For the deep aquifers the q_{unsat}-terms are missing, and the equation reduces to (after dividing by Δt_g):

$$\mu \frac{\Delta \varphi}{\Delta t_g} = \frac{1}{\Delta t_g} \int_{t-\Delta t_g}^{t} (-\text{div } \mathbf{q}^{\mathbf{a}} + q_z - q_d)\, dt + q_b - q_s - q_e \tag{64}$$

Since the heads in the deep aquitards are not included in the set of equations, the storage change in these layers has to be accounted for in a different manner. That is done by adding an extra term to the storage coefficient of the neighbouring aquifers: half of the term DS_{0p} (see Eq. 46) is added to the storage coefficient of the aquifer above, and the other half to that of the aquifer below.

Integration of the drainage flux involves running the surface water submodel in a subloop for the surface water time steps, as follows from the coupling scheme described in §1. Since the (new) groundwater levels are *not* known at the beginning of the time step, the integration of the drainage flux is based on the levels at the *beginning* of the time step (explicit method). For each time step of the surface water model the drainage flux is recomputed, based on the most recent update of the surface water level, and adding to the integrated drainage flux totalizer. After the subloop has progressed to the new time t_g, the update of the groundwater submodel can take place, in which the drainage fluxes are treated as known constants.

Given the above considerations, the total of the flows that are taken as constant in the process of numerically solving Eq. 64 are given by:

$$q_{\text{const}} = q_{\text{b}} - q_{\text{s}} - q_{\text{e}} - \frac{1}{\Delta t_{\text{g}}} \int_{t-\Delta t_{\text{g}}}^{t} q_{\text{d}}\, dt \tag{65}$$

where the integration over t is numerically performed for the time steps of the surface water model.

For the leakage term we use the following expression, derived from integrating the one-dimensional form of Eq. 42, from the middle of one aquifer to the middle of the next:

$$q_z(x,y,l) = \frac{[\varphi(x,y,l-2) - \varphi(x,y,l)]}{0.5D(l-2)/K_z(l-2) + D(l-1)/K_z(l-1) + 0.5D(l)/K_z(l)} + \ldots$$

$$\ldots + \frac{[\varphi(x,y,l+2) - \varphi(x,y,l)]}{0.5D(l+2)/K_z(l+2) + D(l+1)/K_z(l+1) + 0.5D(l)/K_z(l)} \tag{66}$$

where (for being concise the x,y-arguments of D and K_z have been left out above):
$q_z(x,y,l)$ = leakage to layer l (m d^{-1})
$\varphi(x,y,l)$ = hydraulic head in the middle of layer l (m)
$D(x,y,l)$ = thickness of layer l (m)
$K_z(x,y,l)$ = vertical conductivity of layer l (m d^{-1})

The above expression includes the vertical flow resistances within the aquifers themselves. Usually these terms can be neglected. However, when the used schematization involves a large number of layers at set intervals, it is in fact being used as an approximation for fully three-dimensional flow. And in that case the resistances in the 'aquifers' are crucial for the validity of the model.

In the case that the first layer is an aquitard, the leakage to the aquifer below it is computed using the head in the aquitard itself. Since the flow resistance of the

unsaturated zone is accounted for in the soil water submodel, the layer thickness used for Eq.66 is based on the saturated part of this aquitard.

The terms for the regional groundwater flow in Eq. 64 are solved using a finite-element scheme based on the method of Galerkin (1915). This procedure is a special case of the method of weighted residuals (Neuman, 1973; Segerlind, 1984; Wang and Anderson, 1982). In the implementation used for SIMGRO we use a triangular finite-element network, as illustrated by Figure 17. By drawing connection lines between the midpoints

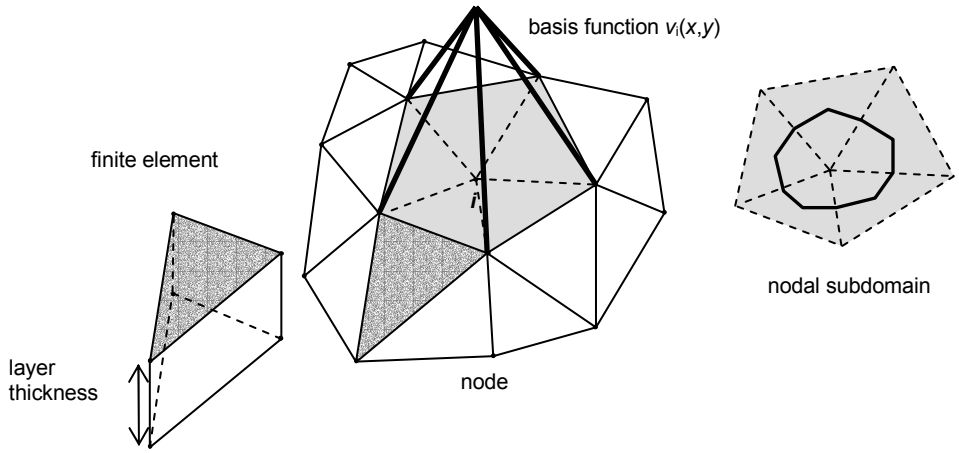

Figure 17 Discretisation of the solution domain into finite triangular elements. The network is repeated for each layer. Piece-wise linear basis functions are used for the' trial solution' (after Bear, 1979). Nodal subdomains are also called 'influence areas'

of the ribs and of the centre-points of the triangles, the so-called influence areas are constructed. These influence areas serve as nodal subdomains for the vertical flux densities in Eqs. 62 and 64. Note that these domains are *not* the same as so-called Thiessen polygons.

In the model implementation the drainage flux is determined in a separate cycle. So Eq. 64 can be rewritten as

$$\mathrm{G}(\varphi) = \frac{1}{\Delta t_{\mathrm{g}}} \int_{t_g - \Delta t_g}^{t_g} \left[\frac{\partial}{\partial x}\left(T_{\mathrm{x}} \frac{\partial \varphi}{\partial x} \right) + \frac{\partial}{\partial y}\left(T_{\mathrm{y}} \frac{\partial \varphi}{\partial y} \right) + q_{\mathrm{z}} \right] dt - \mu \frac{\Delta \varphi}{\Delta t_g} + q_{\mathrm{const}} = 0 \qquad (67)$$

The function G(φ) is used in constructing the numerical solution for this equation. For solving Eq. 67 with the Galerkin method a 'trial solution' is constructed using piece-wise linear basis functions as illustrated in Figure 17. The hydraulic head is then approximated with:

$$\tilde{\varphi}(x, y, t) = \sum_{i=1}^{N} h_{\mathrm{i}}(t)\, v_{\mathrm{i}}(x, y) \qquad (68)$$

where $v_i(x,y)$ is a basis function in the range of [0;1], $h(t)$ the solution of Eq. 67 at the nodal points, and $\tilde{\varphi}$ the piece-wise linear approximation of φ. In the Galerkin method the basis functions are not only used for the piece-wise approximation of φ, but also for the *weighting* of the residuals (e.g. Bear, 1979:

$$\iint_A \mathrm{G}(\tilde{\varphi}(x, y, t))\, v_i(x, y)\, dx dy = 0, \quad \text{for } i = 1,2...,N \tag{69}$$

where A is the flow domain. The component involving -div $\mathbf{q}^a$ concerns the net water balance of the horizontal flows:

$$\sum_j \tilde{Q}_{ji} = \iint_A \left[\frac{\partial}{\partial x}\left(T_x \frac{\partial \tilde{\varphi}}{\partial x} \right) + \frac{\partial}{\partial y}\left(T_y \frac{\partial \tilde{\varphi}}{\partial y} \right) \right] v_i(x, y)\, dx dy, \quad \text{for } i = 1,2...,N \tag{70}$$

where $\sum_j \tilde{Q}_{ji}$ is the net horizontal inflow to a *nodal* subdomain. Note that the above given equation is in terms of a *summation*. It is incorrect to simply interpret the $\tilde{Q}_{ji}$'s as 'flows from one node to the other', because we are here dealing with a finite-element solution, and not a finite-difference one. The equation gives a statement with respect to the net water balance of a nodal subdomain, and not about the individual flows themselves. As put by Pinder and Gray (1977): "The finite element method may be considered as a numerical scheme wherein the algebraic equations represent spatially averaged derivative approximations". Strictly speaking, only in the case of a completely regular network (and isotropic medium) can the flows be interpreted as if it were (integrated) finite differences. But even if that condition is not fulfilled, in most practical applications the interpretation in terms of flows is an acceptable approximation. If desired, a more accurate analysis of the actual flows and flow paths can be made using the method of Cordes and Kinzelbach (1992), which was implemented as post-processing for SIMGRO by Tank and Stuyt (1997).

In for instance Kinzelbach (1986) the derivation is given for numerically computing the net horizontal flow balance with:

$$\sum_j \tilde{Q}_{ji} = \sum_j T_{ji}(h_j - h_i) \tag{71}$$

where T_{ji} is the (symmetric) transmissivity matrix ($m^2\, d^{-1}$). For a phreatic aquifer the transmissivities also depend on the head itself.

In the integration of Eq. 69 the leakage term is taken as constant within the nodal subdomain, but variable with respect to the time t. The integration of the leakage component then takes on the form:

$$\iint_A q_z(x, y, l, t)\, v_i(x, y)\, dx dy = q_{z,i,l}(t) \iint_A v_i(x, y) dx dy = q_{z,i,l}(t) A_i \tag{72}$$

for all i=1,2,…N, and all aquifers (always including the top layer, even if it is an aquitard), where A_i is the area of the nodal subdomain, the 'influence area'. (Note that the basis function is a pyramid with a volume of 1/3 A_b h, where A_b is the area of its base, and h its height, with h equal to unity. The area of the base is three times the size of a nodal subdomain A_i, because each of the subtriangles is equally shared by three neighbours.)

The integration of Eq. 69 with respect to time (see also Eq. 67) is done with a Crank-Nicholson (1947) weighting scheme. By inserting the expressions given in Eqs. 70 and 72 the generated set of equations becomes:

$$A_{\mathrm{i}}\,\mu_{\mathrm{i},l}\,\frac{\Delta h_{\mathrm{i},l}}{\Delta t_{\mathrm{g}}} = (1-W)\left[\sum_{\mathrm{j}} Q_{\mathrm{ji},l} + q_{\mathrm{z,i},l}A_{\mathrm{i}}\right]^{t_{\mathrm{g}}-\Delta t_{\mathrm{g}}} + W\left[\sum_{\mathrm{j}} Q_{\mathrm{ji},l} + q_{\mathrm{z,i},l}A_{\mathrm{i}}\right]^{t_{\mathrm{g}}} + q_{\mathrm{const,i},l}A_{\mathrm{i}} \quad (73)$$

for i=1,2,...N, and all l that are aquifers (always including the top layer, even if it is an aquitard), where

A_{i} = area of nodal subdomain i (m^2)
$\mu_{\mathrm{i},l}$ = storage coefficient of nodal subdomain i, layer l (-)
$\Delta h_{\mathrm{i},l}$ = change of hydraulic head over time interval $[t_{\mathrm{g}}\text{-}\Delta t_{\mathrm{g}}\,;\,t_{\mathrm{g}}]$ in node i, layer l (m)
W = Crank-Nicholson weighting parameter (-)
$\sum_{\mathrm{j}} Q_{\mathrm{ji},l}$ = sum of net horizontal fluxes to nodal subdomain i, layer l ($\mathrm{m}^3\,\mathrm{d}^{-1}$)
$q_{\mathrm{const,i},l}$ = total of flows that are taken constant within the time interval ($\mathrm{m\,d}^{-1}$)
$q_{\mathrm{z,i},l}$ = leakage term given by Eq. 66 ($\mathrm{m\,d}^{-1}$)

Rearranging to a convenient form yields:

$$\begin{aligned} A_{\mathrm{i}}\,\mu_{\mathrm{i},l}\,\frac{\Delta h_{\mathrm{i},l}}{\Delta t_{\mathrm{g}}} &= \left[\sum_{\mathrm{j}} Q_{\mathrm{ji},l} + q_{\mathrm{z,i},l}A_{\mathrm{i}}\right]^{t_{\mathrm{g}}-\Delta t_{\mathrm{g}}} + \ldots \\ &\ldots + W\left[\sum_{\mathrm{j}} \Delta Q_{\mathrm{ji},l} + \left(\frac{\partial q_{\mathrm{z,i},l}}{\partial h_{\mathrm{i},l}}\Delta h_{\mathrm{i},l} + \frac{\partial q_{\mathrm{z,i},l}}{\partial h_{\mathrm{i},l-2}}\Delta h_{\mathrm{i},l\text{-}2} + \frac{\partial q_{\mathrm{z,i},l}}{\partial h_{\mathrm{i},l+2}}\Delta h_{\mathrm{i},l+2}\right)A_{\mathrm{i}}\right] + q_{\mathrm{const,i},l}A_{\mathrm{i}} \end{aligned} \quad (74)$$

for i =1,2,...N, and l that are aquifers, where

$$\sum_{\mathrm{j}} \Delta Q_{\mathrm{ji},l} = \sum_{\mathrm{j}} Q_{\mathrm{ji},l}{}^{t_{\mathrm{g}}} - \sum_{\mathrm{j}} Q_{\mathrm{ji},l}{}^{t_{\mathrm{g}}-\Delta t_{\mathrm{g}}} \quad \text{and} \quad \Delta h_{\mathrm{i},l} = h_{\mathrm{i},l}{}^{t_{\mathrm{g}}} - h_{\mathrm{i},l}{}^{t_{\mathrm{g}}-\Delta t_{\mathrm{g}}} \quad (75)$$

The partial derivatives of $q_{\mathrm{z,i},l}$ are constants, as can directly be seen from Eq. 66. Substitution of Eq. 71 then yields the equations in terms of the hydraulic head *change*:

$$\begin{aligned} A_{\mathrm{i}}\,\mu_{\mathrm{i},l}\,\frac{\Delta h_{\mathrm{i},l}}{\Delta t_{\mathrm{g}}} &= \left[\sum_{\mathrm{j}} Q_{\mathrm{ji},l} + q_{\mathrm{z,i},l}A_{\mathrm{i}}\right]^{t_{\mathrm{g}}-\Delta t_{\mathrm{g}}} + \ldots \\ &\ldots + W\left[\sum_{\mathrm{j}} T_{\mathrm{ji}}(\Delta h_{\mathrm{j},l} - \Delta h_{\mathrm{i},l}) + \left(\frac{\partial q_{\mathrm{z,i},l}}{\partial h_{\mathrm{i},l}}\Delta h_{\mathrm{i},l} + \frac{\partial q_{\mathrm{z,i},l}}{\partial h_{\mathrm{i},l-2}}\Delta h_{\mathrm{i},l\text{-}2} + \frac{\partial q_{\mathrm{z,i},l}}{\partial h_{\mathrm{i},l+2}}\Delta h_{\mathrm{i},l+2}\right)A_{\mathrm{i}}\right] + \ldots \\ &\ldots + q_{\mathrm{const,i},l}A_{\mathrm{i}} \end{aligned} \quad (76)$$

for i=1,2,...N and l that are aquifers. For the deeper aquifers these equations are linear. For the phreatic aquifer the left-hand side is given by the left-hand side of Eq. 62 (or 63). Since the storage function is nonlinear for the phreatic layer (supplied in the form of a piece-wise linear table function), the mean storage coefficient $\mu_{\mathrm{i},1}$ over the $\Delta h_{\mathrm{i},1}$-interval is not known beforehand. For this reason an iterative scheme is the preferred way of obtaining a solution. We currently use a successive-over-relaxation method (SOR), as for instance described by Remson et al. (1971). To apply the method, Eq. 76 is rearranged, with only $\Delta h_{\mathrm{i},l}$ on the left-hand side:

$$A_{\mathrm{i}}\,\mu_{\mathrm{i},l}\,\frac{\Delta h_{\mathrm{i},l}}{\Delta t_{\mathrm{g}}}+W\left(\sum_{j}T_{\mathrm{ji},l}\Delta h_{\mathrm{i},l}-\frac{\partial q_{\mathrm{z,i},l}}{\partial h_{\mathrm{i},l}}\Delta h_{\mathrm{i},l}A_{\mathrm{i}}\right)=....$$

$$...=\left[\sum_{j}Q_{\mathrm{ji},l}+q_{\mathrm{z,i},l}A_{\mathrm{i}}\right]^{t_{\mathrm{g}}-\Delta t_{\mathrm{g}}}+W\left[\sum_{j}T_{\mathrm{ji},l}\Delta h_{\mathrm{j},l}+\left(\frac{\partial q_{\mathrm{z,i},l}}{\partial h_{\mathrm{i},l-2}}\Delta h_{\mathrm{i},l\text{-}2}+\frac{\partial q_{\mathrm{z,i},l}}{\partial h_{\mathrm{i},l+2}}\Delta h_{\mathrm{i},l+2}\right)A_{\mathrm{i}}\right]+q_{\mathrm{const,i},l}A_{\mathrm{i}}$$

$$\Rightarrow\Delta h_{\mathrm{i},l}=\frac{\left[\sum_{\mathrm{j}}Q_{\mathrm{ji},l}+q_{\mathrm{z,i},l}A_{\mathrm{i}}\right]^{t_{\mathrm{g}}-\Delta t_{\mathrm{g}}}+W\left[\sum_{\mathrm{j}}T_{\mathrm{ji},l}\Delta h_{\mathrm{j},l}+\left(\frac{\partial q_{\mathrm{z,i},l}}{\partial h_{\mathrm{i},l-2}}\Delta h_{\mathrm{i},l\text{-}2}+\frac{\partial q_{\mathrm{z,i},l}}{\partial h_{\mathrm{i},l+2}}\Delta h_{\mathrm{i},l+2}\right)A_{\mathrm{i}}\right]+q_{\mathrm{const,i},l}A_{\mathrm{i}}}{\left[\frac{A_{\mathrm{i}}\,\mu_{\mathrm{i},l}}{\Delta t_{\mathrm{g}}}+W\left(\sum_{\mathrm{j}}T_{\mathrm{ji},l}-\frac{\partial q_{\mathrm{z,i},l}}{\partial h_{\mathrm{i},l}}A_{\mathrm{i}}\right)\right]}\qquad(77)$$

Each SOR-iteration consists of first evaluating $\Delta h_{\mathrm{i},l}{}^{\mathrm{j}}$ using Eq. 77, and then extrapolating the result with the over-relaxation factor Ω (all within the same iteration cycle *j*):

$$\Delta h_{\mathrm{i},l}^{\mathrm{j}}=\Delta h_{\mathrm{i},l}^{\mathrm{j}}+\Omega(\Delta h_{\mathrm{i},l}^{\mathrm{j}}-\Delta h_{\mathrm{i},l}^{\mathrm{j}-1})\qquad(78)$$

The disadvantage of every iterative method is that a certain criterion has to be used for halting the iterations; otherwise the computational time becomes excessive. But halting the iterations inevitably involves a violation of the water balance. This error can especially be significant if the conductivity of an aquifer is high, and the nodal subdomains are very small. In order to mend this error, it is first computed by rearranging Eq. 76 to:

$$Q_{\mathrm{loss,i},l}=q_{\mathrm{const,i},l}A_{\mathrm{i}}-\mu_{\mathrm{i},l}\frac{\Delta h_{\mathrm{i,1}}}{\Delta t_{\mathrm{g}}}A_{\mathrm{i}}+\left[\sum_{\mathrm{j}}Q_{\mathrm{ji},l}+q_{\mathrm{z,i},l}A_{\mathrm{i}}\right]^{t_{\mathrm{g}}-\Delta t_{\mathrm{g}}}+...$$
$$...+W\left[\sum_{\mathrm{j}}T_{\mathrm{ji},l}(\Delta h_{\mathrm{j},l}-\Delta h_{\mathrm{i},l})+\left(\frac{\partial q_{\mathrm{z,i},l}}{\partial h_{\mathrm{i,1}}}\Delta h_{\mathrm{i},l}+\frac{\partial q_{\mathrm{z,i},l}}{\partial h_{\mathrm{i},l-2}}\Delta h_{\mathrm{i},l\text{-}2}+\frac{\partial q_{\mathrm{z,i},l}}{\partial h_{\mathrm{i},l+2}}\Delta h_{\mathrm{i},l+2}\right)A_{\mathrm{i}}\right]\qquad(79)$$

where $Q_{\mathrm{loss,i},l}$ is the amount of water that has been lost during the time step in ($m^3\ d^{-1}$). The amount of water is accumulated per node with a continuing balance:

$$\sum Q_{\mathrm{loss,i},l}=\sum Q_{\mathrm{loss,i},l}+Q_{\mathrm{loss,i},l}\Delta t_{\mathrm{g}}\qquad(80)$$

During the next time step part of this water loss is recouped, by adding half of it to the water balance on the right-hand side of Eq. 76, and at the same time reducing the continuing balance of the loss by:

$$\sum Q_{\mathrm{loss,i},l}=0.5\sum Q_{\mathrm{loss,i},l}\qquad(81)$$

It is not advisable to try and recoup all of the accumulated loss straightaway in the next time step, because that can lead to oscillations. By each time step recouping half of the accumulated loss, any water balance error is redressed within a day or two, if the time step of the groundwater model is the commonly used value of 0.25 d. In this way a near-perfect water balance is maintained throughout the simulation period.

4.3.2 Drainage

As regards the drainage flow to watercourses, the flow description given in §4.2.2 was for the theoretical situation with parallel watercourses that have an equal spacing *L*. In practice, the nodal subdomains are criss-crossed by watercourses having varying dimensions, like in the example of Figure 18. A certain watercourse is active as a drainage or infiltration medium if either the groundwater level or the surface water level is higher than the elevation of the bottom of the watercourse, and if the levels differ from each other. In order to apply the given theory in §4.2.2, several adaptations are required.

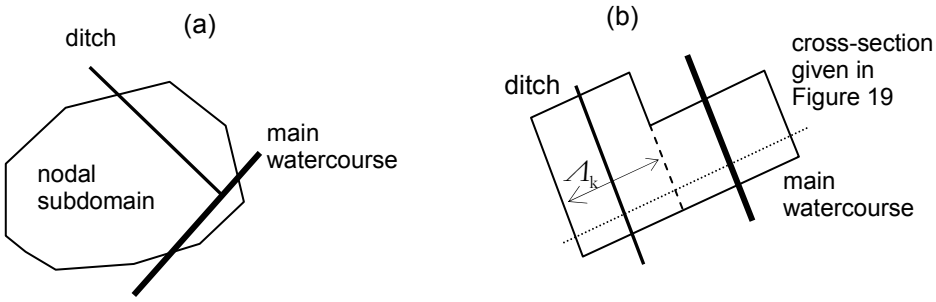

Figure 18 Example of a nodal subdomain that is criss-crossed by watercourses having vary dimensions: practical situation (a), and schematised situation used in the calculation method (b)

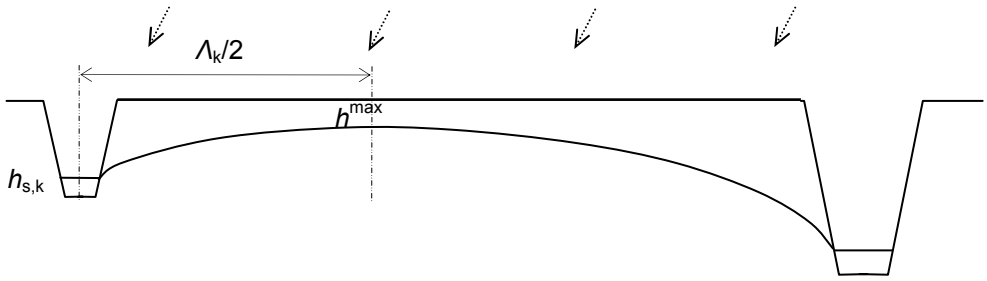

Figure 19 Example of a cross-section of the shallow groundwater for a situation with simultaneous drainage flow to a ditch and a main watercourse (see also Figure 18)

The first adaptation is to group the watercourses into a number of categories *k*, having similar characteristics in terms of:

- the cross-section;
- the entrance resistance;
- surface water level.

Obviously, in practical situations the watercourses are not parallel, and different types can be present. For such situations it is only possible to compute an 'equivalent' spacing, by dividing the area of a subdomain through the length of watercourse (Ernst, 1978):

$$L_k = \frac{A_i}{l_k} \tag{82}$$

where
L_k = equivalent spacing of watercourses in category k (m)
A_i = area of nodal subdomain (m^2)
l_k = total length of watercourses in category k (m).

Ernst (1978) presents and discusses a method for using the equivalent drainage spacing in a regional analysis of different flows to watercourses of varying cross-sections and spacings. The method takes into account the interdependency of the drainage flows to the different categories of watercourses. The route a water droplet takes within the groundwater body depends on the total configuration. Even though the method of Ernst (1978) is theoretically sound, it is not used here for computational reasons. Instead, we use an alternative approach that accounts for combinations of simultaneous infiltration and drainage and for the arising combinations of head losses due to 'horizontal' and 'radial' flows.

Our approach involves the introduction of an entity the 'drainage influence span' as a function of the relative strength of the drainage flux towards a certain category of water courses. For this we first compute the 'drainage subarea' a_k of each category of water-courses according to

$$a_k = \frac{|Q_{d,k}|}{\sum |Q_{d,k}|} A_i \tag{83}$$

where $Q_{d,k}$ is the drainage flux to category of watercourses k within the nodal subdomain in [m^3 d^{-1}]. The underlying assumption of Eq. 83 is a uniformly distributed recharge over the area in the nodal subdomain, whatever the circumstances and the type of drainage medium that is involved (small/large watercourse). The absolute values are used, because it is also possible that infiltration takes place instead of drainage. And, even more complex, it is possible that both drainage and infiltration take place *simultaneously* within the same nodal subdomain. Both directions of flow 'need' a certain part of the soil volume for the flow, so in that sense both are competing for use of the (same) flow medium. For situations with a relatively high density of watercourses, this method entails that the situation in a nodal subdomain is schematized to that of (b) in Figure 18. For each of the watercourse categories, the mean 'drainage influence span' can now be calculated with

$$\Lambda_k = \frac{a_k}{l_k} \tag{84}$$

For situations with $\Lambda_k > \sqrt{A_i}$ the schematization as given in Figure 18 becomes unrealistic, due to the sideways-elongated form of the drainage subarea. That would lead to an *over*-estimate of the horizontal drainage resistance, because the water would have to travel an unrealistic distance in the local flow system. (This does not, however, apply to the radial and entrance resistance. The reason for the horizontal resistance being different is that Λ itself is in the expression for it, as is evident from Eq. 53. But Λ is not

present in the expressions for the other resistances, as given in Eq. 57 for the radial resistance and Eq. 58 for the entrance resistance.) On the other hand, by simply taking Λ_k as $\min(a_k/l_k; \sqrt{A_i})$ the estimate would become too *low*.

In order to arrive at a reasonably sound approximation for the case where Λ_k exceeds $\sqrt{A_i}$ a radial flow formulation can be used as explained in Appendix 2. That method yields a correction factor for the horizontal resistance, as compared to the value obtained by simply using the value of Λ_k as given by Eq. 84. Apart from yielding a correction factor for the horizontal resistance, the method given in Appendix 2 also yields a form factor that differs from the value 2/3 of Eq. 53 (in its simplified linear form). The form factor is needed for the drainage calculation, as will be explained subsequently.

Like in the computation of the vertical leakage flux densities we consider the groundwater level h at the nodal point as being representative for a nodal subdomain, and we thus interpret it as a *mean* level. In the case that this level is higher than the bottom of a watercourse, one can be sure that the watercourse is active, either involving infiltration or drainage. In the case that the level is below the deepest bottom, one can be sure that *none* of the watercourses will be draining. But it is not always so clear-cut. The intermediate situation can occur with a watercourse actively draining, even though the *mean* groundwater level is below the bottom of that watercourse. That this possibility exists has to do with the local head variation caused by the horizontal drainage resistance. For this reason the drainage calculation method also includes the calculation of the (unknown) h^{max}, which is the maximum (local) groundwater level within a nodal subdomain. Put more precisely, that is the level at the culmination point between two watercourses. Examples of cross-sections of the shallow groundwater are given in Figure 19 for the line indicated in Figure 18. It is assumed that h^{max} is the same for all of the drainage subareas, which is of course an approximation. In order to compute it, we first formulate the drainage flow equations as if we already know its value, and also the (as yet unknown) Λ_k's.

For a given h^{max} and Λ_k the drainage flux to a category of water courses k can be computed as (cf. Eq. 60):

$$Q_{d,k} = l_k \Lambda_k q_{d,k} = l_k \frac{h^{max} - h_{s,k}}{\omega_{v,k} + \omega_{h,k} + \omega_{r,k} + \omega_{e,k}} \tag{85}$$

where $h_{s,k}$ is the surface water level in water courses of category k, the drainage base. Subsequently we can compute the mean head elevation within the drainage subarea a_k of the nodal subdomain with (cf. Eq. 59):

$$h_k^m = h_{s,k} + \frac{Q_{d,k}}{l_k}(\omega_{v,k} + \zeta_k \omega_{h,k} + \omega_{r,k} + \omega_{e,k}) \tag{86}$$

where ζ_k is the form factor for the horizontal drainage flow of watercourses in category k. The weighted mean of h_k^m should be equal to the mean groundwater level h in the nodal subdomain:

$$\frac{1}{A_i} \sum a_k h_k^m = h \tag{87}$$

In the calculation procedure we have to solve for the following unknowns: h^{max} and the Λ_k's, the latter being equivalent to solving for the unknown a_k's. For the solution we use an iterative scheme. In the initial step of the very first calculation, we assume that all the categories of watercourses have the same 'drainage influence span', as given by:

$$\Lambda_k^{\,o} = \frac{A_i}{\sum_k l_k} \tag{88}$$

For the next steps of the calculation (and for new time steps), we simply use the last value as a starting point. The iterative scheme involves the following steps:

1. Perform the initialization of the drainage spans Λ_k, the drainage subareas a_k, the head at the culmination point h^{max}.
2. Compute the horizontal drainage resistances ω_h.
3. Compute the $Q_{d,k}$'s with Eq. 85, and compute the sum of $|Q_{d,k}|$; then recompute the drainage subareas a_k using Eq. 83, and the new drainage spans Λ_k using Eq. 84.
4. Compute the mean head $h_k^{\,m}$ within the drainage subarea using Eq. 86, and then compute the mean level in the nodal subdomain $h^{m,j}$, using Eq. 87; compute the new h^{max}.
5. Now compare the value of $h^{m,j}$ with the value h obtained of the regional model. Return to 2 if convergence of $h^{m,j}$ has not been reached.

Since the drainage flux is recomputed for each surface water time step, the strict adherence to the above scheme could lead to a large increase of the computational burden. In order to avoid this, a pragmatic approach is followed, involving at most two iteration cycles per surface water time step.

4.4 Data summary

The input data of the geohydrologic schematization consist of the following parameters given per nodal subdomain:
- thickness of the layers;
- conductivities in the *xy*-plane for aquifers, *xz*-plane for aquitards.

Boundary conditions can be supplied in the form of heads or net fluxes within all nodes of the domain. The flow to a well can either involve a head or a flux boundary condition. In the latter case we assume that it is always possible to extract the desired amount. In order for this assumption to be valid, a separate analysis is required for the detailed situation around a well. The extractions are converted to 'diffuse' flux densities (dividing by area of nodal subdomain).

Drainage characteristics of watercourse categories are supplied in the form of a long list, along with the geometry in the separate nodal domains. The watercourses themselves are described in §5. Here it is relevant to note that a distinction is made between:
- watercourses in the conventional sense, with a cross-section; for these the drainage characteristics given in terms of:
  - entrance resistance and radial resistance;
  - horizontal resistance; this resistance is optional, because it can also be dynamically computed by the model from the basic data (geometry and subsoil conductivities) using the iterative scheme given above;
- field drains, with a radius instead of cross-section; the same resistance data as for water courses;
- gulleys, with the drainage characteristics given in terms of a total drainage resistance for the situation when the gulleys just start draining;
- soil surface, with a drainage depth of zero, and a very low drainage resistance (<1 d).

5 Surface water

5.1 Introduction

Surface water plays a key role in the functioning of many regional hydrologic systems. The interaction with the soil water and groundwater can be very complex. Seen from the perspective of groundwater, surface water acts as a boundary condition for the drainage/infiltration flux; but that flux also influences the surface water dynamics itself. Depending on the local conditions, the mobility of the surface water can range widely. In lakes and in depressions of the soil surface it is relatively immobile. Therefore lakes are modelled as 'visible' groundwater (cf. Figure 13). Depression storage is modelled in combination with the simplified runoff concept as described in §3.2.1 and §3.3.1.

Large-scale lateral movement of surface water (i.e. transcending the scale of nodal subdomains) is assumed to take place through a network of conduits that forms part of the model schematization. In the following, we will confine ourselves to this channel flow.

5.2 Theory

Using the full form of the Saint Venant equations (non-steady gradually varied flow in open conduits) for the whole channel network would lead to an unwieldy integrated model: compared to the soil water and groundwater submodels the surface water model would require a disproportionate amount of computational effort. Therefore a flexible modelling concept is used, involving a simplified model for the smaller channels and a hydraulic model for the larger ones. Here we confine ourselves to describing the simplified concept.

Just like in the soil-water modelling, the dynamics of surface water are simulated with a quasi-steady state method, using a stream of steady-state situations. For the steady states we assume gradually varied non-uniform flow. The momentum equation can for instance be stated as (Chow, 1959)

$$\frac{dy}{dx} = \frac{S_o - Q^2 / C^2 A_f^2 R}{1 - \alpha Q^2 / g A_f^2 D_h} \tag{89}$$

and the continuity (for steady-state flow) as

$$\frac{dQ}{dx} = q_{lat} \tag{90}$$

where
x = distance along the watercourse (m)
y = water depth (m)
z = elevation of the channel bottom (m)
S_o = slope of the channel bottom, dz/dx (-)
Q = discharge ($m^3\ s^{-1}$)

α = energy coefficient (-)
g = acceleration due to gravity ($m^2\ s^{-1}$)
C = Chézy coefficient ($m^{1/2}\ s^{-1}$)
A_f = cross-sectional area of the water normal to the direction of flow (m^2)
R = hydraulic radius (A_f divided by the wetted perimeter) (m)
D_h = hydraulic depth (A_f divided by the width of the free surface) (m)
q_{lat} = lateral inflow per unit of length of the channel ($m^2\ s^{-1}$)

For handling Eq. 89 we use a dynamic metamodelling method: it is first solved in the 'pre-processing' stage using a hydraulic model, covering a wide range of boundary conditions. The results are then stored and subsequently used in the form of hydraulic metafunctions. The transitions between the steady-state flow situations are calculated using the continuity equation in the form of:

$$\frac{\partial A_f}{\partial t} + \frac{\partial Q}{\partial x} = q_{lat} \tag{91}$$

5.3 Model implementation

5.3.1 Schematization and hydraulic metafunctions

The watercourses are divided into trajectories. Structures are assumed located at the end of a trajectory, with the simulated water level pertaining to the upstream situation just before the end. Depending on the detail of the implementation the explicitly modelled watercourses can involve even the smallest of ditches.

For a given schematization of watercourses the storage function is used in the form of:

$$S_n = \Xi_n(h_{s,n}) \tag{92}$$

where S (value) and Ξ (function) represent the storage in the watercourse trajectory n (m^3) in dependency of the water level $h_{s,n}$. For deriving the storage function we assume a constant cross-section within a trajectory. The function also includes the 'added storage' in the ditches that are connected to it within a subcatchment (Figure 3). An example is given in Figure 20.

In the model implementation we make the assumption that at the end of each trajectory there is a *unique* relationship between the water level and the flow rate. This relationship in the form of a metafunction is denoted by:

$$Q_n = \Theta_n(h_{s,n}) \tag{93}$$

where Q_n (value) and Θ_n ($h_{s,n}$) (function) are the outflow ($m^3\ s^{-1}$) from trajectory n. The metafunction $\Theta(h_{s,n})$ can be obtained in various ways, depending on:
- whether there is a weir or other structure at the end of the trajectory;
- whether or not a hydraulic model is used for deriving the metafunctions.

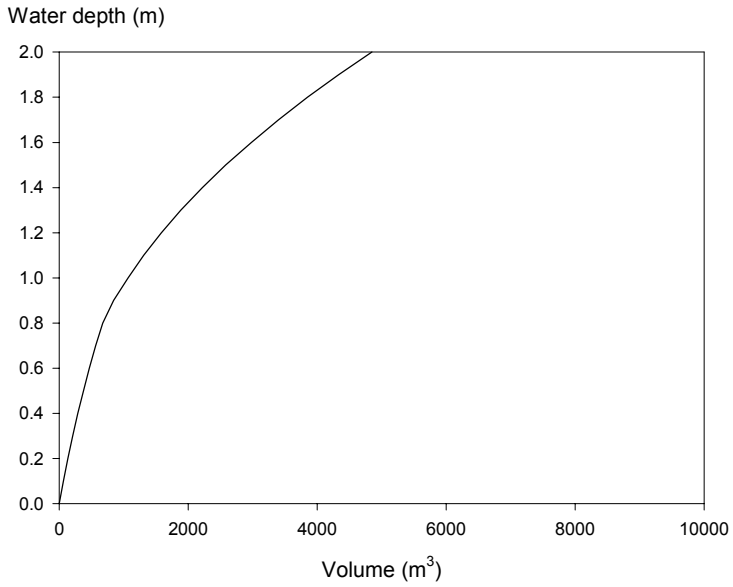

Figure 20 Example of a storage function for a trajectory (bottom width 2 m, side slopes 1:1, length 300 m), with ditches entering the watercourse at a height of 0.8 m (bottom depth of ditches 0.5 m, side slopes 1:1, total length of ditches within subcatchment 1200 m).

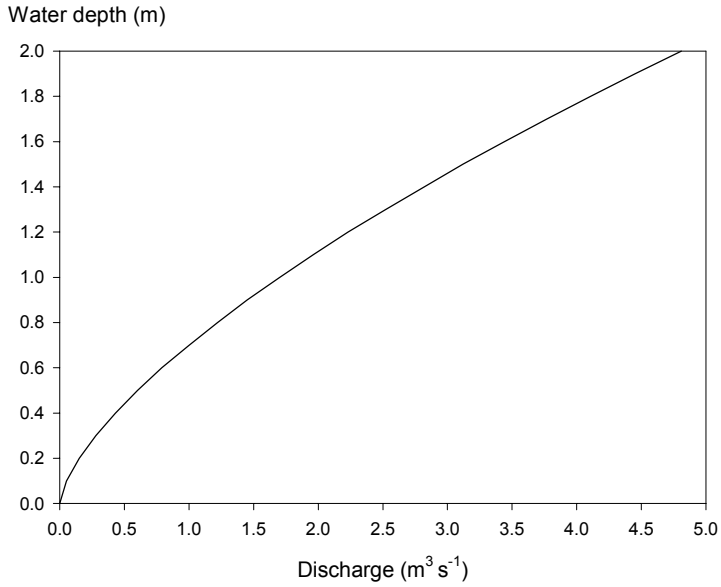

Figure 21 Example of a discharge function for a trajectory (rectangular short-crested weir with a crest width of 1 m, see Eq. 94)

Structures

For structures like weirs and culverts it is possible to use the special relationships describing the flow. For a simple rectangular short-crested weir, for instance, one can use (see Figure 21 for an example):

$$\Theta_{\mathrm{n}}(h_{\mathrm{s,n}}) = 1.7w(h_{\mathrm{s,n}} - h_{\mathrm{c}})^{1.5} \qquad (94)$$

where

$h_{s,n}$ = water level in trajectory n (m)
h_c = elevation of weir crest (m)
1.7 = weir coefficient (dependent on the type of weir) ($m^{0.5}$ s^{-1})
w = width of weir crest (m)

For the management of the crest level the model can employ several types of operational rules, as described in §6.3.1. In the case of a partially submerged weir the flow becomes less than what is given by Eq. 94: both the discharge coefficient and the exponent are influenced by the downstream water level. But to stay within the limitations of the model code we approximate the flow reduction by inserting the downstream water level $h_{s,n+1}$ in Eq. 94, instead of h_c. Another simplified representation of reality is that if the upstream water level rises above the soil surface next to the weir, the water involved in the excess head is assumed to flow freely to the next trajectory.

For a culvert, the relationship is given in terms of the head *difference*:

$$\Theta_n(h_{s,n}, h_{s,n+1}) = c\sqrt{(h_{s,n} - h_{s,n+1})} \tag{95}$$

where $h_{s,n+1}$ is the water level in the trajectory downstream of trajectory n, and c is a discharge coefficient ($m^{2.5}$ s^{-1}) depending on the hydrodynamic properties of the culvert and the in- and outlet design. In situations with the downstream water level below the bottom of the culvert, the bottom-level h_c is used instead of $h_{s,n+1}$.

Open water conduits
For trajectories with unobstructed channel flow the simplest way of deriving the metafunctions is by assuming that the flow is uniform and that the influence of the trajectories on each other is negligible. By the latter is meant that the flow in the trajectories is not influenced by any backwater effects. This method is implemented by using the Chézy formula (made explicit by setting dy/dx=0 in Eq. 89) independently for each of the trajectories. But in many cases this simplification is inadequate. Then the preferred way of deriving the metafunctions is by performing computational experiments with a hydraulic model. In an example (Hermans *et al.,* 2004) using SOBEK (WL|Delft Hydraulics, 2001) the movable weirs were set to their lowest position. Subsequently, the weirs were introduced in SIMGRO using relationships as e.g. given in Eq. 94.

A more sophisticated way of generating the metafunctions is to include the *management* of the weirs in the hydraulic model with which the experiments are made. The disadvantage of that method is, however, that each new water management strategy requires doing the computational experiments anew. Another point is that the spatial distribution of the lateral inflow cannot be accurately foreseen without running the SIMGRO-model first. So of course the metamodelling of surface water has its limitations. In addition, to avoid anomalies in the simulation results, various amendments have been made to the model implementation, as described in §5.3.2.

5.3.2 Dynamics

Water balance
The water balance of a trajectory is written as

$$S_{\mathrm{n}}(t_{\mathrm{s}}) + \int_{t_s-\Delta t_{\mathrm{s}}}^{t_{\mathrm{s}}} Q_{\mathrm{out,n}}(t)dt = S_{\mathrm{n}}(t_{\mathrm{s}}-\Delta t_{\mathrm{s}}) + \int_{t_{\mathrm{s}}-\Delta t_{\mathrm{s}}}^{t_{\mathrm{s}}} [Q_{\mathrm{in,n}}(t) + Q_{\mathrm{lat,n}}(t)]dt \qquad (96)$$

where
$S_{\mathrm{n}}(t_{\mathrm{s}})$ = storage in trajectory *n* (m^3)
$Q_{\mathrm{out,n}}(t)$ = outflow of trajectory *n* ($m^3\ d^{-1}$)
$Q_{\mathrm{in,n}}(t)$ = upstream inflow of trajectory *n* ($m^3\ d^{-1}$)
$Q_{\mathrm{lat,n}}(t)$ = lateral inflow of trajectory *n* ($m^3\ d^{-1}$)

The lateral inflow can be composed of several terms, which can also include extractions. The assumption is that these terms are evenly distributed along a trajectory, so that this also holds for the net inflow given by Q_{lat}.

Solution scheme
Solving for the new water levels and discharges is done in two major steps:
- initially the assumption is made that the outflow from a trajectory (and also the flow direction) is uniquely defined for a certain water level, by the outflow metafunction Θ as given in Eq. 93 (or Eq. 94/95);
- the obtained solution is then checked for hydraulic anomalies (like flow to a trajectory having a higher water level), and if necessary it is corrected.

Given the assumption in the first solution step that the outflow from a trajectory is uniquely defined for a certain water level, it is possible to solve Eq. 96 for each trajectory separately, starting from the upstream end to ensure that the solution is based on the updated value of Q_{in}. In the case that the outflow metafunction Θ is given as Eq. 95, the downstream water level of the preceding time step is used as the second argument. For discharge pumps (§6.3.3), the on/off setting is determined at the start of the time step. If a surface water supply link is active (§6.3.2) the extraction and supply rate are also determined at the beginning of the time step. For the integration of Q_{out} within the time step we use a fully implicit scheme, because it is numerically more stable than a Crank-Nicholson weighting. The water balance equation is therefore used in the form:

$$\begin{aligned} S_{\mathrm{n}}(t_{\mathrm{s}}) + Q_{\mathrm{out,n}}(t_{\mathrm{s}})\Delta t_{\mathrm{s}} = S_{\mathrm{n}}(t_{\mathrm{s}}-\Delta t_{\mathrm{s}}) + [Q_{\mathrm{in,n}}(t_{\mathrm{s}}) + Q_{\mathrm{R,n}}(t_{\mathrm{s}}) + .. \\ Q_{\mathrm{D,n}}(t_{\mathrm{s}}) - Q_{\mathrm{S,n}}(t_{\mathrm{s}}) - Q_{\mathrm{E,n}}(t_{\mathrm{s}}) + Q_{\mathrm{I,n}}(t_{\mathrm{s}}) + Q_{\mathrm{U,n}}(t_{\mathrm{s}})]\Delta t_{\mathrm{s}} \end{aligned} \qquad (97)$$

where:
$Q_{\mathrm{R,n}}$ = surface runoff from nodes within the subcatchment of the trajectory ($m^3\ d^{-1}$);
$Q_{\mathrm{D,n}}$ = drainage to (or infiltration from) the trajectory ($m^3\ d^{-1}$);
$Q_{\mathrm{S,n}}$ = extraction of water for sprinkling ($m^3\ d^{-1}$);
$Q_{\mathrm{E,n}}$ = extraction of water for water supply to another trajectory ($m^3\ d^{-1}$);
$Q_{\mathrm{I,n}}$ = inflow of water supply from another trajectory, using a special link ($m^3\ d^{-1}$);
$Q_{\mathrm{U,n}}$ = inflow of water after being processed in a sewage plant ($m^3\ d^{-1}$)

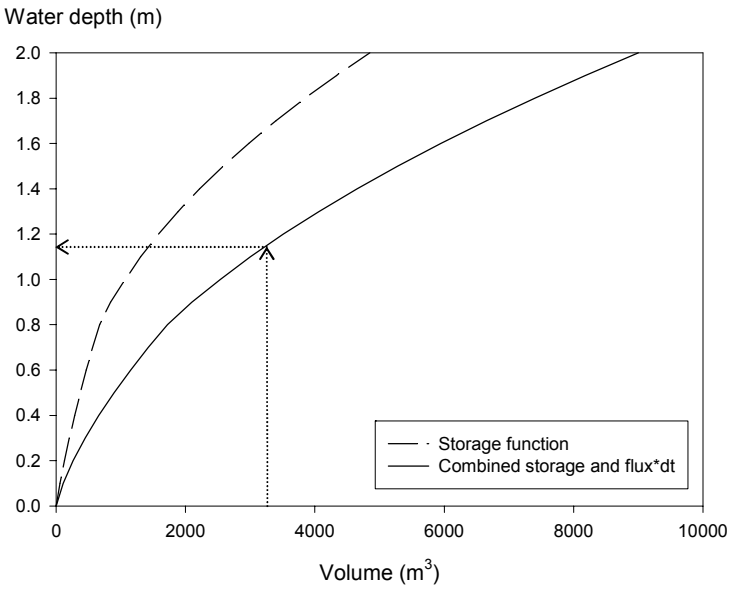

*Figure 22 Combined storage and flux*dt function (Eq. 98, dt=0.01 d) used in solving for the unknown water level and outflow: starting from the evaluated value using Eq. 97 the new water level is found by the inverse table interpolation following the arrow; the outflow is then given by the function shown in Figure 21.*

The surface water system can be highly dynamic, so the time step should be chosen accordingly. Typical values used in the implementation of the model are 0.005 – 0.05 d.

No term is included for the precipitation/evaporation, in order to avoid double counting with the soil-water submodel. We assume that large tracts of surface water are modelled as 'visible' groundwater, with the watercourses simply serving as links to the rest of the network.

For efficient solving of Eq. 97 we prepare a combined storage-flux function (Figure 22) in the form of a table at programme initialization:

$$\sigma_n(h_{s,n}) = \Xi_n(h_{s,n}) + \Theta_n(h_{s,n})\Delta t_s \tag{98}$$

For solving Eq. 97 its right-hand side is first evaluated. The solution for $h_{s,n}$ is then found through an inverse table interpolation of the storage-flux function (arrows in Figure 22). This yields new values for the water level *and* for the outflow (after inserting the new water level in Eq. 93).

It is possible that the outflow from a trajectory *n* is split at a bifurcation (Figure 23). In that case the $\Theta(h_s)$-function given by Eq. 93 is a summation of the flows to the manifold downstream trajectories of *n*. After having computed the new water level and the new outflow, the outflow is divided over the downstream branches according to the $\Theta_{n,n+1}(h_s)$-functions of the separate trajectories diverging from the bifurcation.

Stabilization

The explicit nature of the over-all solution scheme can lead to instabilities, because the levels in the trajectories are solved one-by-one and not as a set. The latter method is customary in hydraulic models, which is inherently more stable. However, the disadvantage of solving a set of equations is the required computational effort. In SIMGRO an alternative way of stabilizing the levels is employed. In the case that the water level

wants to rise faster than a pre-set maximum rate (Δh_{max}), the surplus volume is computed and then temporarily stored. All of this volume is then added to the water balance for the next time step (as an extra term added to Eq. 97). In Figure 24 an example is given of the simulation with and without the described stabilization, for point *c* of Figure 23. From that example it becomes clear that the stabilization is not equivalent to a smoothing operation. In this case the over-all model stabilization affects the distribution of the discharge at the upstream bifurcation (point *b*), leading to a systematic shift in the discharge that passes the weir at *c*.

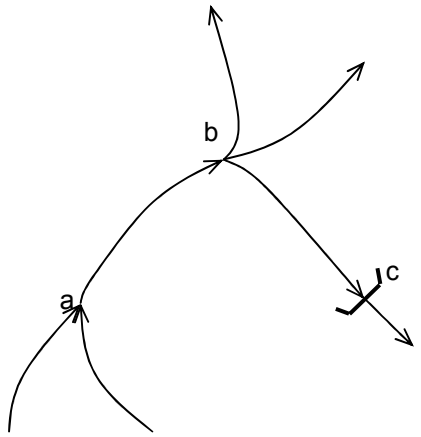

Figure 23 Example of a confluence (a) a bifurcation (b), and a weir (c)

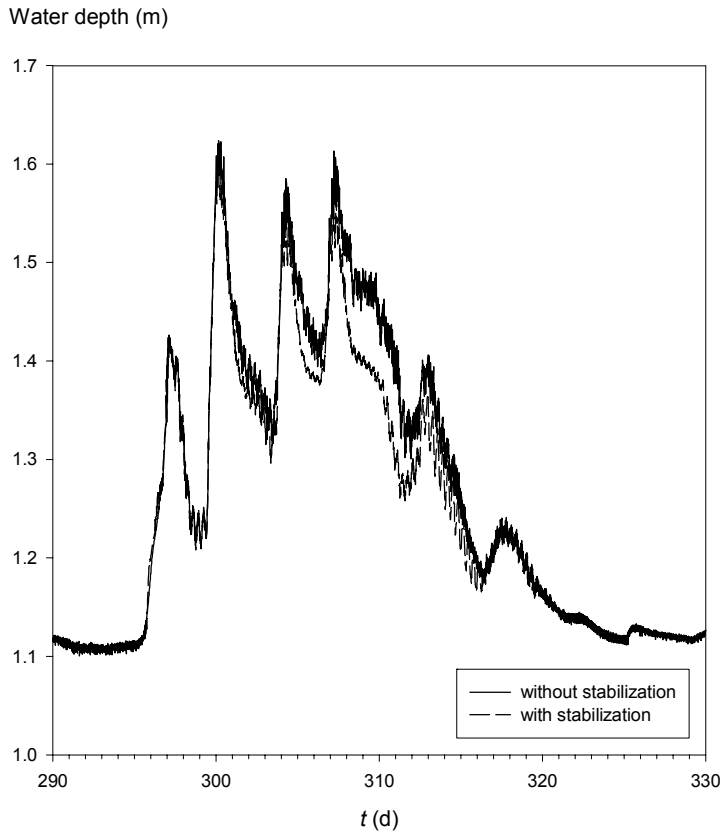

Figure 24 Example of a simulation with and without the stabilization of the explicit calculation scheme. The systematic shift is due to the presence of a bifurcation upstream from the location for which the results are shown. The distribution of water over the branches of that bifurcation is affected by the over-all model stabilization, leading to a lower discharge in this case

Amendments

Before accepting the new discharge and water level as the final solution, a number of checks are made. Modifications are needed in the following instances, which are further explained in the subsequent paragraphs:

- in the presence of a hydraulic structure, and the computed water level becoming higher than the top of the structure, leading to an overflow situation;
- in the presence of an automated weir, with the computed level lower than the target level (see also §6.3.1);
- if the level is lower than the downstream level;
- in the presence of a bifurcation and a higher water level ('flow blocking') in one or more of the branches.

In the presence of a hydraulic structure that gets overflowed (see H_{constr} in Figure 28), the surplus volume is computed and then added to the outflow. The new water level is made exactly equal to the construction height.

In the presence of an automated weir a check is made to see if the target level is reached. If not, part of the outflow is used for filling up until the target level. It can happen that there is not enough water for doing this; the new water level will then be lower than the target, and the outflow is set to zero.

In the case that the downstream water level would otherwise become higher than the upstream one, the flow is temporarily 'put on hold', or the direction is even reversed. For this 'reverse flow' we assume that the friction is zero, because it usually will involve only relatively small flow rates, that are fed by water supply during dry periods (§6.3.2). The frictionless moving of water can be hampered by the discharge function. That is especially relevant if there is an obstruction in the watercourse, like a weir or a culvert (Eq. 94 and 95). Such a situation is taken into account by assuming that the same discharge relationship also holds for flow in the reverse direction, with the up- and downstream levels changed around.

A special case of flow blocking can occur at a bifurcation if in one or more of the downstream branches the water level becomes higher than that in the upstream trajectory. If this occurs the flow to such a branch is (temporarily) set to zero, and divided proportionally over the remaining branches. If *all* of the branches have water levels higher than the upstream one, yet another dividing mechanism is brought into action:

- part of the flow is used for raising the water level in the upstream trajectory to that of the *lowest* level in the downstream branches;
- the remaining part of the flow is sent to the branch with the *lowest* water level.

5.4 Data summary

For practical purposes the following classification into classes of watercourses is used:
1) primary watercourses, involving canals that traverse the region; the level is determined at a supra-regional scale, not in the model;
2) secondary watercourses, forming the main arteries of the regional system;
3) tertiary watercourses, usually the ditches;
4) tile drains;
5) gulleys/soil surface.

For each surface water trajectory that is explicitly modelled, there must be a specification of either:
- the discharge as a function of the water level (Eq. 93);
- the discharge as a function of the water level difference with the next trajectory (e.g. Eq. 95).

In the case of a bifurcation there can be several such functions for the flows to the multiple downstream branches.

For specifying the watercourse characteristics, each sub-section traversing a nodal subdomain must be specified in a list, with for each segment:
- the number of the system that is involved (k=0,1,2,..5); k=0 is reserved for trajectories that do not have any interaction in the form of drainage, but act only as a conduit for the surface water;
- the length of the segment;
- the cross-sectional specifications;
- the nodal subdomain involved;
- the surface water trajectory that the segment is connected with;
- the parameters defining the drainage resistance (§4.3.2).

The use of this table involving the nodal subdomains (instead of a table for the complete trajectories themselves) ensures consistency in the model. The parameters are here used for making tables of the storage function for the main watercourse (Eq. 92). In the groundwater model they are used for the drainage characteristics.

6 Water management

6.1 Introduction

Water management covers many features that have been discussed in the preceding chapters. For instance a small waterway that has been dug as a ditch is of course 'non-natural'. Its dimensioning is part of the water management scheme. Water management is here defined to cover those parts of the system that do not have a pendant in the natural world. A fixed weir, for instance, is analogous to a dam-like obstruction in a river. Accordingly, its modelling has been discussed in §5. A weir that has a movable crest, on the other hand, is distinctly non-natural and therefore discussed below.

6.2 Land use

6.2.1 Urban areas

The water management of urban areas has evolved in the course of time. Originally it was just a question of discharging the rain and sewage water to the surroundings. But untreated water led to the spreading of diseases and to eutrophication. This has largely been remedied by building treatment plants. Recently the focus has further broadened. Whereas in the past urban areas were often considered as a 'separate world' from the surrounding rural area, there is now an increasing awareness that modern water management should be based on an integrated vision. Therefore, the SIMGRO-model has an elaborate set of options for modelling the water management of urban areas, as depicted by the schematic diagram given in Figure 25.

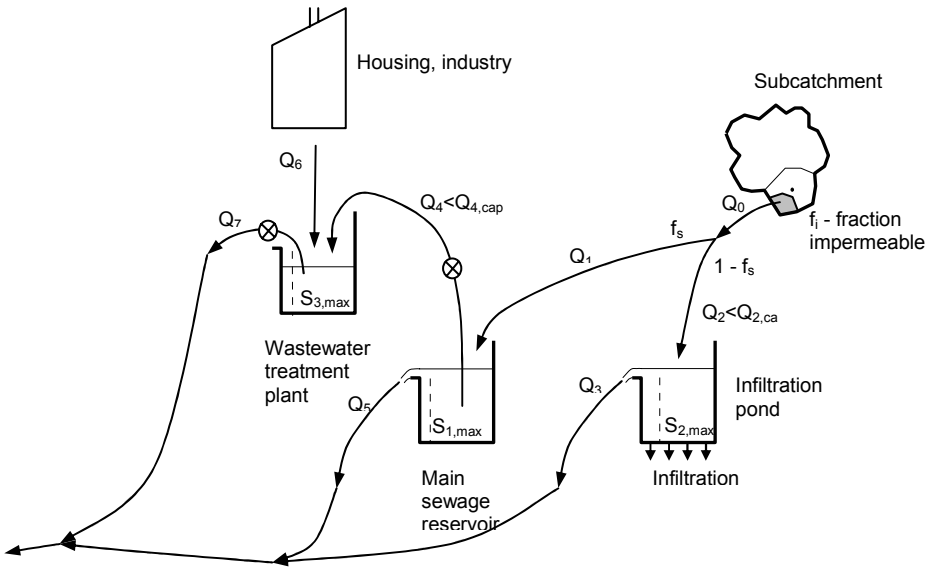

Figure 25 Schematic diagram of storage elements and transmission links in urban areas

The fraction of the paved area is specified per nodal subdomain. The model has an (optional) rainwater infiltration pond. That is a modern feature of urban water management, with the intention of conserving the water by feeding it into the groundwater. The inflow is governed by a dividing fraction $(1-f_s)$, and a maximum capacity $Q_{2,max}$. The water can then infiltrate to the subsoil, or else spill over to the surface water network (Q_3). The other part of the runoff (Q_1) goes to the main sewage reservoir. This reservoir has a 'pump over' capacity ($Q_{4,cap}$) for transporting water to the wastewater treatment plant. In the case of excessive inflow there can be direct spilling into the surface water network (Q_5). The wastewater treatment plant also receives water from housing and industry. After treating the water it is fed back into the surface water network (Q_7). In theory, a direct spill can also occur; but since this is a water quality-calamity, most systems have enough capacity to avoid that happening.

6.2.2 Sprinkled crops

During the growing season, precipitation deficits are likely to occur regularly. If the water content of the root zone drops below the reduction point (cf. Figure 5), crop growth will be reduced. To avoid this, crops may be irrigated. In the Netherlands, sprinkler irrigation is the most common method. Depending on availability and legislation, sprinkling is done from surface water and/or groundwater.

In terms of water use efficiency, the performance of sprinkling systems is comparatively poor. Water losses due to runoff or percolation to the groundwater may be caused by:
- poor timing of sprinkling;
- poor dosing of sprinkling;
- sprinkling irregularities;
- installation leakage.

Additional losses are introduced by wind, evaporation and interception.

Sprinkling requirements are determined for each nodal subdomain and land-use type, for each time step of the soil water/groundwater model. SIMGRO allows the user to specify a sprinkling gift that may be applied with a rotational period. For determining the moment to start sprinkling use is made of the mean pressure head in the root zone. Sprinkling is triggered when this mean pressure head has fallen below a crop-related 'start' value, and discontinued as soon as it exceeds the 'stop' value. Case studies, carried out with this modelling concept have shown that these assumptions cause realistic amounts of sprinkling water to be simulated (Querner and Van Bakel, 1989).

The actual sprinkling gift is determined by both demand and capacity, as

$$Q_s = \min(Q_{s,dem}; Q_{s,cap}) \tag{99}$$

where
$Q_{s,dem}$ = sprinkling demand ($m^3\ d^{-1}$)
$Q_{s,cap}$ = sprinkling capacity ($m^3\ d^{-1}$)

If sprinkling from both groundwater and surface water are enabled, sprinkling from surface water has priority. The total sprinkling capacity is calculated as:

$$Q_{s,cap} = Q^{g}_{s,cap} + Q^{s}_{s,cap} \tag{100}$$

where:
$Q^{g}_{s,cap}$ = sprinkling capacity from groundwater ($m^3\ d^{-1}$)
$Q^{s}_{s,cap}$ = sprinkling capacity from surface water ($m^3\ d^{-1}$)

The groundwater extraction capacity is not considered time dependent, or dependent on the groundwater conditions. Thus the capacity is simply an input parameter. The maximum possible extraction of surface water depends on the prevailing surface water conditions. Below a certain critical water level the sprinkling is discontinued. In order to effectuate this in the model without causing a water balance violation at the moment that the surface water runs dry (or drops below a critical level), the sprinkling water is 'collected' during the preceding time step of the groundwater model, and held in storage until the next one. This algorithm suffices for the time steps of less than 1 d that are usually used in SIMGRO (0.25 d is the most common).

During sprinkling the atmospheric conditions are usually hot, as opposed to conditions that often prevail when there is natural rainfall. Under normal conditions the rainfall of course also evaporates as it falls. However, that has already been discounted: only the rain that actually reaches the ground surface is measured at the gauging station. Therefore, the evaporation of natural rainfall is not accounted for in the model. With respect to the sprinkling water we assume that a certain fraction is lost to evaporation. That is handled as a separate term in the computation of the evapotranspiration, for which no discounting is done with respect to the reference crop evapotranspiration:

$$ET_{act,spr} = f_{spr}\, Q_s / A_i; \qquad P_{s,net} = (1 - f_{spr})\, Q_s / A_i \tag{101}$$

where
$ET_{act,spr}$ = amount of sprinkling water that directly evaporates before reaching the vegetated (soil) surface, expressed per unit area of nodal subdomain ($m\ d^{-1}$)
f_{spr} (-) = fraction of the sprinkling water that is lost to evaporation (-)
A_i = area of nodal subdomain (m^2)
$P_{s,net}$ = the net sprinkling intensity ($m\ d^{-1}$)

6.3 Surface water

6.3.1 Weirs

Weirs can have advanced technology, including a radio-link to a monitoring point. An automated weir has an electro-mechanical gadget for adjusting the height of the crest, which can be programmed for achieving a target level at either the upstream or downstream side. An upstream control weir can for instance be used in conjunction with groundwater management. For that purpose the SIMGRO-code has the possibility of letting the weir/target level settings be determined by groundwater conditions at a monitoring point. Then a weir control scheme must be specified in the form of a piece-wise linear function, with per record:

- a groundwater level in the monitoring point *i*;
- a target level (or crest level) in trajectory *n*.

An example of a target-level control function is given in Figure 26a. The aim of that scheme is to achieve ideal conditions for crop growth (Van Walsum and Van Bakel, 1984; Van Bakel, 1986). In this case the 'ideal' groundwater level is thought to be 4.7 m +MSL, the point where the dashed line (1:1) intersects the function. For groundwater levels higher than the ideal one, the target level is lowered in an attempt to bring the groundwater level down; for groundwater levels lower than the ideal one, the target level is raised.

An example of a downstream control scheme is given in Figure 26b: if the downstream level starts to drop below 1.6 m +MSL, the crest level in the upstream trajectory is lowered in an attempt to maintain the desired water level. Such a type of

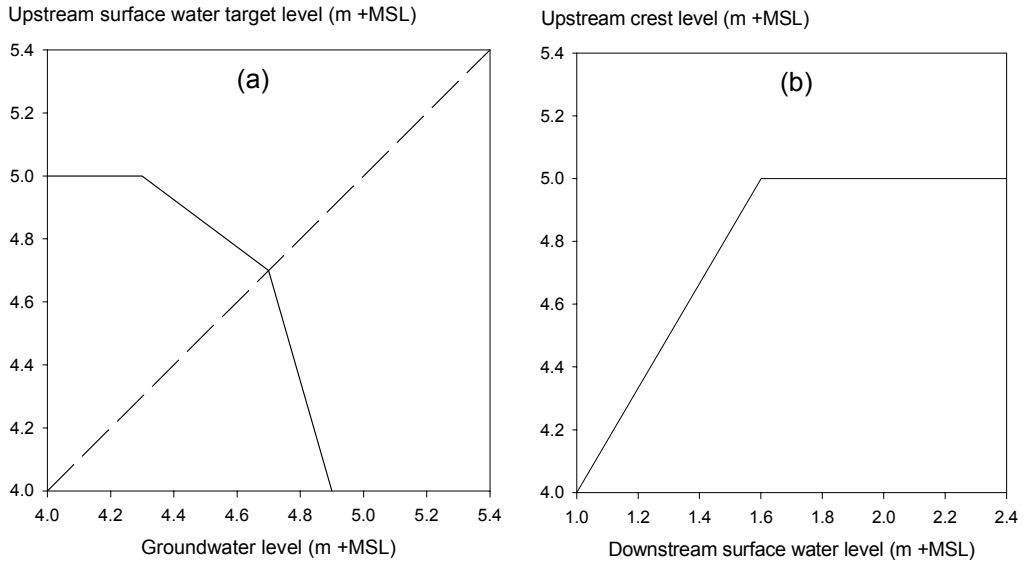

Figure 26 Weir management schemes: a) upstream control based on groundwater monitoring, aimed at optimizing conditions for crop production (soil surface at 5.4 m +MSL); b) downstream control based on surface water monitoring, aimed at stabilizing a downstream water level

scheme is commonly used for regulating demand-driven water supply in an irrigation channel network. But surface water supply can also be needed for maintaining water quality by forcing a certain amount of throughflow, for flushing the system. Then a different kind of control is needed as described in the next paragraph.

6.3.2 Surface water supply links

In SIMGRO it has been made possible to establish special links that involve water transfer from one watercourse to the next, as shown in Figure 27. Such a link does not have to involve an existing connection in the network that is used for calculating the discharge dynamics as described in §5.3.2; neither is there any constraint on creating 'closed circuits' in the network in this manner. (Closed circuits are not allowed for the discharge dynamics, because the algorithm requires a strict upstream to downstream calculation order). No storage is taken into account in the link itself. So in order to remain realistic it should not be very long.

The flow regulation is based upon stepwise adjustment of the supply rate, at each time step of the surface water model (cf. Figure 27):

1. By default, the supply rate is incremented each time step as long as the maximum supply capacity has not been reached.
2. Before actually implementing the new supply rate, the following checks are made. If one of the following conditions is met the flow rate is *decremented* instead:
   - if the level in the extraction trajectory *n* has become lower than the minimum level (the source runs dry);
   - if the water level in the supply trajectory *m* has become higher than the maximum allowed level (over-supply);
   - if the desired flow at the flow control trajectory *k* has been over-stepped (over-supply).

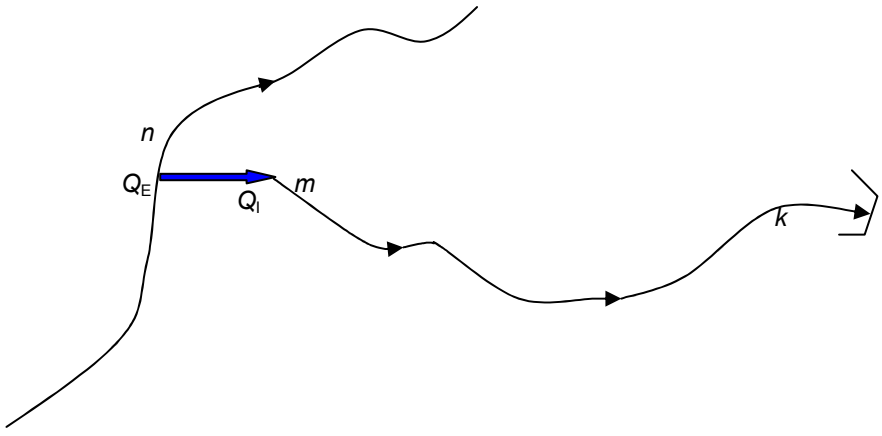

Figure 27 Surface water supply link. Water is transferred from trajectory n to m. Supply control is based on the water levels in n and m, and the flow over the weir at k.

6.3.3 Discharge pumps

For a pump the management can be specified in the form of a switch, with a 'start-level' and 'stop-level' (H_{start} and H_{stop}, Figure 28). If the water level rises above the construction height (H_{constr}), the water is free to move over the top. Such a construction height is also specified in the input data for weirs and culverts.

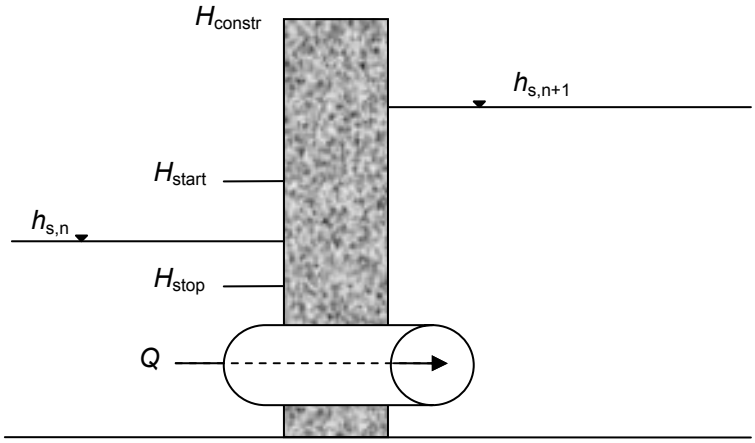

Figure 28 Pumping station, with a start and a stop level for switching the pump on and off. If the water level rises above the construction height Hconstr, the structure overflows and the water is free to move over the top

Literature

Anderson, M.P. and W.W. Woessner, 1992. *Applied groundwater modelling. Simulation of flow and advective transport.* Academic Press, Inc.

Bear, J. 1977. *Hydraulics of groundwater.* Mc-Graw-Hill.

Boesten, J.J.T.I. and L. Stroosnijder, 1986. *Simple model for daily evaporation from fallow tilled soil under spring conditions in a temperate climate.* Neth. J. Agric. Sci., 34, 75-90.

Cordes, C. and W. Kinzelbach, 1992. *Continuous groundwater velocity fields and path lines in linear, bilinear and trilinear finite elements.* Water Res. Res. 28(11):2903-2911.

Crank, J. and P. Nicolson, 1947. *A practical method for numerical evaluation of solutions of partial differential equations of the heat-conduction type.* Proc. Camb Phil. Soc. 43: 50-67.

De Bruin, H.A.R., 1987. *From Penman to Makkink.* Comm. Hydrol. Res. TNO, The Hague. Proc. and Inf. 39:5-31.

De Laat, P.J.M., 1980. *Model for unsaturated flow above a shallow water table, applied to a regional subsurface flow problem.* Doctoral thesis, Agric. University Wageningen. Pudoc, Wageningen.

Dooge, J.C.I. 1959. *A general theory of the unit hydrograph.* J. Geophys. Res. 64: 241-256.

Dumm, L.D. 1954. *Drain spacing formula.* Agr. Eng. 35: 726-730.

Ernst, L.F. 1962. Grondwaterstroming in de verzadigde zone en hun berekening bij aanwezigheid van horizontale evenwijdige open leidingen. Wageningen, Ph.D thesis.

Ernst, L.F., 1978. *Drainage of undulating sandy soils with high groundwater tables. I. A drainage formula based on a constant hydraulic head ratio. II. The variable hydraulic head ratio.* J. Hydrol. 39, 3/4:1-50.

Ernst, L.F. *Wegzijging en kwel; de grondwaterstroming van hogere naar lagere gronden.* Rapport 7. Instituut voor Cultuurtechniek en Waterhuishouding, Wageningen.

Feddes, R.A., P.J. Kowalik, and H. Zaradny, 1978. *Simulation of field water use and crop yields. Simulation monographs.* University of Wageningen, Pudoc.

Feddes, R.A., 1987. *Crop factors in relation to Makkink reference- crop evapotranspiration.* Comm. Hydrol. Res. TNO, The Hague. Proc. and Inf. 39: 33-44.

Feddes, R.A., P. Kabat, P.J.T. van Bakel, J.J.B. Bronswijk and J. Halbertsma, 1988. *Modelling soil water dynamics in the unsaturated zone - state of the art*. J. Hydrol. 100: 69-111.

Feitsma, K.S. 1969. *Grondverbetering in het noordwestelijk deel van Oostelijk Flevoland*. Cultuurtechn. Tijdschr. 9: 86-98.

Freeze, R.A. 1971. *Three dimensional, transient saturated and unsaturated flow in a groundwater basin*. Water Resour. Res. 7(2): 347-366.

Freeze, R.A. and R.L. Harlan, 1969. *Blueprint for a physically based,digitally simulated hydrological response model*. J. Hydrol. 9: 237-258.

Gash, J.H.C., 1979. *An analytical model of rainfall interception by forests*. Q. J. R. Meteor. Soc. 105, 43-55.

Groenendijk,P., M. van Elswijk (SERC), J.Huygen, J.G. Kroes, A.J. Otjens, M.F.R. Smit, A.A. Veldhuizen en J.F. Wesseling, 1999. *MultiSwap als applicatie van het Framework Integraal Waterbeheer*. Technisch Document 60. Alterra (Staring Centrum), Wageningen.

Heij, G.J. 1989. *River-groundwater relationships in lower parts of the Netherlands*. J. Hydrol. 108: 35-62.

Hermans, A.G.M., P.E.V. van Walsum, J. Runhaar, & P.J.T. van Bakel. 2004. *Duurzaam waterbeheer Langbroekerwetering; Fase 1: Modelbouw, calibratie en bepaling van het Actueel Grond- en Oppervlaktewaterregime*. Wageningen, Alterra, Alterra-rapport 914.

Huyakorn, P.S. and G.F. Pinder. 1983. *Computational methods in subsurface flow*. Academic Press, Inc.

Jousma, G., and H.Th.L. Massop. 1996. *Intreeweerstanden; inventarisatie en analyse*. TNO-grondwater en Energie, Delft. Rapport GG-R-96-15(A).

Kinzelbach, W., 1986. *Groundwater modelling. An introduction with sample programs in basic*. Vol. 25, Developments in Water Science, Elsevier, Amsterdam.

Kraijenhoff van de Leur, D.A. 1958. *A study of non-steady groundwater flow with special reference to a reservoir coefficient*. De Ingenieur, 70, B87–B94.

Kraijenhoff van de Leur, D.A. 1977. *Diffusion-type elements for runoff models*. Lecture notes. Wageningen, Vakgroep Hydraulica en Afvoerhydrologie.

Kroes, J.G., J.C. van Dam (eds.). 2003. *SWAP 3.0.3 Reference manual*. Wageningen, Report 773, Alterra.

Molen, W.H. van der. 1972. Waterbeheersing (collegdictaat). Wageningen, Vakgroep Cultuurtechniek..

Neuman, S.P., 1973. *Saturated-Unsaturated seepage by finite elements*. Proc. ASCE, J.Hydraul. Div. 99 (HY12): 2233-2250.

Pinder, G.F. and W.G. Gray. 1977. *Finite element simulation in surface and subsurface hydrology*. Academic Press, London.

Press, W.H., B.P. Flannery, S.A. Teukolsky, W.T. Vetterling, 1986. *Numerical Recipies; The Art of Scientific Computing*. Cambridge University Press, Cambridge, USA.

Querner, E.P. , 1988. *Description of a regional groundwater flow model SIMGRO and some applications*. Agric. Water Man. 14: 209-218.

Querner, E.P. and P.J.T. van Bakel, 1989. *Description of the regional groundwater flow model SIMGRO*. Wageningen, DLO-Staring Centrum, Report 7.

Remson, I., G.E. Hornberger and F.J. Molz. 1971. *Numerical methods in subsurface hydrology*. Wiley & Sons, New York.

Richards, L.A., 1931. *Capillary conduction of liquids through porous mediums*. Physics 1: 318:333.

Rijtema, P.E. 1965. *An analysis of actual evapotranspiration*. Agricultural Reports 659. PUDOC, Wageningen. 107 pp.

Schouwenaars, J.M. 1990. *Problem-oriented studies on plant-soil-water relations*. Doctoral Thesis. Wageningen, Agricultural University.

Smith, G.D., 1978. *Numerical solution of partial differential eqs: finite difference methods*. 2nd Ed., Clarendon Press, Oxford, UK.

Tank, R.G.B.M. and L.C.P.M. Stuyt, 1997. *Zicht op grondwaterstromingspatronen met de modulen SIMPATH en SIMSYS*. Wageningen, SC-DLO, Rapport 470 (in Dutch).

Van Bakel, P.J.T. 1986. *A systematic approach to improve the planning, design and operation of surface water management systems: a case study*. Wageningen, Ph. D. thesis.

Van Walsum, P.E.V. and P.J.T. van Bakel, 1983. *Berekening van de effecten van infiltratie op de gewasverdamping in het herinrichtingsgebied, met een aangepaste versie van het model*

SWATRE. Wageningen, Instituut voor Cultuurtechniek en Waterhuishouding, Nota 1434.

Van Walsum, P.E.V. 1994. *Gebruik van SWATRE voor de berekening van afvoerkenmerken*. Wageningen, DLO-Staring Centrum, Rapport 366.

Van Walsum, P.E.V., T. Vergroesen, P.E. Dik, M. Haasnoot, E. Verschelling. 2003. *Waterwijs Laag Nederland. Een eerste aanzet to ontwikkeling van een planvormend systeem voor het landgebruik en waterbeheer*. Wageningen, Alterra, Rapport 871.

Veldhuizen, A.A., A. Poelman, L.C.P.M. Stuyt and E.P. Querner. 1998. *Software documentation for SIMGRO V3.0; Regional water management simulator*. Technical Document 50. SC-DLO, Wageningen.

Chow, V.T. 1959. *Open-channel hydraulics*. McGraw-Hill, New York.

Walton, W.C. 1970. *Groundwater resource evaluation*. McGraw-Hill, New York.

Wang, H.F. and M.P. Anderson, 1982. *Introduction to groundwater modelling. Finite difference and finite element methods*. W.H. Freeman and Company, New York.

Wesseling, J. 1957. *Enige aspecten van de waterbeheersing in landbouwgronden*. Ph. D. thesis. Versl. van Landbouwk. Onderz. 63.5. Pudoc, Wageningen.

WL | Delft Hydraulics, 2001. *SOBEK Rural, managing your flow*. Manual version 2.07, WL| Delft Hydraulics, Delft.

Wosten, J.H.M., G.J. Veerman, W.J.M. de Groot, J. Stolte. 2001. *Waterretentie- en doorlatendheidskarakteristieken van boven- en ondergronden in Nederland: de Staringreeks*. Vernieuwde uitgave 2001. Alterra-rapport 152. Alterra, Wageningen.

Appendix 1 Drainage resistances in a multiple layered aquifer system

The schematization used for deriving expressions which relate the phreatic head to drain discharge in a multiple aquifer system is depicted in Figure A1.1.

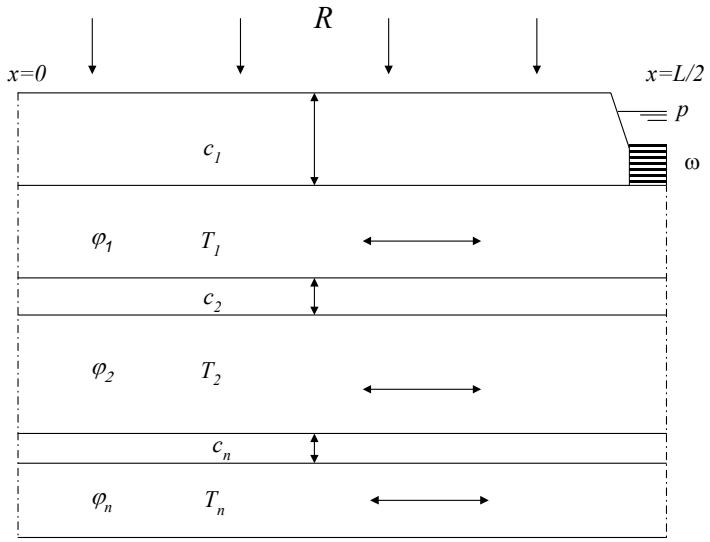

Figure A1.1 Schematization used in the derivation of expressions for the drainage resistance in an multi-layered aquifer system

The set of second order linear differential equations describing the hydraulic heads in the aquifers as a function of distance:

$$\begin{pmatrix} \frac{d^2\varphi_1}{dx^2} \\ \frac{d^2\varphi_2}{dx^2} \\ \cdot \\ \frac{d^2\varphi_n}{dx^2} \end{pmatrix} = \begin{pmatrix} \frac{1}{T_1 c_2} & -\frac{1}{T_1 c_2} & \cdot & 0 \\ -\frac{1}{T_2 c_2} & \frac{1}{T_2 c_2}+\frac{1}{T_2 c_3} & \cdot & 0 \\ \cdot & \cdot & \cdot & \cdot \\ 0 & 0 & \cdot & \frac{1}{T_n c_n} \end{pmatrix} \begin{pmatrix} \varphi_1 \\ \varphi_2 \\ \cdot \\ \varphi_n \end{pmatrix} + \begin{pmatrix} -\frac{R}{T_1} \\ 0 \\ \cdot \\ 0 \end{pmatrix} \tag{102}$$

The general solution to the homogeneous equation can be written as (Ernst, 1983; Bruggeman 1999):

$$\begin{pmatrix} \varphi_1 \\ \varphi_2 \\ \cdot \\ \varphi_n \end{pmatrix}_h = \begin{pmatrix} b \\ b \\ \cdot \\ b \end{pmatrix} + \begin{pmatrix} A_1 x & \beta_{1,2}\left(A_2 \cosh(\frac{x}{\sqrt{\lambda_2}}) + B_2 \sinh(\frac{x}{\sqrt{\lambda_2}}) \right) & \cdot & \beta_{1,n}\left(A_n \cosh(\frac{x}{\sqrt{\lambda_n}}) + B_n \sinh(\frac{x}{\sqrt{\lambda_n}}) \right) \\ A_1 x & \beta_{2,2}\left(A_2 \cosh(\frac{x}{\sqrt{\lambda_2}}) + B_2 \sinh(\frac{x}{\sqrt{\lambda_2}}) \right) & \cdot & \beta_{2,n}\left(A_n \cosh(\frac{x}{\sqrt{\lambda_n}}) + B_n \sinh(\frac{x}{\sqrt{\lambda_n}}) \right) \\ \cdot & \cdot & \cdot & \cdot \\ A_1 x & \beta_{n,2}\left(A_2 \cosh(\frac{x}{\sqrt{\lambda_2}}) + B_2 \sinh(\frac{x}{\sqrt{\lambda_2}}) \right) & \cdot & \beta_{n,n}\left(A_n \cosh(\frac{x}{\sqrt{\lambda_n}}) + B_n \sinh(\frac{x}{\sqrt{\lambda_n}}) \right) \end{pmatrix} \tag{103}$$

where λ_i's are the eigenvalues of the systems equation and $\beta_{i,j}$'s are elements of the transposed eigenmatrix. Note that the first eigenvalue is identical to 0 and yields therefore a linear 'x' term in the solution to the homogeneous equation.

The coefficients $A_1..A_{n-1}$ and $B_1..B_{n-1}$ as well as a and b are integration constants to be solved by substitution of the boundary conditions

The particular solution is found by elaboration of the recharge term in the systems equation and reads (Ernst, 1983):

$$\begin{pmatrix}\varphi_1\\ \varphi_2\\ .\\ \varphi_n\end{pmatrix}_p = -\frac{R}{\sum_{i=1}^{n} T_i}\begin{pmatrix}\frac{x^2}{2}+c_1\sum_{j=1}^{n}T_j\\ \frac{x^2}{2}+c_1\sum_{j=1}^{n}T_j+c_2\sum_{j=2}^{n}T_j\\ .\\ \frac{x^2}{2}+\sum_{i=1}^{n}\left\{c_i\sum_{j=i}^{n}T_j\right\}\end{pmatrix} \tag{104}$$

So the complete solution is written as:

$$\begin{pmatrix}\varphi_1\\ \varphi_2\\ .\\ \varphi_n\end{pmatrix} = \begin{pmatrix}b\\ b\\ .\\ b\end{pmatrix} + \begin{pmatrix} A_1 x & \beta_{1,2}\left(A_2\cosh(\frac{x}{\sqrt{\lambda_2}})+B_2\sinh(\frac{x}{\sqrt{\lambda_2}})\right) & \cdot & \beta_{1,n}\left(A_n\cosh(\frac{x}{\sqrt{\lambda_n}})+B_n\sinh(\frac{x}{\sqrt{\lambda_n}})\right)\\ A_1 x & \beta_{2,2}\left(A_2\cosh(\frac{x}{\sqrt{\lambda_2}})+B_2\sinh(\frac{x}{\sqrt{\lambda_2}})\right) & \cdot & \beta_{2,n}\left(A_n\cosh(\frac{x}{\sqrt{\lambda_n}})+B_n\sinh(\frac{x}{\sqrt{\lambda_n}})\right)\\ . & . & . & .\\ A_1 x & \beta_{n,2}\left(A_2\cosh(\frac{x}{\sqrt{\lambda_2}})+B_2\sinh(\frac{x}{\sqrt{\lambda_2}})\right) & \cdot & \beta_{n,n}\left(A_n\cosh(\frac{x}{\sqrt{\lambda_n}})+B_n\sinh(\frac{x}{\sqrt{\lambda_n}})\right)\end{pmatrix}$$
$$-\frac{R}{\sum_{i=1}^{n} T_i}\begin{pmatrix}\frac{x^2}{2}+c_1\sum_{j=1}^{n}T_j\\ \frac{x^2}{2}+c_1\sum_{j=1}^{n}T_j+c_2\sum_{j=2}^{n}T_j\\ .\\ \frac{x^2}{2}+\sum_{i=1}^{n}\left\{c_i\sum_{j=i}^{n}T_j\right\}\end{pmatrix} \tag{105}$$

The first boundary to consider is the horizontal flow rate at the water divide at x=0. By definition this flow rate equals zero. This condition is only met when A_1 and $B_2..B_n$ are identical to 0. It reduces the general solution to:

$$\begin{pmatrix}\varphi_1\\ \varphi_2\\ .\\ \varphi_n\end{pmatrix}=\begin{pmatrix}1 & \beta_{1,2}\cosh(\frac{x}{\sqrt{\lambda_2}}) & \cdot & \beta_{1,n}\cosh(\frac{x}{\sqrt{\lambda_n}})\\ 1 & \beta_{2,2}\cosh(\frac{x}{\sqrt{\lambda_2}}) & \cdot & \beta_{2,n}\cosh(\frac{x}{\sqrt{\lambda_n}})\\ . & . & . & .\\ 1 & \beta_{n,2}\cosh(\frac{x}{\sqrt{\lambda_2}}) & \cdot & \beta_{n,n}\cosh(\frac{x}{\sqrt{\lambda_n}})\end{pmatrix}\begin{pmatrix}b\\ A_2\\ .\\ A_n\end{pmatrix}-\frac{\mathrm{R}}{\sum_{i=1}^{n}T_i}\begin{pmatrix}\frac{x^2}{2}+c_1\sum_{j=1}^{n}T_j\\ \frac{x^2}{2}+c_1\sum_{j=1}^{n}T_j+c_2\sum_{j=2}^{n}T_j\\ .\\ \frac{x^2}{2}+\sum_{i=1}^{n}\left\{c_i\sum_{j=i}^{n}T_j\right\}\end{pmatrix} \quad (106)$$

The remaining integration constants A_2.. A_n and b are found by substitution of the boundary conditions which hold for $x=L/2$:

$$\varphi_1(\frac{L}{2})=p-\Omega RL;\qquad -T_2\frac{d\varphi_2}{dx}\Big]_{x=L/2}=0;\qquad -T_n\frac{d\varphi_n}{dx}\Big]_{x=L/2}=0 \quad (107)$$

where Ω is the combined radial/entry resistance coefficient and p is the surface water level. The set of n linear equations with n unknowns A_i is formed by:

$$\begin{pmatrix}1 & \beta_{1,2}\cosh(\frac{L}{2\sqrt{\lambda_2}}) & \cdot & \beta_{1,n}\cosh(\frac{L}{2\sqrt{\lambda_n}})\\ 0 & -T_2\frac{\beta_{2,2}}{\sqrt{\lambda_2}}\sinh(\frac{L}{2\sqrt{\lambda_2}}) & \cdot & -T_2\frac{\beta_{2,n}}{\sqrt{\lambda_n}}\sinh(\frac{L}{2\sqrt{\lambda_n}})\\ . & . & . & .\\ 0 & -T_n\frac{\beta_{n,2}}{\sqrt{\lambda_2}}\sinh(\frac{L}{2\sqrt{\lambda_2}}) & \cdot & -T_n\frac{\beta_{n,n}}{\sqrt{\lambda_n}}\sinh(\frac{L}{2\sqrt{\lambda_n}})\end{pmatrix}\begin{pmatrix}b\\ A_2\\ .\\ A_n\end{pmatrix}=\begin{pmatrix}p-\Omega RL\\ 0\\ 0\\ 0\end{pmatrix}-\frac{RL}{2\sum_{i=1}^{n}T_i}\begin{pmatrix}0\\ T_2\\ .\\ T_n\end{pmatrix} \quad (108)$$

Solving this equation can be done using an ordinary matrix solver. It is not necessary to specify a realistic value for the surface water level, since this parameter is in fact a reference level for all the layers. In order to find an expression for the drainage resistance the hydraulic head as a function of the distance x to the line drain in the upper aquifer is needed:

$$\varphi_1(x)=b+\sum_{i=2}^{n}A_i\ \beta_{1,i}\cosh(\frac{x}{\lambda_i})-\frac{R\,x^2}{2\sum_{i=1}^{n}T_i}-R\,c_1 \quad (109)$$

The drainage resistance is defined by:

$$\Gamma_d=\frac{\varphi_1(0)-p}{R} \quad (110)$$

To derive an expression for the 'horizontal' component of the drainage resistance the radial resistance coefficient Ω could be set to zero. The hydraulic head in the upper aquifer at $x=L/2$ is identical to the surface water level p. So we have:

$$\Gamma_h = \frac{\varphi_1(0) - \varphi_1(\frac{L}{2})}{R} \tag{111}$$

From Eq. (108) it can be seen that the constants $A_1..A_{n-1}$ are linearly proportional to the recharge rate R, hence the 'horizontal' component of the drainage resistance reads:

$$\Gamma_h = \frac{L^2}{8\sum_{i=1}^{n} T_i} + \sum_{i=2}^{n} A_i \ \beta_{1,i}(1 - \cosh(\frac{L}{2\lambda_i})) \tag{112}$$

For application in regional groundwater flow models (e.g. SIMGRO, MODFLOW) the drainage resistance is multiplied by the so-called *form factor* ζ. Then the expression should be written as:

$$\zeta\ \Gamma_h = \frac{\frac{2}{L}\int_{o}^{L/2}\varphi_1(x)dx - \varphi_1(\frac{L}{2})}{1} = \frac{L^2}{12\sum_{i=1}^{n} T_i} + \sum_{i=2}^{n} A_i \ \beta_{1,i}(\frac{2\lambda_i}{L}\sinh(\frac{L}{2\lambda_i}) - \cosh(\frac{L}{2\lambda_i})) \tag{113}$$

Appendix 2 Drainage resistance of a short watercourse segment

Here a description is given of the flow within a drainage subarea involving a short water course segment. As indicated in section 4.3.2, if the length of a watercourse segment is shorter than $\sqrt{a_k}$ (with a_k as the spatial extent of the drainage subarea in m^2) the local drainage flow can not be described basing on the assumption that the flow takes place within a rectangle along the segment. That is because this assumption would imply a sideways-elongated subrea, which is contradictory to the idea of the drainage calculation method, involving a droplet taking the shortest route to a watercourse. And certainly if it concerns the *only* segment within a nodal subdomain, the assumption of a rectangular flow area is very erroneous, yielding a too *high* estimate of the horizontal drainage resistance. If the on the other extreme one would try to remedy this by simply computing the resistance as if the equivalent spacing were equal to $\sqrt{a_k}$ (or $\sqrt{A_i}$ in the case of just one segment within the whole nodal subdomain), then part of the horizontal resistance would simply be ignored. That would yield a too *low* estimate of the horizontal resistance.

In order to make an intermediate calculation of the resistance with respect to the above given extremes, we here follow an approach that does not schematise the subarea to a rectangle, but to a quadrant of a circular island, with the watercourse segment following a circular course (figure A2.1). In the area on the outside of the watercourse (A_2), there is converging radial flow towards the watercourse. In the area on the inside of the watercourse (A_1) there is diverging radial flow. Along the boundary we have a zero gradient in the normal direction, and thus a zero boundary flux. Inside the area assume a uniform intensity of the drainage flux q_d. Thus the conditions are satisfied for being able to superimpose the local flow on the regional flow (see Section 4.2).

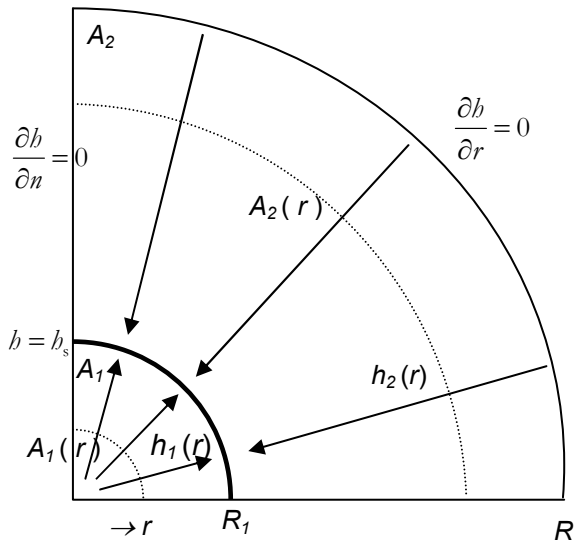

Figure A2.1 Schematization of the flow within a drainage subarea to flow within a quadrant of a 'circular island to a watercourse' with level hs, involving converging radial flow on the outside of the watercourse, and diverging radial flow on the inside of it

Let the length of the watercourse segment be given by l. Then the radius R_1 of the subquadrant enclosed by the watercourse (Fig. A2.1) is given by:

$$l = \tfrac{1}{2}\,\pi R_1 \quad \Rightarrow R_1 = 2\,l / \pi \tag{114}$$

The total area A of the quadrant equals the sum of the area on the inside (A_1) and the area on the outside the watercourse (A_2). So we have:

$$A = A_1 + A_2 = \tfrac{1}{4}\pi R^2 \Rightarrow R = 2\sqrt{A / \pi} \tag{115}$$

where R is the radius of the quadrant (m). For the area on the inside of the watercourse we have:

$$A_1 = \tfrac{1}{4}\pi R_1^2 = \tfrac{1}{4}\pi\,(2\,l / \pi)^2 = l^2 / \pi \tag{116}$$

In the derivation we use the area $A_1(r)$ for calculating the accumulated discharge between the origin and radius length r:

$$A_1(r) = \tfrac{1}{4}\pi r^2 \quad \text{for} \quad r \le R_1 \tag{117}$$

Similarly, we have for the area on the outside of the watercourse:

$$A_2 = \tfrac{1}{4}\pi(R^2 - R_1^2) \quad \text{and} \quad A_2(r) = \tfrac{1}{4}\pi(R^2 - r^2) \quad \text{for} \quad R_1 \le r \le R \tag{118}$$

Now we can describe the flow on the inside of the watercourse with:

$$q_1(r) = A_1(r) q_d \qquad \text{and} \qquad q_1(r) = -\tfrac{1}{4}\,2\pi\, r\, \frac{dh_1}{dr}\, KD$$

$$\Rightarrow \tfrac{1}{4}\pi\, r^2\, q_d = -\tfrac{1}{2}\pi\, r\, \frac{dh_1}{dr}\, KD \quad \Rightarrow -\frac{q_d}{2KD}\, r\, dr = dh_1$$

$$\Rightarrow h_1(r) - h_s = -\frac{q_d}{2KD} \int r\, dr = -\frac{q_d}{2KD}(\tfrac{1}{2}r^2 + C_1) = \frac{q_d}{4KD}(R_1^2 - r^2) \tag{119}$$

where the constant C_1 is derived from the boundary condition $h_1(R_1) - h_s = 0$.

For the flow on the outside of the watercourse we have:

$$q_2(r) = A_2(r) q_d \qquad \text{and} \qquad q_2(r) = \tfrac{1}{4}\,2\pi\, r\, \frac{dh_2}{dr}\, KD$$

$$\Rightarrow \tfrac{1}{4}\pi\,(R^2 - r^2)\, q_d = \tfrac{1}{2}\pi\, r\, \frac{dh_2}{dr}\, KD \quad \Rightarrow \frac{q_d}{2KD}\frac{(R^2 - r^2)}{r} dr = dh_2 \Rightarrow$$

$$\Rightarrow h_2(r) - h_s = \frac{q_d}{2KD} \int (\frac{R^2}{r} - r)\, dr = \frac{q_d}{2KD}(R^2 \ln r - \tfrac{1}{2}r^2 + C_2) \tag{120}$$

From the boundary condition $h_2(R_1)$ - $h_s = 0$ we then obtain:

$$C_2 = \tfrac{1}{2} R_1^2 - R^2 \ln R_1 \tag{121}$$

$$\Rightarrow h_2(r) - h_s = \frac{q_d}{2kD}[R^2 \ln \frac{r}{R_1} + \tfrac{1}{2}(R_1^2 - r^2)] \tag{122}$$

The mean elevation for area A is given by:

$$\bar{h} = \frac{1}{A}\{\int_0^{R_1} h_1(r)\frac{2\pi r}{4}dr + \int_{R_1}^{R} h_2(r)\frac{2\pi r}{4}dr\} = \frac{1}{A}\{A_1 \bar{h}_1 + A_2 \bar{h}_2\} \tag{123}$$

For area A_1 we have:

$$\bar{h}_1 = \frac{1}{A_1}\int_0^{R_1} h_1(r)\frac{2\pi r}{4}dr = \frac{q_d \pi}{8A_1 KD}\int_0^{R_1} r(R_1^2 - r^2)\,dr = \frac{q_d \pi}{8A_1 KD}\,[R_1^2 \tfrac{1}{2} r^2 - \tfrac{1}{4} r^4]_0^{R_1}$$

$$= \frac{q_d \pi}{32 A_1 KD} R_1^4 = \frac{q_d \pi}{32 \cdot \tfrac{1}{4}\pi R_1^2 KD} R_1^4 = \frac{q_d}{8KD} R_1^2 \tag{124}$$

For area A_2 we have:

$$\bar{h}_2 = \frac{1}{A_2}\int_{R_1}^{R} h_2(r)\frac{2\pi r}{4}dr = \frac{1}{A_2}\frac{q_d}{2KD}\frac{2\pi}{4}\int_{R_1}^{R}(R^2 r \ln r - \tfrac{1}{2} r^3 + C_2 r)\,dr$$

$$= \frac{q_d}{2(R^2 - R_1^2)KD}[R^4(\ln \frac{R}{R_1} - \tfrac{3}{4}) + R^2 R_1^2 - \tfrac{1}{4} R_1^4] \tag{125}$$

Insertion of Eqs. 124 and 125 into Eq. 123 yields for the mean head elevation above the surface water level:

$$\bar{h} = \frac{1}{\tfrac{1}{4}\pi R^2}\left(\frac{\tfrac{1}{4}\pi R_1^2 q_d}{8KD} R_1^2 + \frac{\tfrac{1}{4}\pi(R^2 - R_1^2) q_d}{2(R^2 - R_1^2)KD}[R^4(\ln \frac{R}{R_1} - \tfrac{3}{4}) + R^2 R_1^2 - \tfrac{1}{4} R_1^4]\right)$$

$$\bar{h} = \frac{q_d}{2KD}\left(R^2(\ln \frac{R}{R_1} - \tfrac{3}{4}) + R_1^2\right) \tag{126}$$

The form factor is derived by dividing the mean head elevation by $h_2(R)$ as given by evaluating Eq. 120:

$$\zeta_h^{QUAD} = \frac{\bar{h} - h_s}{h_2(R) - h_s} = \frac{\frac{q_d}{2KD}\left(R^2(\ln\frac{R}{R_1} - \tfrac{3}{4}) + R_1^2 \right)}{\frac{q_d}{2kD}\left(R^2 \ln\frac{R}{R_1} + \tfrac{1}{2}(R_1^2 - R^2) \right)}$$

$$\Rightarrow \zeta_h^{QUAD} = 1 - \frac{\tfrac{1}{4}R^2 - \tfrac{1}{2}R_1^2}{\left(R^2(\ln\frac{R}{R_1} - \tfrac{1}{2}) + \tfrac{1}{2}R_1^2 \right)} \qquad (127)$$

For the rectangular drainage subarea we expressed the horizontal drainage resistance in the unit [d m^{-1}]. For being able to compare the value with those obtained from a radial formula, the resistance is converted to the unit [d], using:

$$\gamma_h^L = L\omega_h \qquad (128)$$

where ω_h is computed with Eq. 53, and the 'unmodified' L from Eq. 84. In the case that $L > \sqrt{A_i}$ we make a comparison with the value obtained by applying the simple 'fix' of using **min**$(L; \sqrt{A_i})$ instead of L in Eq. 128. The latter result we denote by γ_h^{LM}. For comparing with the method using the radial flow field in a quadrant we compute the horizontal resistance by dividing the maximum elevation $h_2(R)$ (Eq. 120) through the drainage intensity:

$$\gamma_h^{QUAD} = \frac{h_2(R) - h_s}{q_d} = \frac{1}{2KD}[R^2(\ln\frac{R}{R_1} - \tfrac{1}{2}) + \tfrac{1}{2}R_1^2] \qquad (129)$$

For the example calculations we use the following fixed parameters:
A = 10 000 m^2
R = 112.8 m
KD = 10 m^2 d^{-1}
In the calculation examples we compare the results for the 'rectangular' drainage subarea, and for the radial one as described above.

*Table A2.1 Calculation examples, for comparing results obtained with 'rectangular' drainage formula and 'radial' formula. The rectangular formula using unmodified L are given with the superscript ^{L}, those with the modified L (**min**$(L; \sqrt{A_i})$ with the superscript ^{LM}, and the ones derived from the radial formula within a quadrant with the superscript ^{QUAD}*

l (m)	R_1 (m)	γ_h^L (d)	ζ_h^L (-)	γ_h^{LM} (d)	γ_h^{QUAD} (d)	ζ_h^{QUAD} (-)
100.0	63.7	125	0.67	125	147	0.61
50.0	31.8	500	0.67	250	513	0.74
25.0	15.9	2000	0.67	500	935	0.84
12.5	8.0	8000	0.67	1000	1372	0.89
6.25	4.0	32000	0.67	2000	1812	0.91